Martin Marietta Report
MCR-76-321

National
Aeronautics and
Space
Administration

Final Report

VIKING LANDER SPACECRAFT BATTERY

September 1976

Prepared by

Martin Marietta Corporation
P.O. Box 179
Denver, Colorado 80201

Prepared For

Jet Propulsion Laboratory
California Institute of Technology
Pasadena, California

Under Contract JPL GM-649000

Martin Marietta
Report No. MCR-76-321

Final Report

VIKING LANDER SPACECRAFT BATTERY

September 1976

Prepared by

Duane R. Newell
Martin Marietta Corporation
P. O. Box 179
Denver, Colorado 80201

Prepared for

Jet Propulsion Laboratory
California Institute of Technology
Pasadena, California

Under Contract JPL GM-649000

This report was prepared for the Jet Propulsion Laboratory, California Institute of Technology, sponsored by the NASA under Contract NAS7-100. Martin Marietta Aerospace is responsible for the Viking Lander Spacecraft which is part of the overall Viking Project managed by the Viking Project Office at Langley Research Center (NASA).

ACKNOWLEDGEMENTS

The writer wishes to acknowledge the support received from the following individuals in preparing this report. Mr. Matt Imamura, as the program manager, for his critique and recommendations on the report organization and content. Messrs. John Sanders and Ken Farley for their helpful suggestions and guidance concerning the initial cell development and evaluation efforts and their technical contributions and support for the various sections. Messrs. Jim Masson and Harlan Nassen for contributing the sections on prelaunch activities and in-flight performance. Mr. Guy Rampel of General Electric, Gainesville, Florida, for his review and suggestion on the organization and contents of the cell description and manufacturing sections. Mr. Sam Bogner, JPL project manager, and Mr. Aiji Uchiyama of JPL for their review and comments. Mrs. Carol Shafer for her efforts in preparing the report sections for review.

ABSTRACT

The Viking Lander spacecraft required the use of a heat sterilizable battery to meet the biological cleanliness requirements imposed on a spacecraft landing on the Mars surface. The design, development, fabrication, qualification, test, and flight performance of the battery developed to meet this requirement are presented herein.

The battery consists of twenty-four, 8-ampere-hour sealed nickel-cadmium cells that were qualified to withstand up to 200 hours of heat at a temperature of 125°C in a discharged open circuit condition. Nonwoven polypropylene was the separator material used. Two batteries are packaged in one assembly and two assemblies are flown on a spacecraft.

Battery charging is accomplished normally at rates of C/15, C/7.5, and C/5. Trickle charge rates of C/40 and C/160 are used during the cruise portion of the mission. During the entry and landing phase, the batteries are discharged to 70% of the nameplate capacity. After landing the batteries perform a load leveling function and are used whenever the load exceeds the radioisotope thermoelectric generator (RTG) power capability. During battery recharging operations, three batteries are used to supply the peak loads while the remaining battery is charged.

CONTENTS

Table

I. INTRODUCTION

The Viking mission to search for life on the Mars surface presented some formidable problems relative to the development of an energy storage system for the spacecraft. The environmental requirements developed for the spacecraft included a requirement for sterilization to insure that a biologically clean spacecraft will land on the Mars surface. This requirement ultimately led to the development of a heat sterilizable battery.

The spacecraft design developed for the mission consisted of two separate vehicles joined together during the long journey to Mars. The two vehicles were designated the Orbiter and the Lander. The Orbiter remains in Mars orbit acquiring and relaying data to Earth after the Lander separates and descends to Mars to perform its 90-day mission of analyzing the Mars surface. Only the Lander and its components required sterilization before the launch.

This report presents the cell selection process, design development, manufacture, test, and initial flight performance of the battery system for the Viking Lander spacecraft power system. The power subsystem contains four eight-ampere-hour (A-h) heat sterilizable, nickel-cadmium batteries packaged in two separate assemblies. The battery system was required to have a minimum beginning of life capability of 1140 watt-hours (W-h).

The report is divided into seven major sections describing the program requirements, cell evaluation testing, cell design and manufacturing, battery design, system integration testing, engineering evaluation testing, and initial flight performance.

II. SUMMARY

The Viking Lander was the first spacecraft to fly a sterilized nickel-cadmium battery on a mission to explore the surface of a planet. This report documents the significant results of the battery development program from its inception through the design, manufacture, and test of the flight batteries which were flown on the two Lander spacecraft. The flight performance during the early phase of the mission is also presented.

A. DESIGN CONSIDERATION

The basic mission requirements were as follows:

1) A 11-month cruise from Earth to Mars;
2) Orbiting Mars for up to 80 days before landing;
3) Operating for 90 days on the Mars surface;
4) Provide a biolotically clean spacecraft.

Based on these mission requirements, the following key battery design requirements were derived:

1) The batteries shall be capable of being heat sterilized at temperatures up to 135°C.
2) The battery shall be capable of operating after 11 months of discharged open circuit stand.
3) The batteries shall be capable of operating after trickle charging at a C/160 rate for 80 days while approaching and in Mars orbit.
4) During entry and landing, the batteries shall be capable of being discharged to 70% of their rated capacity.
5) The batteries shall provide up to 200 cycles at a 50% depth-of-discharge during the landed operations.
6) The batteries shall be capable of being charged over a temperature range from 4 to 32°C.

5. DEVELOPMENT TEST PROGRAM

The initial development effort was concentrated in developing a sealed 40 A-h silver-zinc (Ag-Zn) cell due to its high energy density capability. This approach was abandoned due to problems which could not be solved within the schedule and cost allocations.

The problems encountered included:

1) Loss of capacity after sterilization;
2) Case leaks after sterilization;
3) Terminal to case seals;
4) Outgassing and degradation of case material.

A backup nickel-cadmium (Ni-Cd) cell development program was initiated in 1971 when it became apparent that there were significant problems connected with the silver-zinc development program. When the major problems with the nickel-cadmium development were solved, the silver-zinc program was phased out.

An 8 A-h Ni-Cd cell was selected. This size was dictated largely by the low power capability of the radioisotope thermoelectric generators on the Lander. Load analyses and power margin assessment predicted a maximum charge rate of 1.5 amperes with an average rate between 0.8 and 1.0 amperes. To meet the redundancy requirements, four 24-cell batteries were used in each spacecraft.

Two nickel-cadmium cell manufacturers, Eagle Picher, and General Electric were involved in the nickel-cadmium development program. Their major tasks were to:

1) Qualify a separator material to the sterilization requirements;
2) Determine adequacy of cell manufacturing processes to meet the sterilization requirement;
3) Develop inspection criteria, procedures, and tests for producing high reliability cell;
4) Design, fabricate, test, and qualify candidate cells to the Viking acceptance criteria.

The significant obstacles to overcome included the selection of a separator material and developing procedures that minimize degradation in performance characteristics during sterilization.

Polypropylene separator material was found to be compatible with the sterilization temperatures by both vendors. However, its hydrophobic characteristic introduced the problem of how to provide an adequate amount of electrolyte and still maintain an adequate oxygen recombination rate and prevent an early separator dryout. General Electric developed and introduced a heat treatment process during fabrication which improved the separator wettability. This process permitted an increase in the electrolyte quantity from 1.5 to 2 cc over the quantity supplied in nonheat treated cells, while still avoiding the excessive pressure during overcharge. Based on their success, GE was selected to supply the cells for the Viking development and flight test program.

The cells fabricated by Eagle Picher developed high pressures during charge due to an inadequate oxygen recombination rate which was found to be due to excessive electrolyte. Eagle Picher later solved this problem and they were designated as a second source for the Lander battery cells.

An extensive development program was undertaken at Martin Marietta Aerospace to evaluate the vendor designs and to develop techniques and procedures for sterilizing and determining the cell and battery performance characteristics. A method for sterilizing the cells was developed which introduced little or no degradation in cell performance. Before sterilization the cells were discharged at a C/2 rate to 1.0 V followed by the application of a one-ohm load to each cell for 24 hr. During exposure to heat, the cells were kept in an open circuit condition. Cells sterilized in any other condition suffered extensive capacity loss and in some cases physical damage.

The effect of long duration trickle charging at a C/160 rate to maintain the batteries in a charged condition during portions of the 11-month interplanetary cruise to Mars were evaluated. This evaluation showed that the batteries could be maintained at their rated capacity (8 A-h); however, there was a significant degradation in the cell voltage during the first discharge after removal of the trickle charge. It was found that this voltage degradation can be erased after cycling the cells a few times.

The thermal dissipation characteristics of the cells were determined for various operating conditions using the calorimetry technique developed by Martin Marietta. These data were used to predict the battery and Lander internal temperature for the various battery operating modes.

C. FLIGHT CELL AND BATTERY DESIGN, FABRICATION, AND TESTING

The cell design that evolved as a result of the development program provided a cell with the following characteristics:

Capacity:	8 A-h (nameplate)
Weight:	373 gm (lot average)
Dimensions:	7.59 cm x 2.26 cm x 8.64 cm including terminals
Case Material:	304L stainless steel
Terminal Seal:	General Electric - all nickel braze
Plates:	11 positive
	12 negative
Separator:	Polypropylene (nonwoven)
Electrolyte:	34% potassium hydroxide

The cells were matched in watt-hour capacity after experiencing 64 cycles of charge and discharge using C/15, C/10, and C/7.5 charge rates and a C/2 discharge to a 1.0 V cutoff in a 21°C temperature

controlled environment. Watt-hour capacity matching between 1.5 to 3% of the average cell capacity was achieved for the flight batteries and spares.

The cells were qualified to withstand both a sterilization temperature of 135°C for 40 hr and 110°C for 54 hr in a discharged open circuit condition.

Due to the limited space and volume available on the Lander, two 24-cell batteries were packaged in one assembly. Heat rejection from the battery to the Lander structure was through a center plate which divided the two batteries and the base plate. Each assembly weighed 22.9 kg and required a mounting area of 30.48x20.32 cm. Each battery had separate power and instrumentation connectors. The instrumentation connector was used during laboratory testing to provide access to each of the battery cells for voltage monitoring.

The batteries were subjected to electrical checkout tests after assembly and then sterilized at an acceptance level temperature of 121°C for 54 hours. Environmental acceptance tests consist of sinusoidal and random vibration in each of the three axes of the battery assembly.

Two battery assemblies were mounted side by side on each Lander to insure that each assembly was exposed to the same environment. A total of 13 battery assemblies were fabricated to support the prototype, development, and Lander ground test programs. Eight batteries were built for the flight test program of which four were allocated for the two Landers. Four spare batteries were provided.

D. SYSTEM INTEGRATION AND TESTING

Lander system tests at the factory and the launch site were performed with test support batteries. One battery failure involving high internal cell impedance was observed during the factory testing.

Failure analysis of the cells in this battery revealed that the most probable cause of this was the improper battery operation during tests in which the battery was left in a charged condition for long periods of time with high impedance instrumentation loads connected. The slow discharge rates during these periods led to the development of large CdOH crystals on the negative plate with a corresponding increase in plate porosity. It was theorized that this increase in negative plate porosity along with the typical increase of positive plate thickness resulted in the electrolyte migrating from the separator into the plates. The separator dry-out was the primary cause of the cells developing high internal impedances. This failure illustrated the need for adequate battery operating and maintenance procedure to insure that the batteries are used properly.

Life cycle tests are in progress on two batteries made up of spare Viking cells. Over 11,000 cycles have been achieved at various recharge fractions at several temperatures, of which 4,000 cycles were performed at 25% depth-of-discharge in a temperature environment between 40 and 50°C.

E. INITIAL FLIGHT PERFORMANCE

During the early phase of the mission, the batteries were charged and used to support the in-flight checkout of the Lander subsystems. All batteries were charged at the C/15 rate until the temperature compensated cutoff voltage was reached. They were recharged once during the test and again at the completion of the checkout sequences.

One of the four batteries on each Lander was placed on a C/40 trickle charge for the duration of the cruise to Mars. The other three batteries were each discharged into a telemetry isolation

resistor (10.3 kilo-ohm). The three batteries not on trickle charge were allowed to discharge as low as 2.5 Vdc into a fixed 19.3 kilo-ohm resistor. This resulted in several cells developing a reverse voltage due to over discharge. This had no detrimental effect on subsequent battery performance and proved to be an effective reconditioning method.

The batteries on trickle charge reached a temperature of 31°C and remained there for the duration of the cruise. The batteries were recharged successfully and used during the Orbiter-Lander preseparation checkout. At the completion of this checkout, all four batteries were placed on the C/160 trickle charge while awaiting the selection of an acceptable landing site.

All batteries performed satisfactorily during the Mars landing phase and operation on Mars surface.

III. CONCLUSIONS AND RECOMMENDATIONS

The single most critical requirement of the Viking battery development program was to meet the sterilization requirement. Twenty-one batteries containing over 1,000 cells were subjected to this requirement without a failure. The cells have demonstrated the capability of being trickle charged at a C/40 rate at a temperature of 31°C for over six months and still meet the performance requirements.

A heat treatment process was developed for the cells to improve the separator wettability and consequently increase the quantity of electrolyte supplied to the cell. This process should be considered for cells manufactured with polypropylene separators regardless of whether a sterilization requirement exists. The increase in the electrolyte quantity will tend to prevent premature separator dryout thus extending the cell life.

The design of a nickel-cadmium cell using polypropylene separator material requires close control of the electrolyte quantity to insure an adequate oxygen recombination rate. However, inadequate electrolyte can also lead to premature separator dryout and subsequent failure. Since the margin between the two limits is small, it is recommended that a lower limit be established for the electrolyte quantity. If an adequate oxygen recombination rate cannot be achieved with this minimum allowable electrolyte, the cell must be rejected.

A carbonate reduction process was incorporated into the cell manufacturing processes beginning with the flight cell production. A comparison of test data on cells built with and without the carbonate reduction process leads to the conclusion that a definite improvement in cell characteristics was obtained. Cell voltages during the cell matching tests were typically 5 to 10 mV lower during charge and a corresponding increase in voltage during discharge was noted.

A decrease in the end-of-charge voltage spread among the cells was also observed. In general, it was concluded that a reduction in the cell internal impedance had been achieved. It is recommended that this process be considered for new designs for improving existing designs.

A battery failure occurred during the prototype spacecraft test program. This failure was attributed to improper battery usage in which the battery was allowed to remain mostly in charged open circuit condition with intermittent charging for long periods without cycling. The conclusion reached in the investigation of this problem was that an adequate control of battery maintenance and operation is required during spacecraft testing. It is recommended that a battery maintenance and operating criteria document be prepared and used to support spacecraft testing, especially if flight batteries are used.

A change was incorporated into the cells on the type of cell terminal after the prototype cell program. This change was made at the recommendation of the cell manufacturer and was due to numerous industry reports of seal failures. The new terminal was developed by General Electric and used on all nickel braze. It was felt that this terminal had a better chance of surviving the rigors of sterilization than the original terminal design. Over 1,200 cells built with all nickel braze had no seal failure. Over 1,000 of these cells were sterilized. Based on this record, it is recommended that the selected terminal design be considered for any new cell procurement.

The cell matching procedure for the test support and flight batteries was based on the watt-hr capacity at the end of 64 charge/discharge cycles. During the 64 cycles the cells were charged at C/15, C/10 and C/7.5 rates. Each discharge was at a C/2 rate to a cell voltage of one volt. The charge/discharge A-h ratio varied from 1.4 to 1.6. All testing was performed at 21.1^{o}C. Both watt-hr

and ampere-hr data was obtained for the last several cycles. The cells were ranked and selected based on the watt-hr capacity on the 64th cycle. Equivalent results could have been obtained using the A-h capacity. A cell matching percentage of 1.5 to 3% was attained for the flight batteries. This method for testing and matching cells is recommended whenever the requirement for a high depth of discharge exists.

The life cycle testing has proven that the cells with polypropylene separators have a high cycle life capability and are suitable for consideration on low earth and synchronous orbit type missions.

The concept of maintaining the batteries in discharged state during flight and then charging them just before their required usage was proven to be acceptable. Since the batteries were discharged at launch, recharged just before the in-flight checkout discharged after the checkout, and finally recharged several months later in preparation for Mars orbit insertion and landing.

Reconditioning was accomplished on the Lander batteries by discharging each battery into a 19.3-ohm load bank to approximately 1.1 V per cell during the final phases of the launch and then allowing the telemetry isolation resistor (19.3 kΩ) to slowly drain the battery during flight to Mars. This technique was used twice during the mission, once immediately after launch and again after the in-flight checkout. Cell voltage polarity reversals were observed during laboratory evaluation tests. However, the discharge current was not sufficient to produce any pressure and no apparent degradation in cell performance was observed during subsequent operation. This reconditioning method involving the use of a fixed resistor deserves consideration for application on the other planetary or Earth-orbiting missions.

During the course of inspection and analysis of failed cells, several plates were found with manufacturing defects which did not meet the cell specification. Examples of these defects are severe blistering along one side, no coining along one edge but with a double width coining on the opposite edge, rust spots on the positive plate

edges in one cell, and a lump of silicon grease between the plate pack and case. Considering the limited number of cells that were dissected, it was concluded that an improvement in the quality assurance at the manufacturer was required if the goals of the high reliability cell specifications are to be achieved.

IV. DESIGN CONSIDERATIONS

A. MISSION AND SYSTEM CONSIDERATIONS

During the initial phases of the development program, numerous analyses and trade studies were performed to develop design criteria and select candidate subsystems and components. Some of the more significant factors considered were derived from the mission sequence and objectives. The planned Viking mission sequence included an 11-month interplanetary cruise from Earth to Mars, up to 80 days of Mars orbital operations, 2 to 6 hr of deorbit coast followed by a 10- to 15-min terminal descent phase to the Mars surface, and finally a 90-day operational period on the Mars surface acquiring, analyzing, and transmitting scientific data back to Earth. A pictorial representation of the mission profile is shown in Figure IV-1.

The Viking spacecraft consists of a two-stage vehicle. The Orbiter stage remains in a Mars orbit performing scientific experiments and relaying data received from the Lander stage back to earth. The Orbiter is powered by a solar array/battery power system. During the cruise phase, the Orbiter electrical power system is used to power the Lander subsystem.

The Lander stage was designed to separate from the Orbiter while in Mars orbit and land on the Mars surface using a combination of a parachute and retropropulsion to achieve a soft landing. As a consequence of the landing requirement, the Lander and its components were required to be sterilized to prevent contamination of the Mars surface.

The design that evolved as a result of the sterilization requirement consisted of a spacecraft that was completely enclosed in a bioshield. The bioshield's purpose was to maintain the Lander in a sterile condition after sterilization. Figure IV-2 shows the general configuration of the Lander vehicle as it is packaged in the time of launch. The bioshield cap is jettisoned shortly after the spacecraft is placed in the interplanetary cruise trajectory.

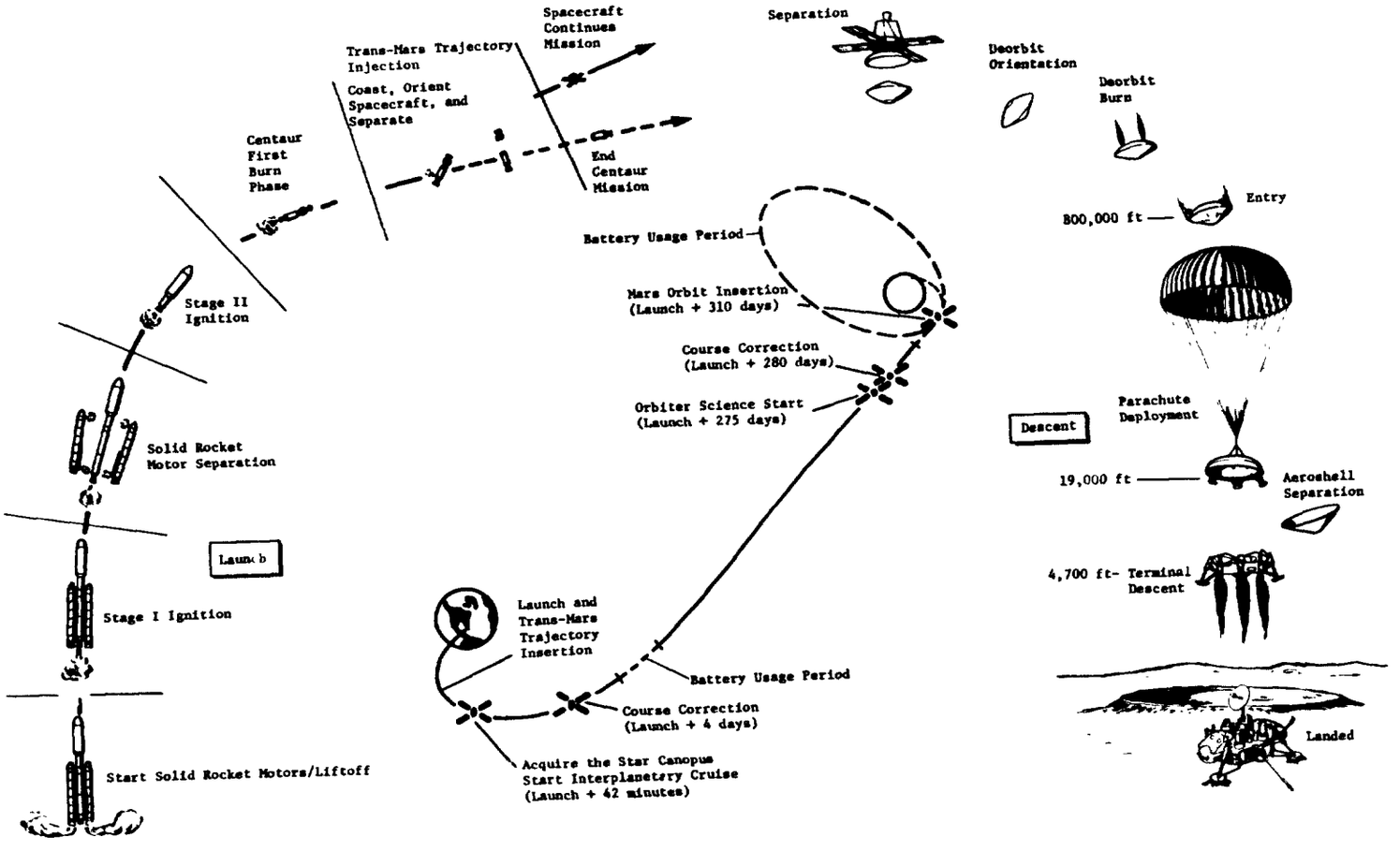

Figure IV-1 Viking Mission Sequence

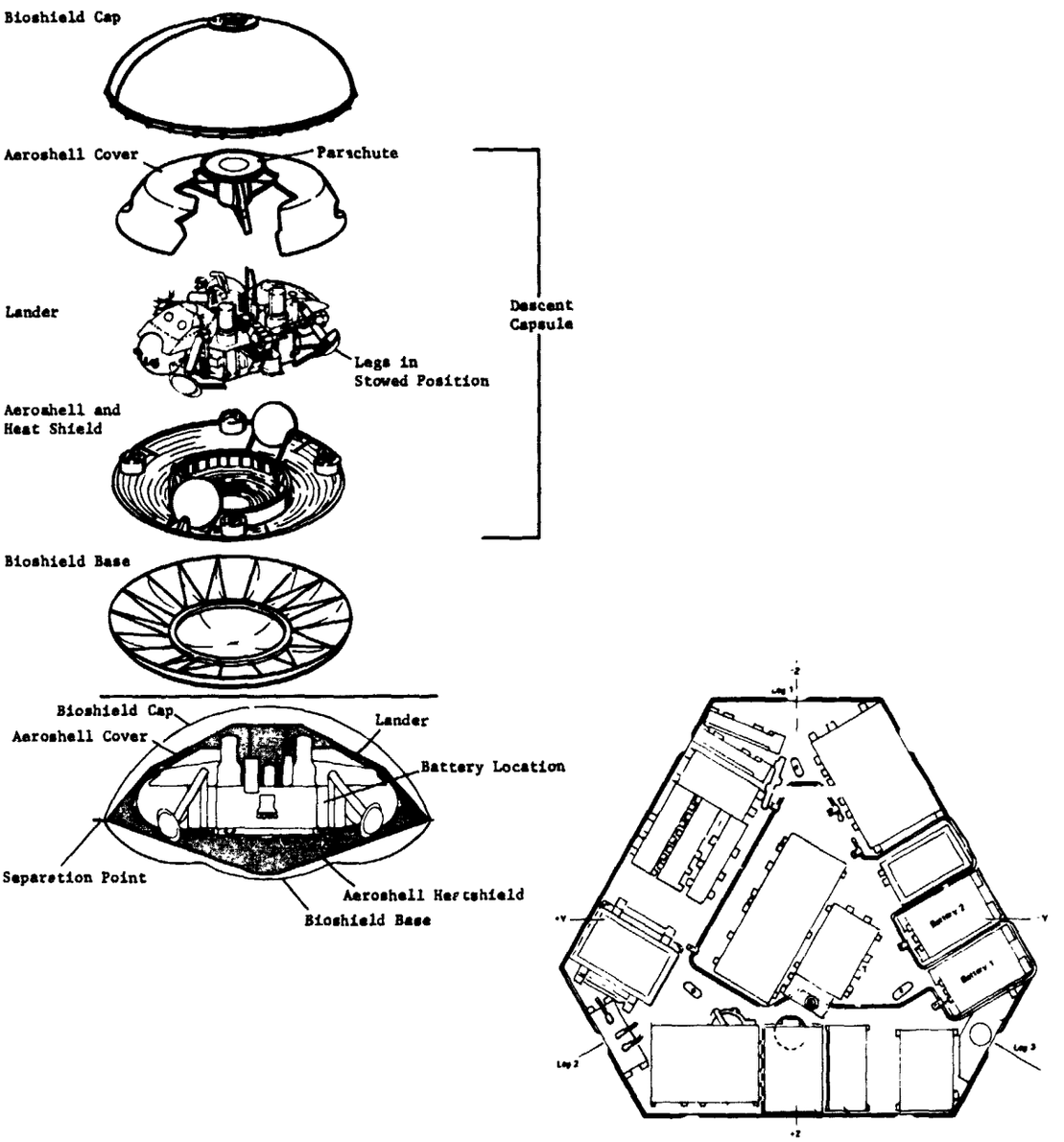

Figure IV-2 Lander Assembly

The following paragraphs describe how each of these mission phases contributed to the selection of a power system and energy storage components.

1. Interplanetary Cruise

The long term (11 months) interplanetary cruise in essentially a dormant condition posed the problem of how to store the batteries during this time period. Because of the thermal problems associated with operating the Lander RTGs with the bioshield cover and aeroshell in place, the Lander electrical power requirements during cruise were supplied by the Viking Orbiter. During this period, the RTGs were stored in a shorted condition to prevent thermal degradation during cruise.

An evaluation of the various battery storage methods including trickle charging, charged open circuit stand, and total discharge stand was made to select the method offering the least risk and performance degradation. It was decided to discharge the batteries before launch and keep them discharged until just before Mars orbit insertion. At that time the batteries were to be subjected to 1½ cycles to prepare them for use during the subsequent operations.

2. Mars Orbital Operation

Once the Viking spacecraft was in a Mars orbit, the landing sites would be surveyed and the final selection of a suitable landing site would be made. During this period which could last for up to 50 days, the batteries are maintained in a fully charged state in preparation for an Orbiter-lander preseparation checkout and the subsequent deorbit coast and landing operations. The method selected for keeping the batteries in a fully charged state was to apply a low rate trickle charge. A C/160 charge rate was found acceptable for maintaining the batteries charged without overheating the components.

3. Deorbit Coast and Landing

A variable entry and landing window period ranging from 2.5 to 6 hr in duration was programmed for this phase. The length of this period was dependent upon the time required to get from orbit to the selected landing site and land. Using the maximum duration allowable of six hours, the projected battery capacity required was determined to be 24 A-h. This particular phase imposed the maximum power demand on the batteries and therefore battery sizing was based on these requirements.

4. Landed Operation

The environmental conditions predicted for the surface of Mars introduced the primary constraints on the selection of a power source for the Lander. Blowing sand and dust storms precluded the use of solar arrays as a source of the power required. Radioisotope thermoelectric generators (RTGs) were the only competitive power source available when other factors such as weight and mission duration were considered.

RTGs are typically low-power low-voltage devices. Their limited power capability led to a requirement to provide an energy storage capability which could be used to supply power during peak demand periods. The RTG configuration selected consists of two 35-W (end-of-mission) units connected in series to provide a total capability of 70 W at 8.8 Vdc. Since only the power remaining after the lander subsystem requirements were met was available for battery charging, the 70 W of available RTG power also restricted the battery recharge capability.

B. BATTERY DESIGN AND PERFORMANCE CONSIDERATIONS

The cell size, number of cells, number of batteries, and packaging configuration were determined from the Lander power requirements, reliability and redundancy considerations, environment conditions, and the Lander configuration.

The bus voltage and the battery voltage were set at a nominal 28 V. This decision was influenced by the requirement to provide power conditioning of the RTG output and the availability of components and subsystems designed for 28-Vdc operation. A limit of 75% depth-of-discharge was imposed on the batteries to insure an adequate safety margin against cell overdischarge and voltage reversals. This 75% depth-of-discharge led to a requirement for a total battery capacity of 32 A-h based on the 24 A-h required during entry.

1. Battery Charging

Two RTGs and four chargers were provided. During the time that the Orbiter and Lander are mated, the Orbiter power system supplies the necessary power to redundant chargers on the Lander. After separation, the Lander RTGs supply the power to another set of chargers. Since the RTGs supply all the power requirements of the Lander, including battery charging, the charge rate varies as a function of the Lander subsystem power demands. A load analysis based on the planned operational sequences for the Lander subsystems indicated that the charging would occur in the 0.8- to 1.5-A range. A computer-generated load profile for the landing phase and a typical day on the Mars surface are shown in Figures IV-3 and IV-4. These figures also show the energy available from the batteries. The RTG energy in excess of the Lander requirements is available for recharging the batteries. During periods when the Lander power requirements exceed the RTG capabilities, the batteries supply the required energy.

The low charge rate capability of the RTGs along with the 32-A-h battery requirements results in a low charge efficiency. In the power-limited condition of landed operation, it was deemed desirable to improve the battery charge efficiency. This was accomplished by dividing the 32 A-h capacity requirement into four batteries, each using 8 A-h cells. This provided a C/10 charge rate resulting in an acceptable charge efficiency.

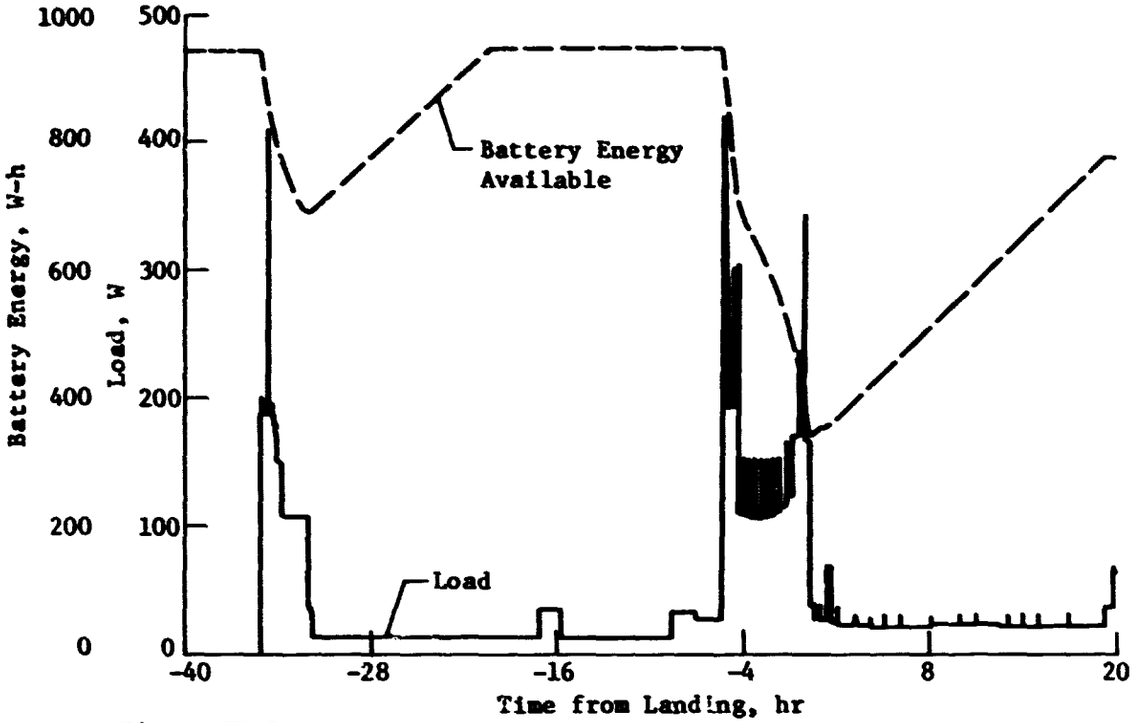

Figure IV-3
Lander Power Profile and Remaining Battery Energy from Preseparation Checkout through Landing

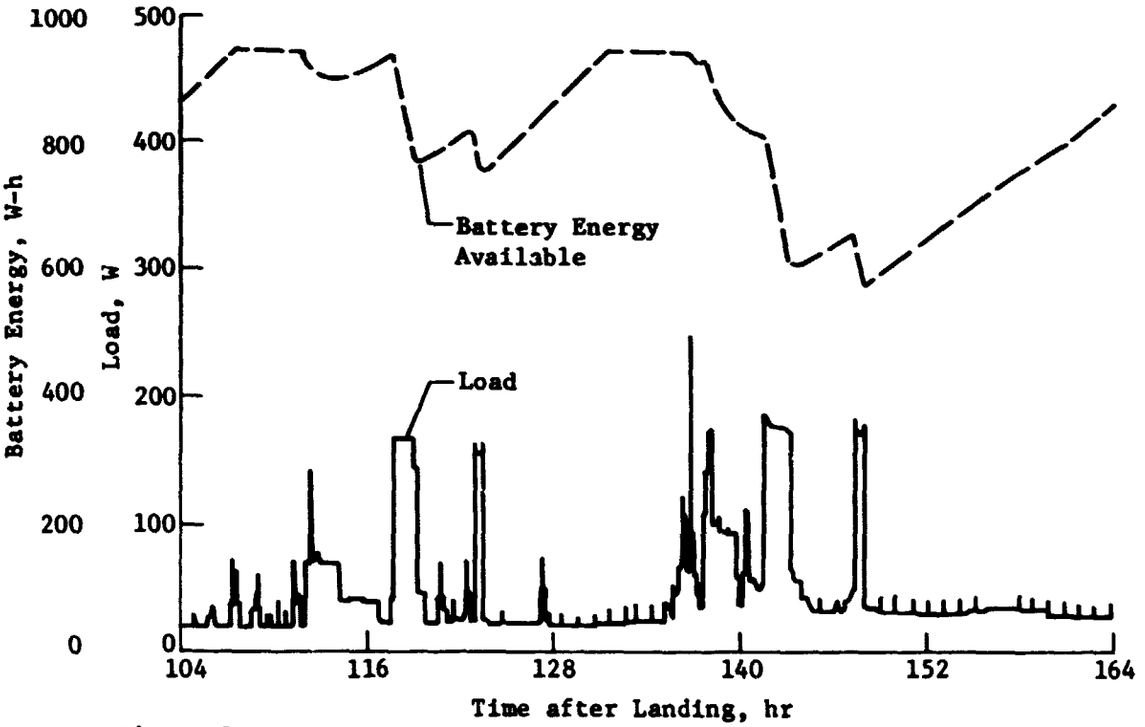

Figure IV-4
Lander Power Profile and Remaining Battery Energy for a Typical Operation on Mars Surface

The selection of an 8 A-h cell along with the limited charge rates available from the RTGs led to an operational sequence in which three of the four batteries were connected to the Lander distribution buses while the fourth battery was switched to the charge bus.

The three batteries that are connected to the load bus perform a load leveling function. They supply power only when the demand exceeds the RTG capability. The fourth battery is charged using whatever power is available from the RTGs. The recharge sequence uses a combination of voltage and temperature or time to control the end-of-charge. A time span of one hour was selected for the sequential charge regime. If the battery reached the voltage-temperature end of charge criteria during this time span, the charge was terminated. However, the battery remained connected to the charge bus until the end of the one-hour period. At that time, the computer switched the battery to the load bus and replaced it with one of the three that were feeding the load bus. In this manner each battery was connected to the load bus for three hours and then switched to the charge bus for one hour (if required) for recharging. The upper curve in Figures IV-3 and IV-4 shows the variation in battery energy available during the landing phase and for a typical day on the Mars surface. It can be seen from this data that several cycles are required to completely recharge the batteries after heavy load periods.

Redundancy

A redundancy analysis was made to determine the impact on the mission capabilities due to the loss of battery capacity. The results of this analysis were used in selecting the number of batteries. The initial load analysis defined a requirement for 24 A-h. (32 A-h with 75% depth-of-discharge to meet the worst-case mission requirements which occurs during deorbit coast and terminal descent.) By reducing the deorbit coast time from 6 to 2.5 hr (nominal mission) the mission objectives could be met with 18 A-h of capacity while still maintaining the 75% depth-of-

discharge limitation. This indicated that if the 32 A-h were divided into four 8 A-h batteries, the Mars landing could be accomplished and the 90 days of landed operation completed with the loss of one battery. This analysis was consistent with the selection of an 8 A-h cell based on the charge rates available from the RTGs.

3. Sterilization

Heat sterilization of the components and the assembled Lander vehicle after ground checkouts were completed and the vehicle was ready for installation on the launch pad was required. Sterilization at temperatures between 111.6 and 123.3°C with exposures ranging from 40 to 54 hr was required for the Lander and its components. This requirement led to a development program whose purpose was to evaluate various electrochemical couples and materials and finally select one for use in the Lander batteries.

4. Environmental Constraints

The battery storage and operating temperature extremes were derived from the earth-induced environments, interplanetary space environments, and finally Mars orbital and surface environments. Temperature extremes of 0 to 40°C were established to cover the various mission phases. Dynamic environments were derived using a composite environment which included the launch, Mars entry, and the landing phase. The environmental test requirements are given in Section V, Table V-5 and Figures V-39 thru V-41.

5. Spacecraft Physical Constraints

The battery configuration was determined from the space available on the Lander for installation and the method used to dissipate the heat produced during charge and discharge. The volume available for installing batteries was 2.86×10^4 cm^3 (1750 $in.^3$). The installation area was located in a compartment thermally isolated from space. Heat losses during charge or discharge could not be dissipated into space but had to be conducted into the Lander structure. This dictated a packaging design in which the heat produced during charge and discharge could be conducted through the battery case into the mounting structure.

6. Battery Requirements

The battery requirements, that were developed as a result of the mission constraints and Lander requirements discussed in the previous paragraphs are summarized as follows.

Energy:	944 W-h
Capacity:	32 A-h
Depth-of-Discharge:	75% maximum
Cell Size:	8 A-h
Charge Rate:	C/10 nominal
Thermal Control:	Passive-heat conduction into the Lander structure.

C. PROGRAM SCHEDULE AND MILESTONES

Figure IV-5 shows the Viking program span with the schedule of key milestones that significantly influenced battery development. The schedule shows the start date for the Ag-Zn cell development effort, the initiation of a backup nickel-cadmium cell as the prime candidate when the mission was rescheduled to a 1976 landing. Battery fabrication and delivery requirements to support the Lander acceptance test schedule and to meet the September-October 1975 launch windows were as shown.

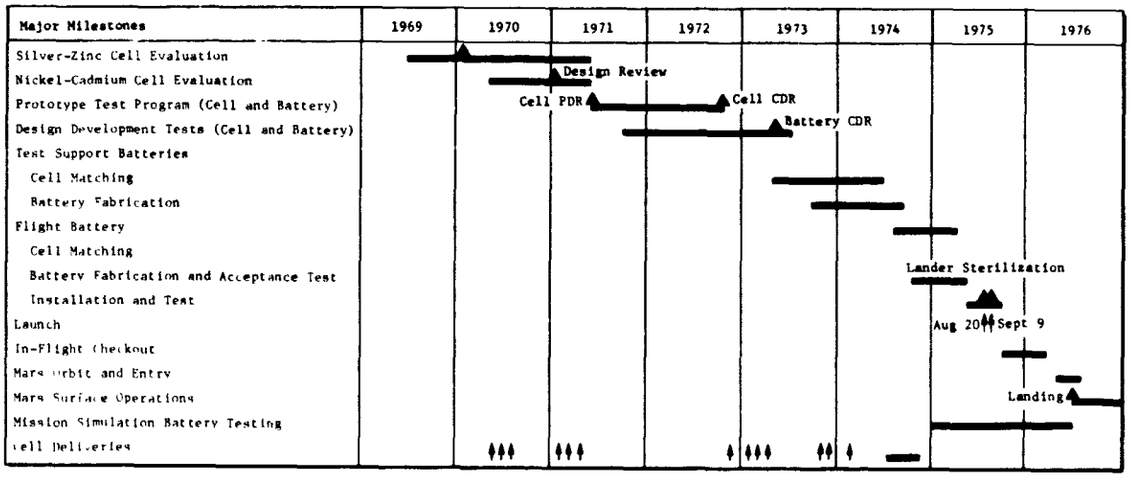

Figure IV-5 Battery Program Schedule

V. DEVELOPMENT TEST PROGRAM

A. CELL CANDIDATES AND EARLY DEVELOPMENT EFFORT

This section presents a summary of the initial development efforts Martin Marietta made to evaluate electrochemical sources for possible use on the Viking Lander. Rationale are presented to substantiate the final selection of the nickel-cadmium cell for the Lander battery.

1. Silver-Zinc Cell Development

The initial battery cell development effort consisted of a program to design, fabricate, and test sealed heat-sterilizable silver-zinc (Ag-Zn) cells. This program was awarded to Electric Storage Battery Incorporated (ESB) in 1969. ESB was required to fabricate and test 180 cells and to supply 100 cells to Martin Marietta for testing. The AgZn cell development program was initiated because of the severe weight limitation for the Lander electrical power system.

The initial ESB design consisted of a 30 A-h sealed cell (Model No. 387) which used six positive and seven negative plates. The cell case and covers were fabricated from polyphenlene oxide. Furane Epocast 31B with 9216 catalyst was used to seal the cover and exterior "O" rings on the terminals. The interior recesses for the cell terminals were filled with Isochem 911B/911A epoxy. Irradiated polypropylene was used as a positive plate absorber. When the mission duration was extended and the cells were required to meet a 22-month service life, a manganese-dioxide treatment was given to the separator material to fill the oversize pores to reduce the silver migration rate. The cells that received the manganese-dioxide treatment were designated Model 390 cells.

The three major areas of concern associated with this program were:

Cycling and Life Capability - The initial battery requirements included six cycles at 70% depth-of-discharge during checkout before Mars landing and 100 cycles at 20% depth-of-discharge after landing. Landed operation occurs after two months of battery storage and 11 months of prelaunch checkout and interplanetary cruise.

Sterilization - The cells were prepared for sterilization by discharging until an open circuit voltage of 0.2 to 0.9 V was reached. Sterilization at temperatures of 135°C for periods of up to 180 hr was performed during the evaluation testing.

Development Program - A limited time span for a development program existed since the Electrical Power System Design review was initially scheduled for June of 1971 when a decision on the selection of a battery cell was required.

The major problems that were encountered during the development program were as follows:

Leaks - Numerous problems were encountered with developing reliable seals between the cell lids, case, and terminals. Leaks were experienced both before and after sterilization.

Pressure - Excessive pressure was experienced when the batteries were charged following sterilization. Pressures ranging from 344 to 413 kPa (50 to 60 psig) were developed during the formation charge following the 140 hr exposure to 135°C temperature. Sources for this pressure included:

1) Gassing of residual amines from epoxies;
2) Procedural problems during the bakeout cycle at the cell manufacturer during fabrication; and
3) Fundamental degradation of cell materials (separator, case, etc).

Weight Loss - Cell weights before and after sterilization were compared. This comparison showed a typical loss of four grams during sterilization. This was attributed to the porosity

of the polyphenylene-oxide cell cases, and resulted in water loss through the case material during high temperature exposure.

2. Nickel-Cadmium Cell Development

Due to the problems encountered with the development of the Ag-Zn cell, a backup program was initiated to develop a sterilizable nickel-cadmium cell. The nickel-cadmium cell was given primary status when the program was redefined and the launch date changed from 1973 to 1975. The major factor considered in this decision was the inability of the Ag-Zn cell to perform satisfactorily after sterilization; however, the program redefinition also increased the operating life requirement of the batteries from 14 to 22 months. The longer life requirement raised some doubt as to whether the Ag-Zn cells could be qualified to meet this requirement. The Ag-Zn cell development effort was finally cancelled in September of 1971.

Two suppliers (General Electric and Eagle Picher) were placed on contract to perform the following nickel-cadmium cell development tasks:

1) Evaluate and select a separator material;
2) Perform evaluation tests and confirm the capability of their designs to perform satisfactorily after sterilization; and
3) Manufacture and deliver 188 cells to Martin Marietta for evaluation in a prototype test program.

The nickel-cadmium cell development program was oriented toward developing a heat-sterilizable cell that would meet the requirements discussed in the previous sections.

Both cell manufacturers performed evaluation tests on candidate separator materials. Both manufacturers selected Pellon's FT2140 for the prototype cell. General Electric later qualified WEX1242 which was produced by the General Aniline Film Corporation (GAF) as a back-up separator material. However, no cells were fabricated using this material for the prototype test program.

Separator selection criteria generally consisted of determining whether the material would survive the high temperature exposure required and still retain the properties necessary to act as an acceptable separator. Some of the more significant properties evaluated

were wettability, dimensional stability, and degradation in a potassium hydroxide environment at elevated temperatures (135°C) for long durations (200 hr).

The vendors performed numerous tests to optimize the cell design. Three of the interrelated parameters that required evaluation were oxygen recombination rates, negative precharge adjustment, and the quantity of electrolyte permissible.

General Electric determined that a heat treatment increased the wettability characteristic of polypropylene separator material. They modified their cell manufacturing process sequence to take advantage of this characteristic. A special heat treatment process consisting of subjecting the cells to a temperature of 125°C for 20 hr was added during the final stages of assembly and test.

Following the heat treatment, the cells were overcharged and the final electrolyte quantity adjustment made. The negative precharge adjustment was then made and the cells were prepared for final acceptance testing. An additional benefit was obtained from the heat treatment process. It was found that the allowable quantity of electrolyte was increased by 1.5 to 2 ccs.

The effects of sterilization were evaluated for the following cell conditions: (1) discharged and shorted, (2) open circuit discharged, and (3) charged. Sterilization of charged cells was eliminated due to the large loss in capacity and physical damage to the plates. Eagle Picher reported a 15 to 20% loss in capacity when cells were sterilized in the discharged shorted condition. Little or no capacity loss was experienced when each cell was totally discharged with a one-ohm load per cell for 24 hr and then sterilized in an open circuit condition. In some cases, a small increase in capacity was obtained after sterilization. This increase was partially attributed to the reconditioning (deep discharge) before sterilization. The cells exhibited an elevated charge voltage profile during the first charge after sterilization. Early charging was done at a C/15 rate to prevent excessively high voltages. The charge rate was increased to a C/10 rate as the cell design parameters (i.e., electrolyte quantity and precharge level) were developed. The

high voltage condition after sterilization was attributed to changes in the electrolyte distribution, which were caused by the high temperatures. Cycling gradually corrected this condition and the cell performance reverted to normal.

Based on the vendor test results, the deep discharge open circuit condition was selected for the battery sterilization procedures.

B. PROTOTYPE CELL AND BATTERY TEST PROGRAM

The cells that were delivered by each vendor were placed in a prototype cell and battery evaluation program. Test plans are summarized in Figures V-1 and V-2. The basic goals of the test program were as follows:

1) Evaluate vendor designs and select a supplier for the subsequent production build;
2) Determine procedures and techniques necessary to sterilize nickel-cadmium cells and batteries;
3) Determine performance characteristics before and after sterilization;
4) Determine capability of cells to survive dynamic environmental exposures;
5) Evaluate capability of cells to accept float (trickle) charging at low rates;
6) Determine thermal characteristics;
7) Determine capability for providing 200 50% depth-of-discharge cycles at both 4.4 and 26.7°C; and
8) Evaluate prototype battery design during exposure to sterilization and dynamic environments.

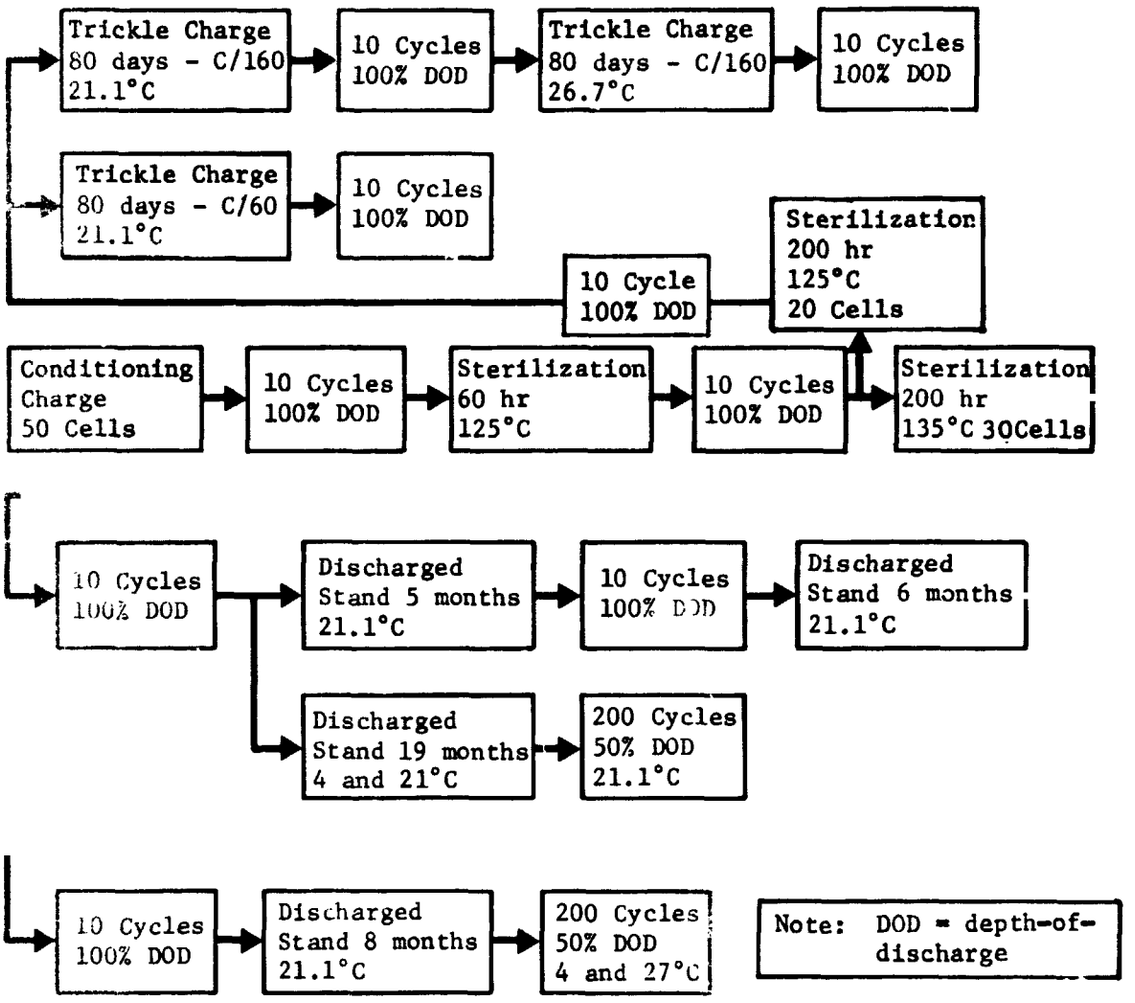

Figure V-1 Prototype Cell Test Plan

The following paragraphs summarize the significant results of this program.

1. Eagle Picher Cell Evaluation

The Eagle Picher prototype cell experienced high end-of-charge voltages and pressure buildup. The cell specification required that the cells must be capable of accepting charge at a C/10 rate for 16 hr before sterilization; however, the cell voltages increased rapidly in the 11.5- to 12.5 hr time range to greater

than 1.5 V. Cell cases began to bulge and pressures exceeded the capability of the pressure gages (1.1 MPa). Vendor tests showed that the actual pressure was in the range of 4.1 MPa (600 psig). This pressure decayed to zero during the subsequent open circuit stand (24 to 48 hr).

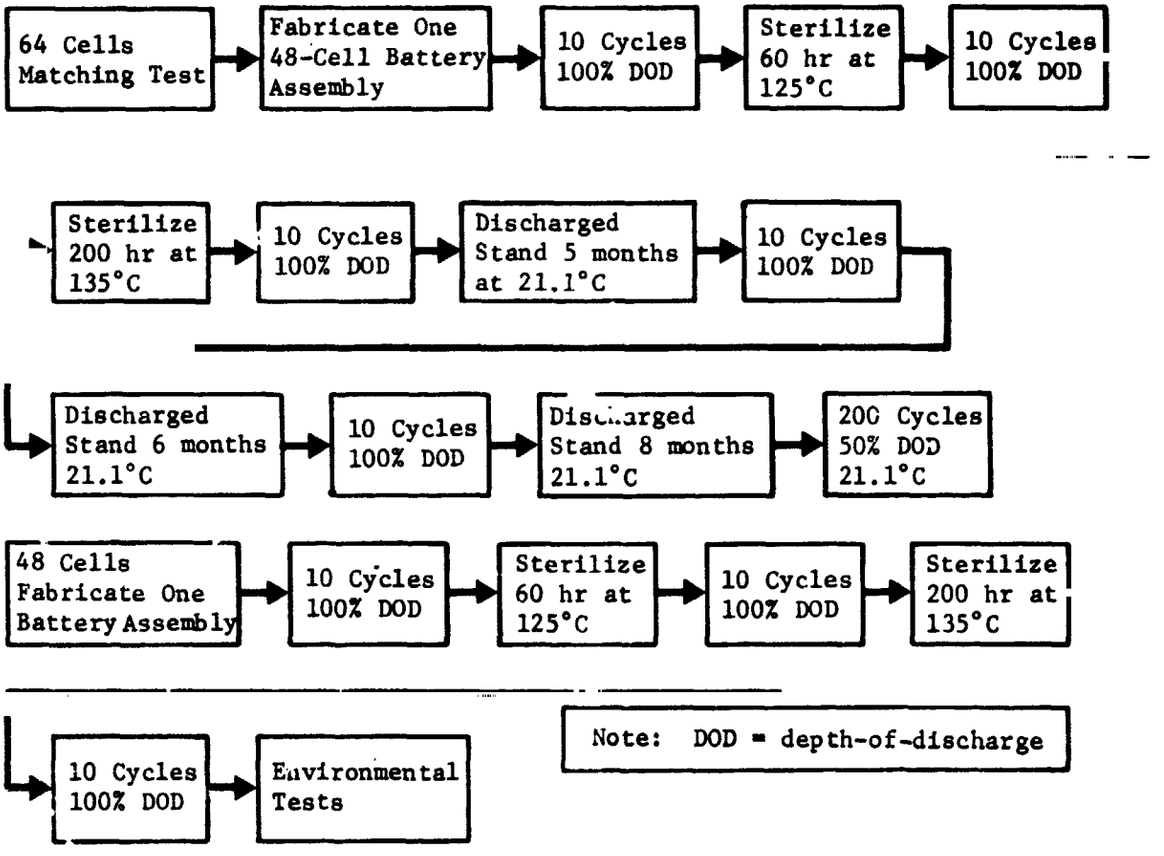

Figure V-2 Prototype Battery Test Plan

The pressure decay indicated that oxygen was the gas generated and over a period of time the gas recombined at the negative plates. The fact that the oxygen did not recombine rapidly was attributed to too much electrolyte in the cells. This conclusion was also supported by the high voltage at the end-of-charge which is typical of flooded vented cells where the cadmium electrode is reaching full charge.

The cells were subjected to the 60-hr sterilization at 125°C and then charged to determine if sterilization had any effect on the end-of-charge voltage and oxygen recombination rate. The charge after sterilization was terminated early due to high voltages. It was decided to continue with the 200-hr sterilization at 135°C to determine if the additional high temperature exposure would facilitate improved electrolyte absorption and distribution and would improve oxygen recombination. This additional exposure failed to improve the cell performance. At this point the Eagle Picher cell testing was terminated until new cells could be fabricated with less electrolyte.

Concurrent with the cell testing, two prototype battery assemblies were fabricated using the Eagle Picher cells. One battery assembly was scheduled for sterilization followed by dynamic environmental testing. The other was placed in electrical characterization, sterilization, and life test program.

The sterilization portion of the test program was completed but the following problems were noted.

1) The battery assembly base plate warped during exposure to heat. This problem will be discussed in subsequent paragraphs in this section;
2) Similar problems with high pressures and voltages at the end-of-charge were experienced with the batteries as with the cells.

As a result of these problems, the Eagle Picher cell evaluation was terminated and the prototype test program continued with only the General Electric cells. Eagle Picher continued an in-house development effort on the nickel-cadmium cell to provide a second source for the Viking program. Additional cells were fabricated and tested by Eagle Picher to determine an optimum quantity of electrolyte and to eliminate the pressure problems. This effort was successfully concluded by Eagle Picher and they were designated as a second source for the battery cells.

2. General Electric Cell Evaluation

One significant anomaly was identified during the electrical cycling and sterilization testing of General Electric prototype cells. After the 200-hr sterilization at 135°C, one cell exhibited high voltage immediately upon start-of-charge. The cell performed normally before and after sterilization for 60 hr at 125°C. The high voltage during charge indicated an increase in internal cell impedance which suggested an abnormal internal cell dryness. A chemical leak check confirmed that the cell had experienced no electrolyte leakage.

The cell was returned to General Electric to determine the nature of the problem. A small hole was drilled near to the top of the cell and a small quantity of electrolyte was introduced. Subsequent electrical performance of the cell was normal. This confirmed that the quantity of electrolyte of this cell was marginal.

General Electric conducted an electrolyte quantity investigation of all cells that had been delivered. A comparison was made of dry cell weight and wet cell weight to determine electrolyte quantity. Fourteen cells were identified as having a low electrolyte quantity; however, of the 14 cells only one exhibited any abnormal characteristics during testing at Martin Marietta.

The cause for the low electrolyte quantity was traced to a procedure in which the electrolyte quantity is either added or removed to adjust the operating pressure to a nominal 137.9 kPa (20 psig) during overcharge. In this case, too much electrolyte was removed. As a result of this investigation, the minimum allowable electrolyte quantity was set at 27.93 grams of 34% KOH. Cells with less than 27.93 grams were to be rejected.

3. Electrical Characteristics

In addition to the sterilization, trickle charge and life tests were performed to further characterize the prototype cell electrical performance at various charge and discharge rates over the predicted

temperature range. Cell voltages during charge and discharge (see figs. V-3 and V-4) represent the results of testing 188 prototype cells that were sterilized and then subjected to the tests. Testing was performed in temperature controlled ($\pm 1.1^{\circ}C$) test chambers. Figures V-5, V-6, and V-7 show the variation of the cell discharge voltages as a function of the load current for temperatures of 10, 21.1 and $26.7^{\circ}C$. Data were obtained for cell depth-of-discharges ranging from 0 to 90%. This datum was obtained by discharging four cells at a C/2 rate and every 10 min interrupting the discharge and applying 5 sec pulse loads of 2, 4, 6, 8, and 10 A.

An effective series resistance was calculated based on the following equation:

$$ESR = \frac{VOC - VL}{10\ A}$$

where

VOC was the cell open circuit voltage.

VL was the cell voltage at a 10 A load.

The ESR was found to be nearly constant at 0.005 ohms up to 80% depth-of-discharge and also only slightly dependent on temperature.

The main objective of the electrical characterization tests was to establish the end-of-charge voltage versus temperature cutoff criteria over a temperature range from 4 to $32^{\circ}C$. These data were obtained by subjecting two 24-cell prototype batteries to a series of charge-discharge cycles using an end-of-charge voltage that varied from 33.5 to 36.8 V. Data were obtained at 10 different voltages over this range. Charging was performed at C/40, C/15, C/10, C/7.2, and C/5.3) for each of the 10 end of charge voltage limits. A C/2 discharge to a end-of-discharge voltage of 27 V was used to determine the state of charge achieved for each test condition. The end-of-charge voltage versus temperature criteria is shown in Figure V-8 for a charge rate between C/10 and C/7.5.

4. Trickle Charging

Trickle charging was proposed for the time during Mars orbital operation when the batteries must be maintained in a charged condition. Thus, the effects of trickel charging on cell capacity were evaluated.

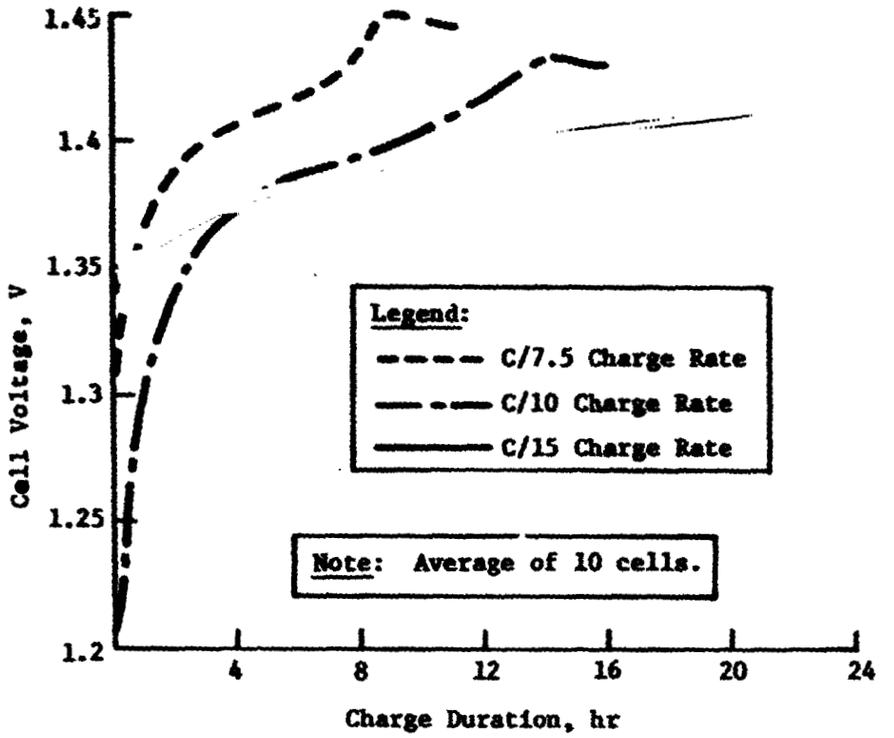

Figure V-3
Typical Cell Charge Voltage Characteristics at 21.1°C for C/15, C/10, and C/7.5 Charge Rates

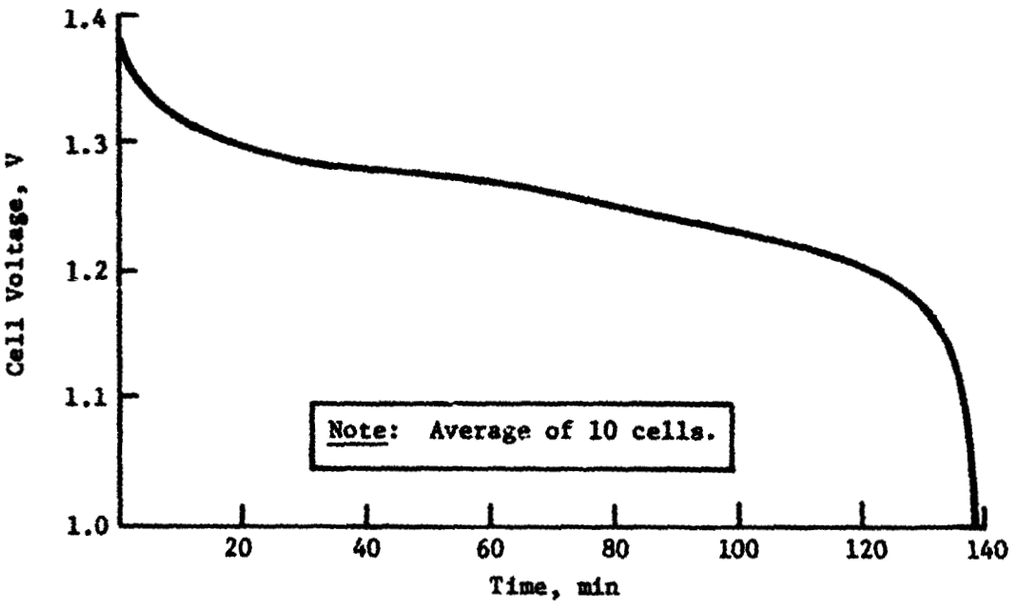

Figure V-4
Typical Discharge Voltage Characteristic for a C/2 Discharge at 21.1°C

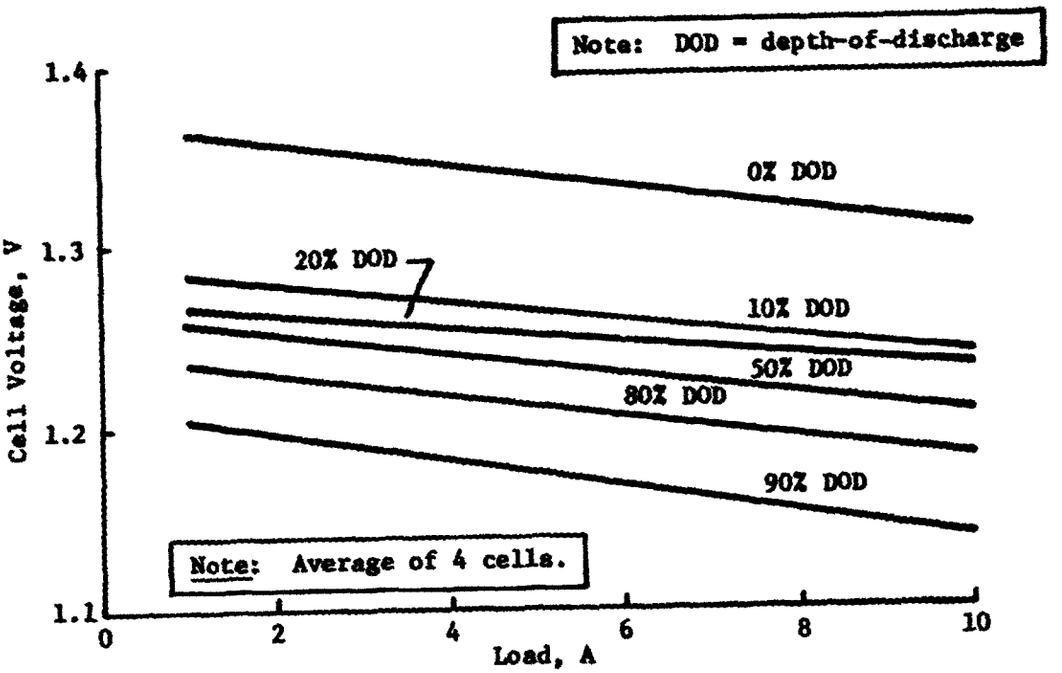

Figure V-5
Cell Voltage as a Function of Load Current at 26.7°C

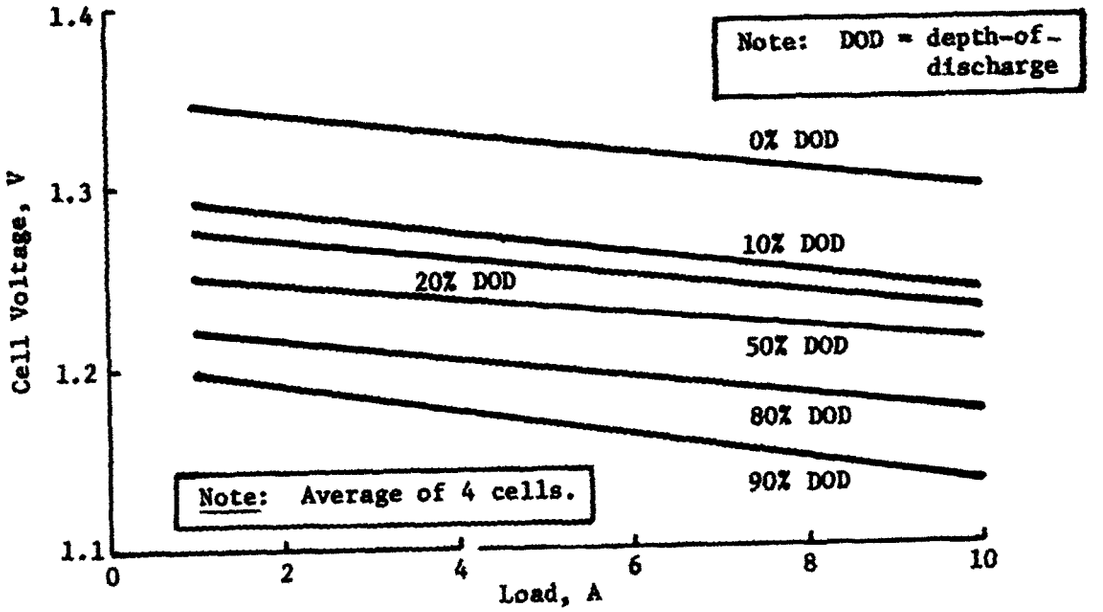

Figure V-6
Cell Voltage as a Function of Load Current at 21.1°C

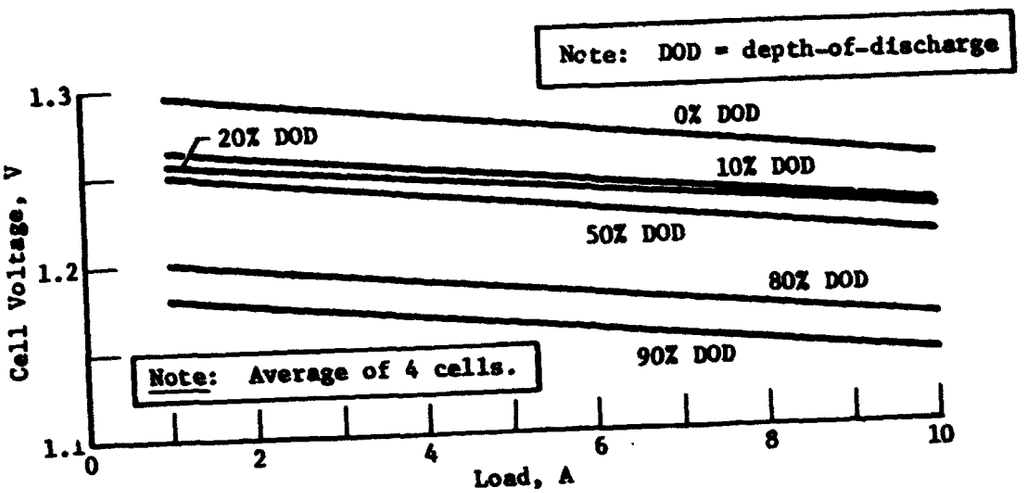

Figure V-7
Cell Voltage as a Function of Load Current at 10°C

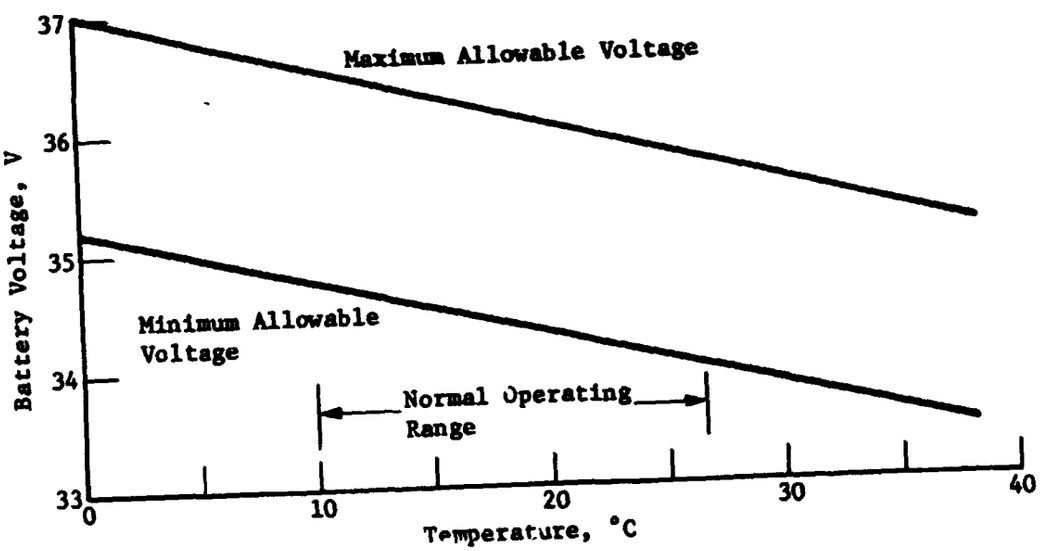

Figure V-8
Battery End-of-Charge Voltage Limits for a C/10 to C/7.5 Charge Rate

The primary concern with the trickle charge mode-of-operation was the loss in available capacity due to a depressed voltage (second plateau) during discharge. Since the batteries must be capable of supplying energy to a 75% depth-of-discharge during the entry and landing phase, the loss in capacity due to extended periods of float charging was a major concern in predicting the available energy.

Trickle charging at rates between C/60 and C/40 had been evaluated by the aerospace industry to support synchronous orbit operations; however, the inability to reject large amounts of heat from the interior of the Lander prohibited the use of these rates and led to the selection of a much lower C/160 trickle charge rate.

Two groups of cells were placed on trickle charging after being charged and discharged to determine their initial characteristics. The two sets of cells were tested as follows:

Set 1, Test A) 10 cells at (21.1°C), C/160 (50 mA) charge rate;

Set 2, Test A) 10 cells at (26.7°C), C/160 (50 mA) charge rate;

Set 1, Test B) 10 cells at (21.1°C), C/60 (130 mA) charge rate.

Test B for the first set of cells was performed after Test A. The test duration was set at 80 days. This was based on 50 days in Mars orbit and 30 days before Mars orbit insertion. At the completion of each of the trickle charging tests, the cells were discharged to 1.16 V per cell (Lander lower bus voltage limit) to determine the amount of available capacity. Several cycles of C/10 charge for 16 hr followed by a C/2 discharge to approximately 1.16 V were performed to identify changes in the cell characteristics. The cells in Test A were discharged to 0.6 V on the sixth cycle after trickle charge testing to determine if a second plateau existed and to recondition the cells.

Individual cell voltages were measured near the end of each of the trickle charges to determine the spread in voltage among

each group of 10 cells. These data are shown in Table V-1. These data show that the comparable cell voltages were obtained from the C/60 and C/160 trickle charge tests at the 21.1°C test temperature. The average cell voltage at the 26.7°C float temperature was 0.03 V lower than the test data obtained from the 21.1°C test.

Typical charge-discharge curves are shown in Figures V-9 through V-14 to illustrate how the cell electrical characteristics changed as a result of the trickle charge for 80 days. The charge voltage data in Figure V-9 show a five-millivolt reduction in voltage after the trickle charging as compared to the prefloat test data. The discharge curves in Figure V-10 show approximately a 20-mV reduction in discharge voltage for the first discharge after the float charging. However, the third discharge after float shows that the voltage recovered to the prefloat level for the first half of the discharge duration and then exhibited a lower voltage characteristic for the remainder of the discharge. This discharge was continued down to a cell voltage of 0.6 V to recondition them and to identify the extent of the second plateau. The cells exhibited an increase in both ampere-hour capacity and discharge voltage after the reconditioning discharge. Approximately one ampere-hour of additional capacity was obtained. The cell voltage increased by approximately five millivolts over the prefloat test level and by 10 to 15 mV above the voltage on discharge immediately after float. The charge voltage data in Figure V-9 show a corresponding increase in charge time before the overcharge condition was reached for the charges after reconditioning.

The initial discharge after the float period for the 26.7°C test (Fig. V-11) at a C/160 rate provided a capacity of 11 A-h. Subsequent discharges provided only 10.4 and 10.1 A-h. The first discharge was at a depressed voltage which recovered on subsequent discharges. During the first charge after float (Fig. V-12), the cells exhibited a reduced voltage profile; however, the subsequent charges were typical of nickel-cadmium cells. The capacity after the float test was comparable to the capacity obtained from the cells after the reconditioning that was performed as a part of the 21.1°C test.

Table V-1 Cell Voltages at the Trickle Charging, 80 Days

Cell No.	C/160 at 21.1°C Volts	C/160 Charge at 26.1°C Volts	C/60 Charge at 21.1°C Volts
1	1.377	1.366	1.415
2	1.367	1.365	1.409
3	1.404	1.366	1.415
4	1.407	1.364	1.406
5	1.406	1.365	1.386
6	1.408	1.366	1.381
7	1.405	1.366	1.353
8	1.406	1.352	1.406
9	1.406	1.366	1.423
10	1.373	1.366	——
Average	1.396	1.364	1.399

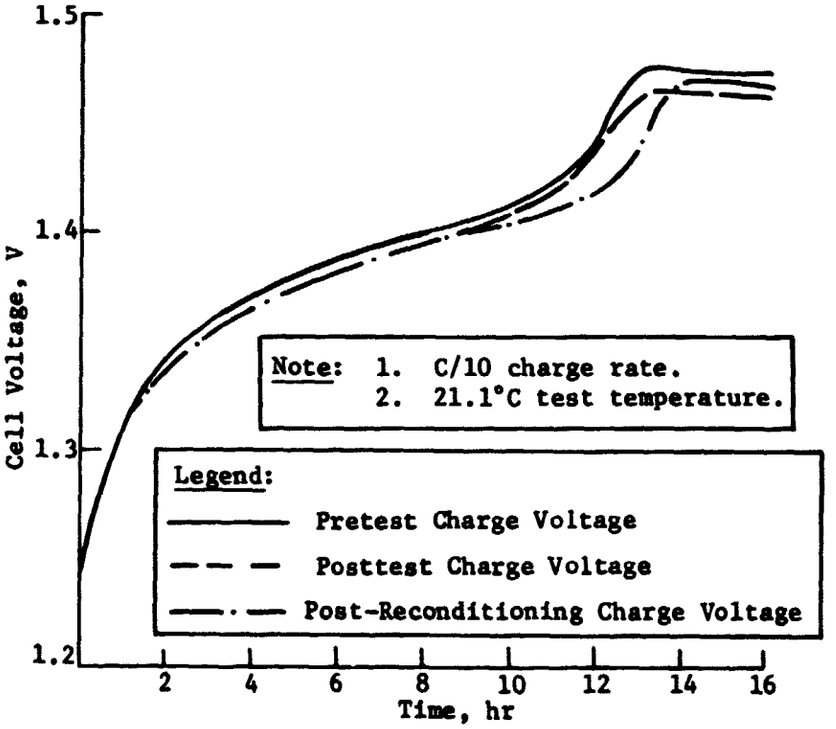

Figure V-9 Cell Charge Voltage Profiles during Trickle Charge

The (C/60) trickle charge test (Fig. V-13) produced the largest capacity (11.5 A-h) during the first discharge after trickel charging; however, the C/60 test at 26.7°C provided a slightly lower capacity with a lower discharge voltage. The increased capacity was attributed to the reconditioning performed on the cells before the start of the C/60 float test.

It was concluded as a result of these tests, that the C/160 trickle charge rate was adequate to keep the batteries fully charged over a temperature range of 21.6 to 26.7°C.

5. Cell Sterilization

As shown in Figure V-1, sterilization tests at the cell level were performed in two steps. The initial test was performed on 50 cells at 125°C for 60 hr. Following the heat exposure, the cells were charged and discharged for 10 cycles using a 100% depth-of-discharge (discharge terminated at a cell voltage of 1.0 V) to identify any changes to the cell characteristics and to determine if the changes were permanent or subject to changes by cycling. Following the 60-hr heat exposure, the cells were divided into groups of 20 and 30 cells. The 20-cell group was sterilized for 200 hr at 125°C. The 30-cell group was sterilized for 200 hr at 135°C. After sterilization, the cells were again cycled ten times using a C/10 charge rate for 16 hr and a C/2 discharge rate to a cell voltage of 1.0 V. Figure V-15 contains the charge voltage profile for the pre-sterilization charge and the charge after each of the sterilizations. Figure V-16 shows similar data for the discharges. These data show some loss in capability to accept a charge as shown by the reduction in time required to reach an overcharge condition An increase in voltage, especially at the end-of-charge also indicated that the cell impedance had increased. A gradual recovery from the high voltage conditions was evident after repeated cycling which suggested that the problem may have been caused by a change to the electrolyte distribution which was corrected by cycling the cells.

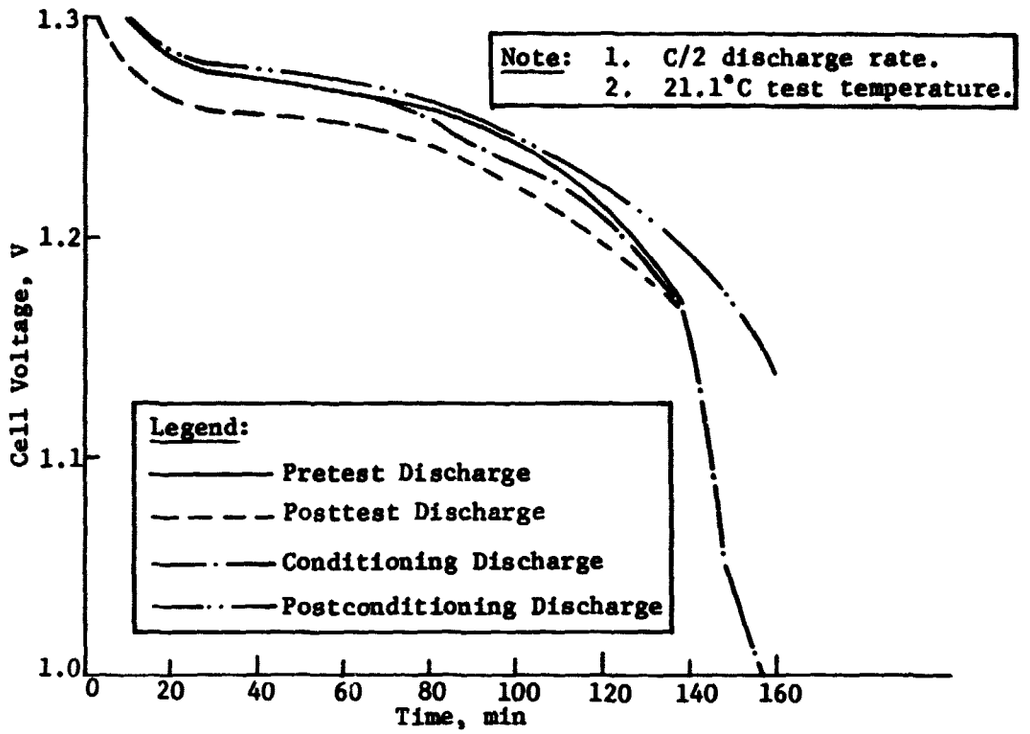

Figure V-10 Cell Discharge Voltage Profiles during Trickle Charge

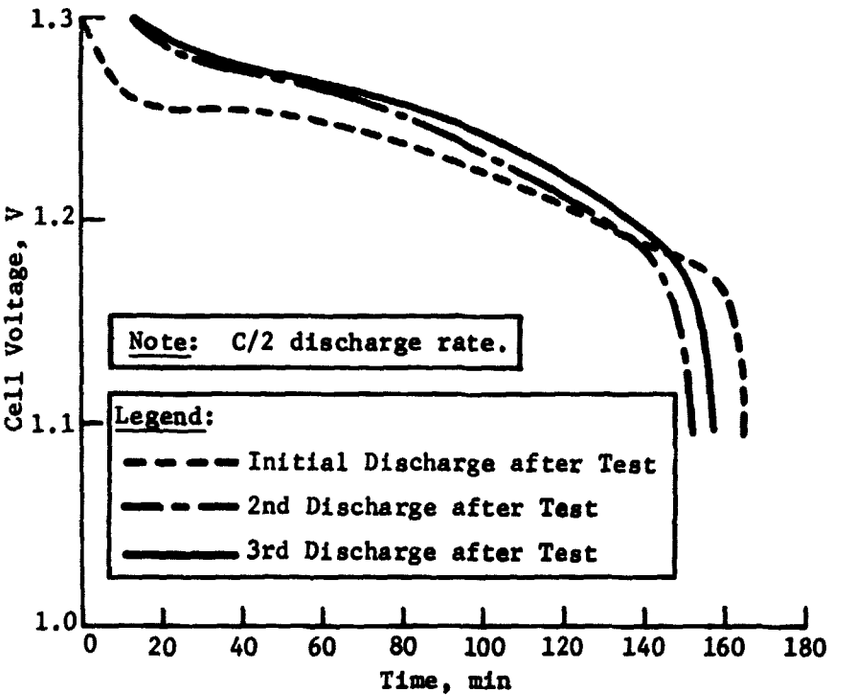

Figure V-11
Cell Discharge Voltage Profiles after C/160 Trickle Charge at 26.7°C

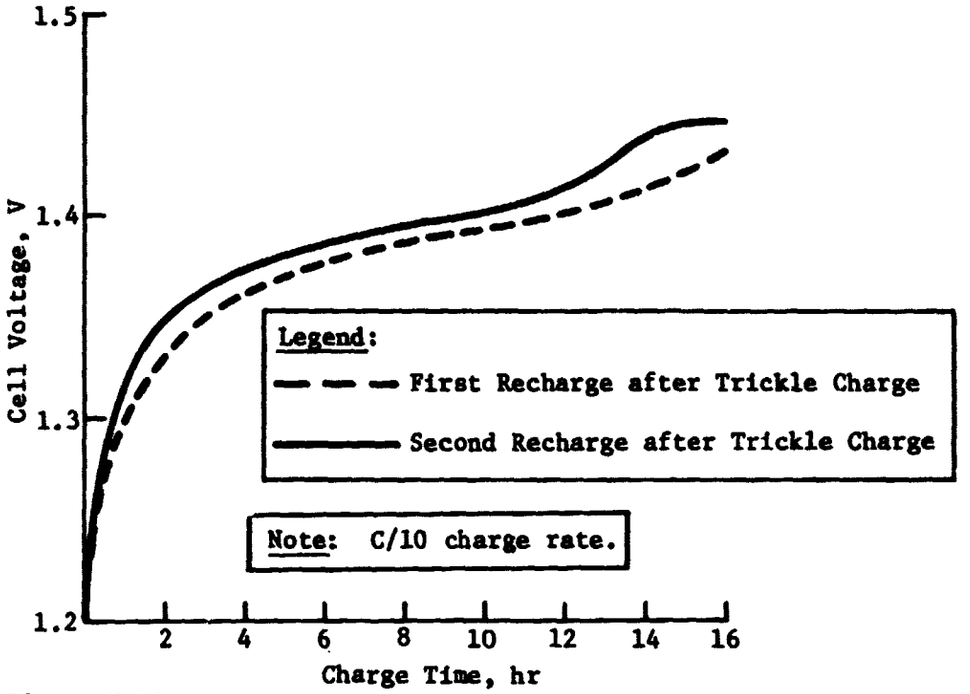

Figure V-12
Cell Charge Voltage Profiles after C/160 Trickle Charge Test at 26.7°C

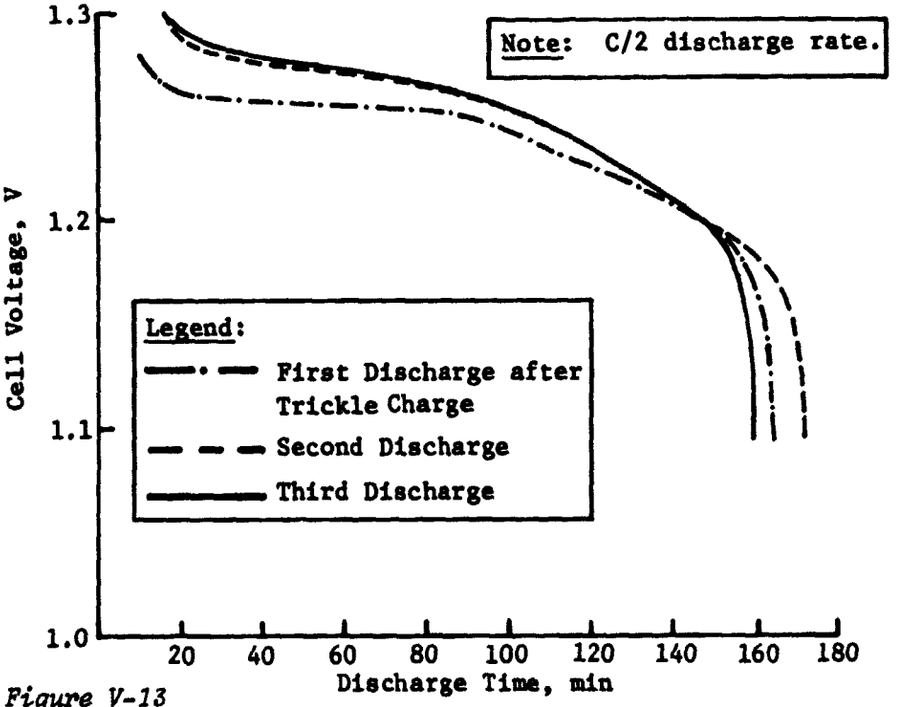

Figure V-13
Cell Discharge Voltage Profiles after C/60 Trickle Charge Test at 21.1°C

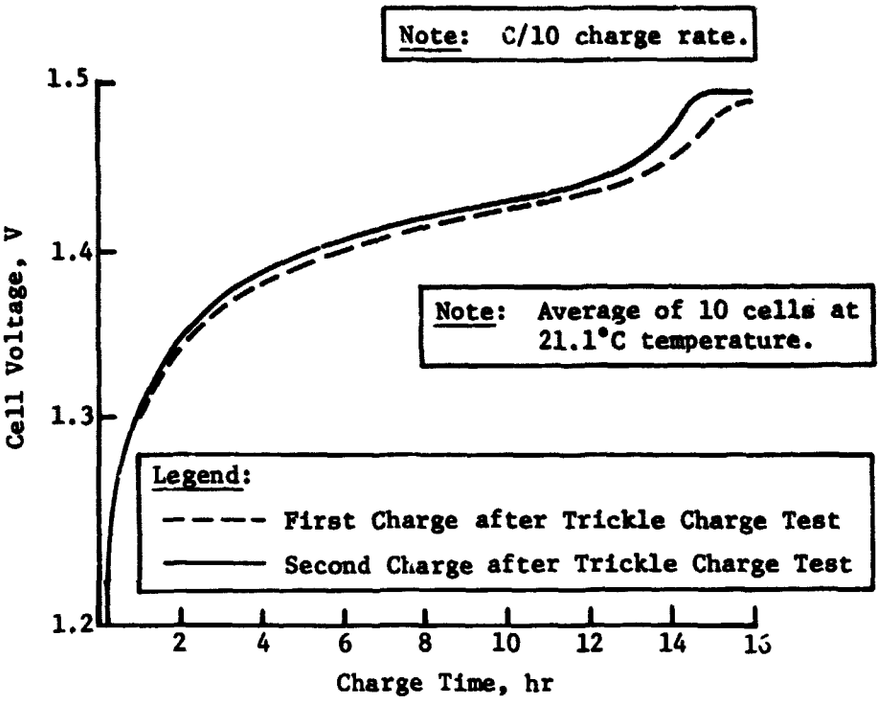

Figure V-14
Recharge Voltage Profile after C/60 Trickle Charge Test at 21.1°C

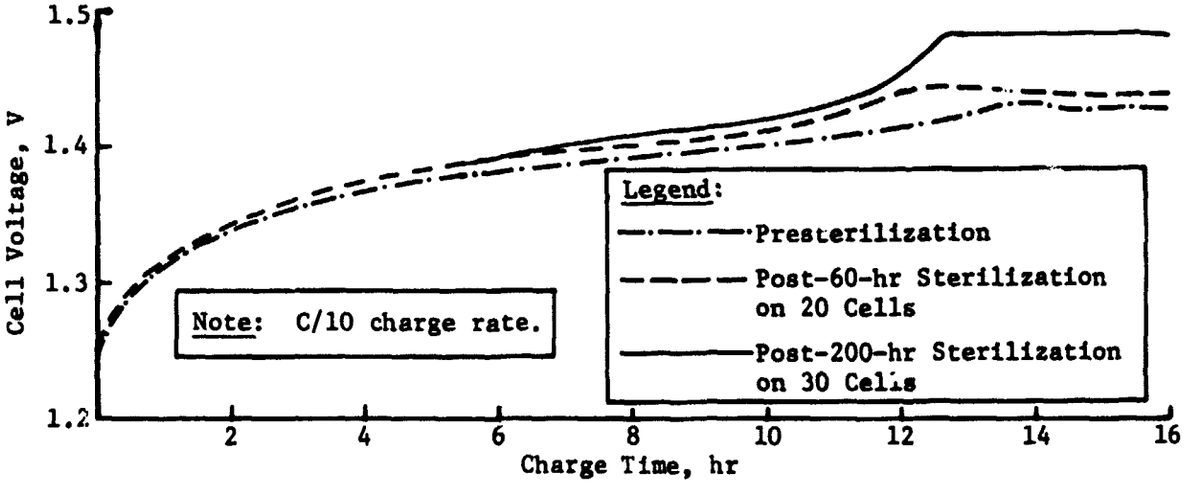

Figure V-15
Cell Charge Voltage Characteristics before and after Sterilization at 135°C

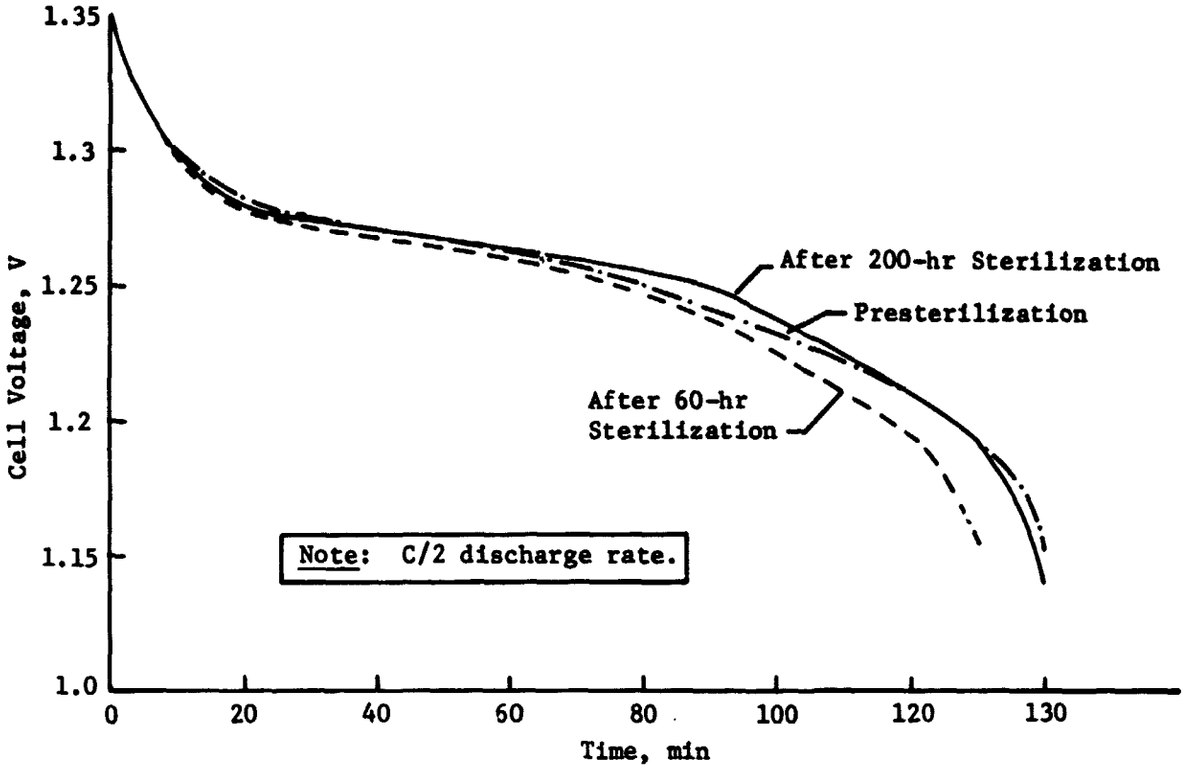

Figure V-16
Cell Discharge Voltage Characteristics before and after 60 and 200 hr of Sterilization

The conclusion reached as a result of the cell sterilization t ·ts, was that no significant degradation in capacity was induced as a result of the 260 hr of exposure to the high temperatures. Temporary increases in voltage during charge were produced; however, these voltages decreased gradually after cycling.

It was concluded that the original restriction to a low rate (C/15) conditioning charge applied only after the cells had been allowed to stand in an inactive discharged condition for a long period of time. A C/10 charge rate could be used immediately after sterilization.

The results of these tests, which included sterilization durations far in excess of that required for the flight hardware, proved that sealed nickel-cadmium cells built with polypropylene separators would meet the Viking program sterilization and performance requirements.

6. Battery Sterilization

Both the General Electric and Eagle Picher batteries were subjected to sterilization tests to evaluate the battery design and materials. Figures V-17 and V-18 show the battery electrical characteristics before and after sterilization. As shown in Figure V-17, there is a significant increase in the cell voltage during charging as compared to the presterilization charge data. This same characteristic was noted during the cell sterilization tests. This phenomenon tends to diminish as additional charge/discharge cycles are accumulated on the cell during subsequent testing.

The Eagle Picher battery exhibited an abnormally high voltage after only 10 of the 16 hr programmed for charge during the first charge after the 60-hr sterilization at 125°C (see Fig. V-19). Further testing on this battery was terminated because excessive cell pressure was generated during charge. This resulted in bulging cases and deformed covers.

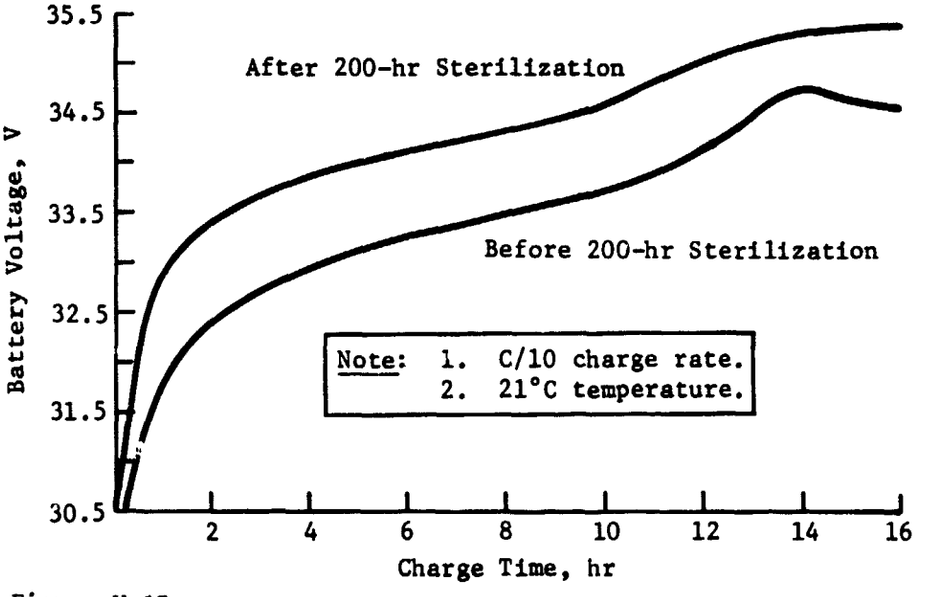

Figure V-17
Battery Charge Voltage Characteristics before and after 200 hr of Sterilization at 135°C (General Electric Battery)

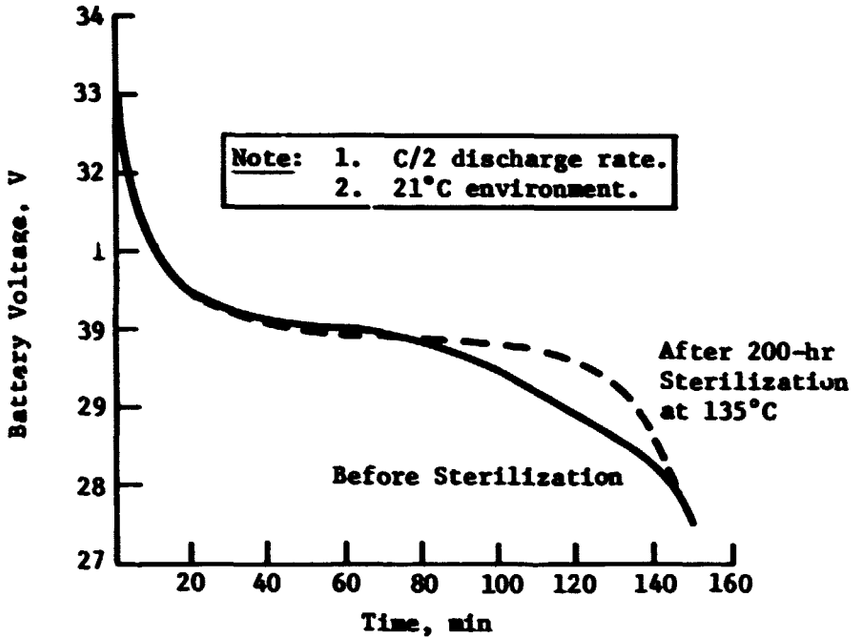

Figure V-18
Battery Discharge Characteristics before and after Sterilization for 200 hr at 135°C (General Electric Battery)

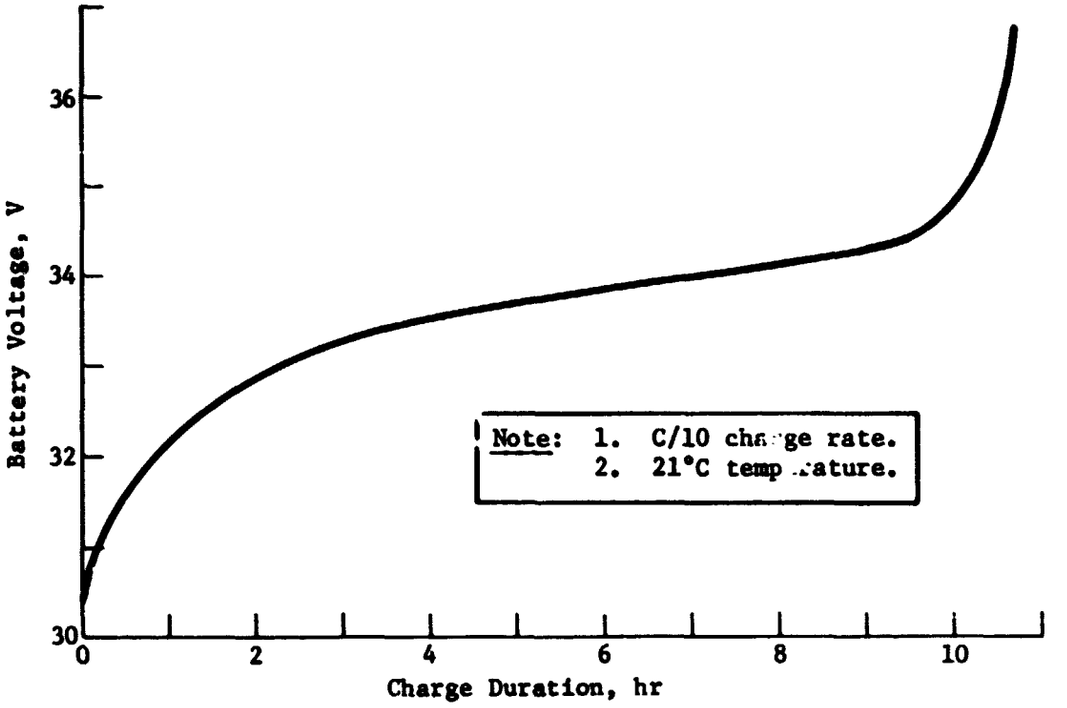

Figure V-19

Charge Voltage Characteristic for Eagle Picher Battery after 60-hr Sterilization at 125°C

7. Thermal Efficiency Tests

The design and material changes, such as the use of polypropylant separator material and the limited electrolyte quantity, that were made to accommodate the heat sterilization requirements of the Viking program resulted in changes to the cell electrical characteristics and efficiencies as compared to conventional sealed nickel-cadmium cells. The heat rejection capabilities of the proposed battery design and the Lander structure were limited; therefore, an accurate assessment of the heat losses produced during charge and discharge operations was required to provide the capability to accurately predict the battery and Lander temperatures. A test program was initiated to evaluate the instantaneous charge and discharge thermal output and hence thermal and electrical efficiency over a range of temperatures and charge rates. Table V-2 summarizes the various charge rates and temperatures for the test program.

Table V-2 Test Conditions for Thermal Efficiency Tests

Test No.	Temperature, °C	Charge Rate	Charge Duration, hr	End-of-Charge Voltage, Vdc	Discharge Rate
1	32.2	C/7.5	9:58	1.430	C/2
2	32.2	C/10	16:22	1.431	C/2
3	32.2	C/15	30:07	1.418	C/2
4	26.7	C/7.5	10:00	1.428	C/22
5	26.7	C/10	16:05	1.469	C/2
6	26.7	C/15	30:14	1:441	C/2
7	18.3	C/7.5	10:05	1.482	C/2
8	18.3	C/10	16:21	1.489	C/10
9	18.3	C/15	29:59	1.472	C/2

The method selected for performing the thermal efficiency tests differs from the conventional calorimetric approach. Instead of allowing the cell temperature to vary during the test (introducing a variation in efficiency), the test method used maintains the cell temperature to within ±1°C by varying the rate at which heat is removed or added to the cell during the test. The resulting data are then independent of temperature changes and represent efficiencies for a particular test temperature throughout the charge-discharge cycle.

The data obtained are not typical of the usual performance conditions a nickel-cadmium battery is subjected to. These data are useful in predicting the operating efficiency if the temperature and approximate state-of-charge is known. These data were used to develop a thermal model of the battery which was used in a computer program to predict the Lander temperatures for the various operational modes.

Figure V-20 shows the test configuration which illustrates how the heat flow was measured during the charge-discharge phases. The tests were performed in a vacuum of 10^{-7} torr to minimize conduction losses.

Heat flow to or from the test cell was measured using heat flux sensors which were calibrated in btu ft^2 -hr. Data were recorded on strip-chart recorders and time correlated to the charge and discharge phases to facilitate relating the measured heat loss to the state-of-charge of the cell.

The system was calibrated by supplying a known quantity of heat to the cell and measuring the heat flow through the flux sensors while maintaining the cell temperature constant. Accuracies of 4% in efficiency were obtained during the testing.

During the charge phase, oxygen is produced at the positive electrode. When this oxygen reaches the negative electrode it eventually chemically recombines with the cadmium metal producing $Cd(OH)_2$ and heat. The oxygen recombination reaction continues after the charge has been terminated due to residual oxygen gas in the cell. During the thermal efficiency

testing, a period of time was allocated after the charging was completed to measure the heat produced by the oxygen recombination reaction and the heat stored in the cell mass. This quantity of heat was added to the losses during charging for calculating the charge efficiency.

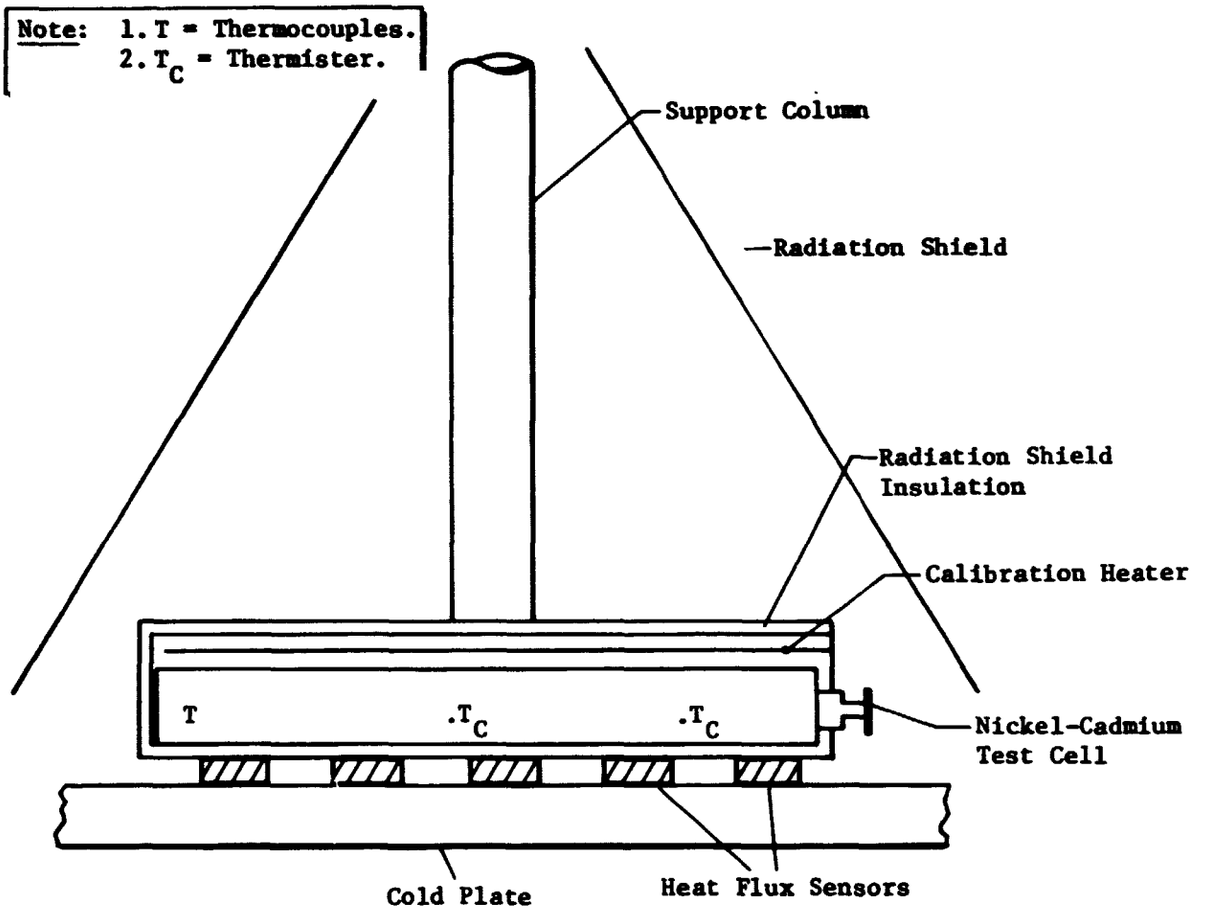

Figure V-20 Thermal Efficiency Test Configuration

The data shown in Figures V-21 through V-24 are examples of the relationship between the heat losses and the cell voltage during the charge and discharge tests. These data include heat losses for charge rates of C/7.5, C/10, and C/15. Tests at each of the charge rates were performed at three temperatures (18.3, 26.7, and 32.2°C). The discharges were performed at C/2 and C/10 rates. Only one discharge figure was included due to similarity of discharge data at the three temperatures. These data were used to predict battery losses and temperature profile during charge and discharge.

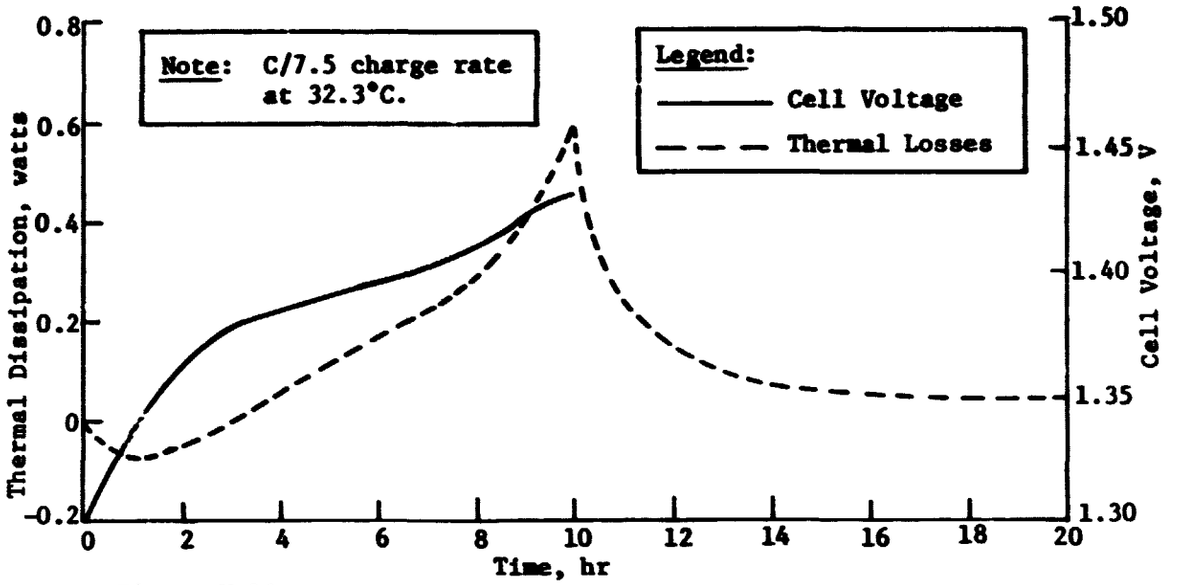

Figure V-21
Cell Voltage and Thermal Losses during Charge at C/7.5 Rate

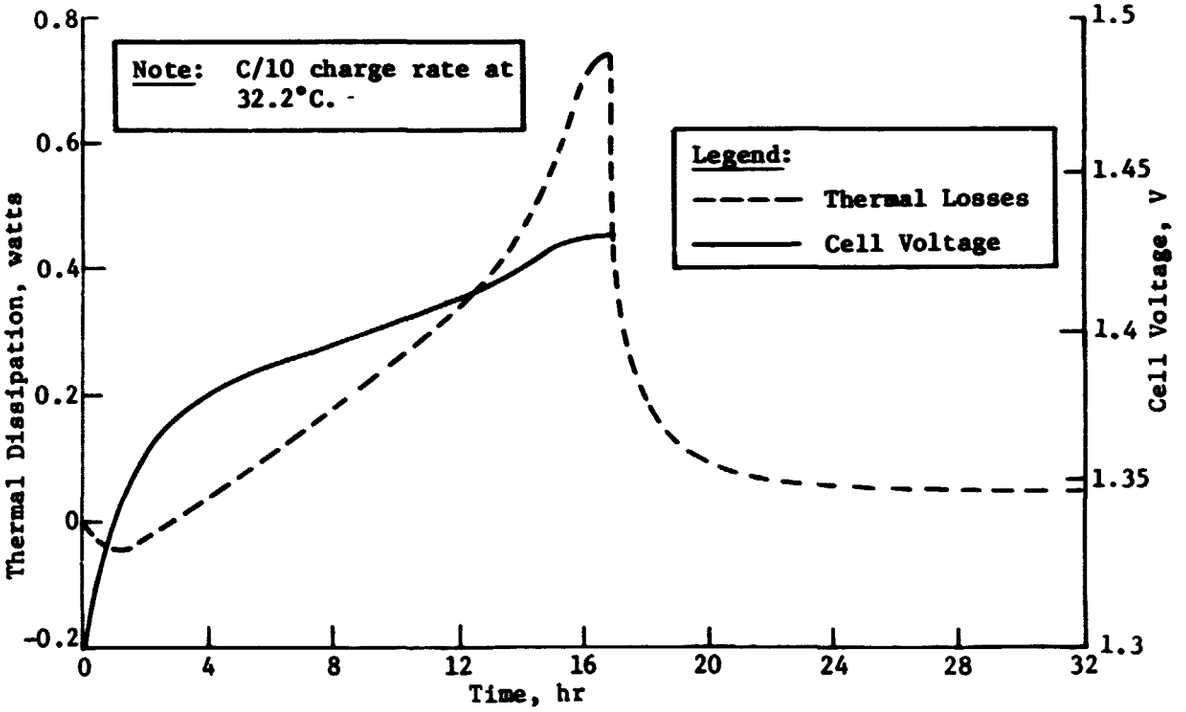

Figure V-22
Cell Voltage and Thermal Losses during Charge at a C/10 Rate

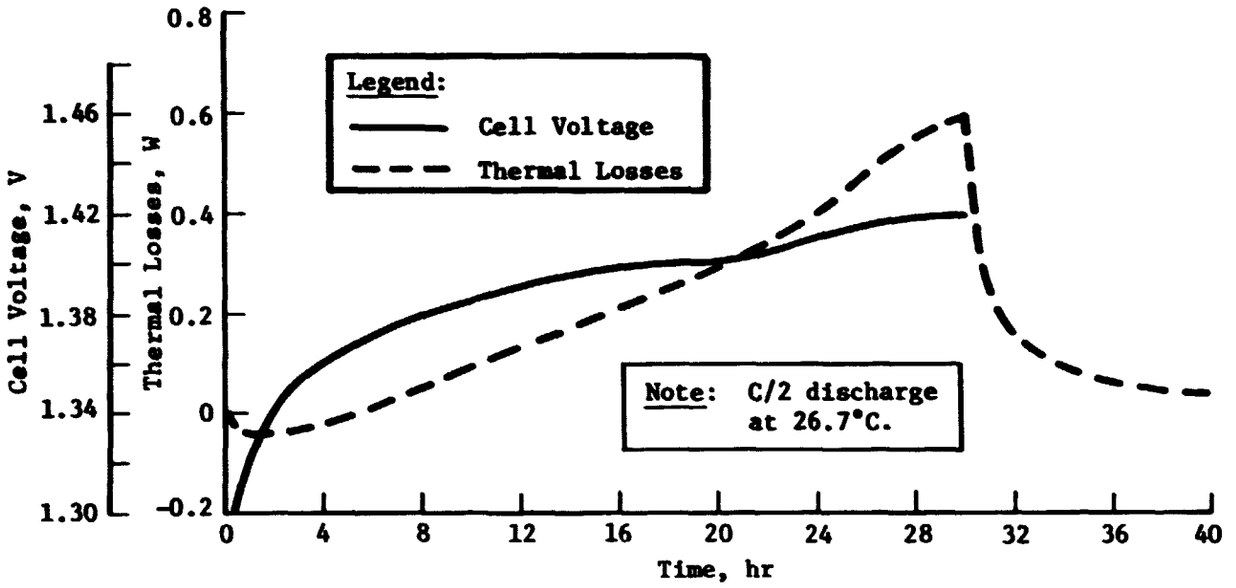

Figure V-23 Cell Voltage and Thermal Losses during Charge at C/15 Rate

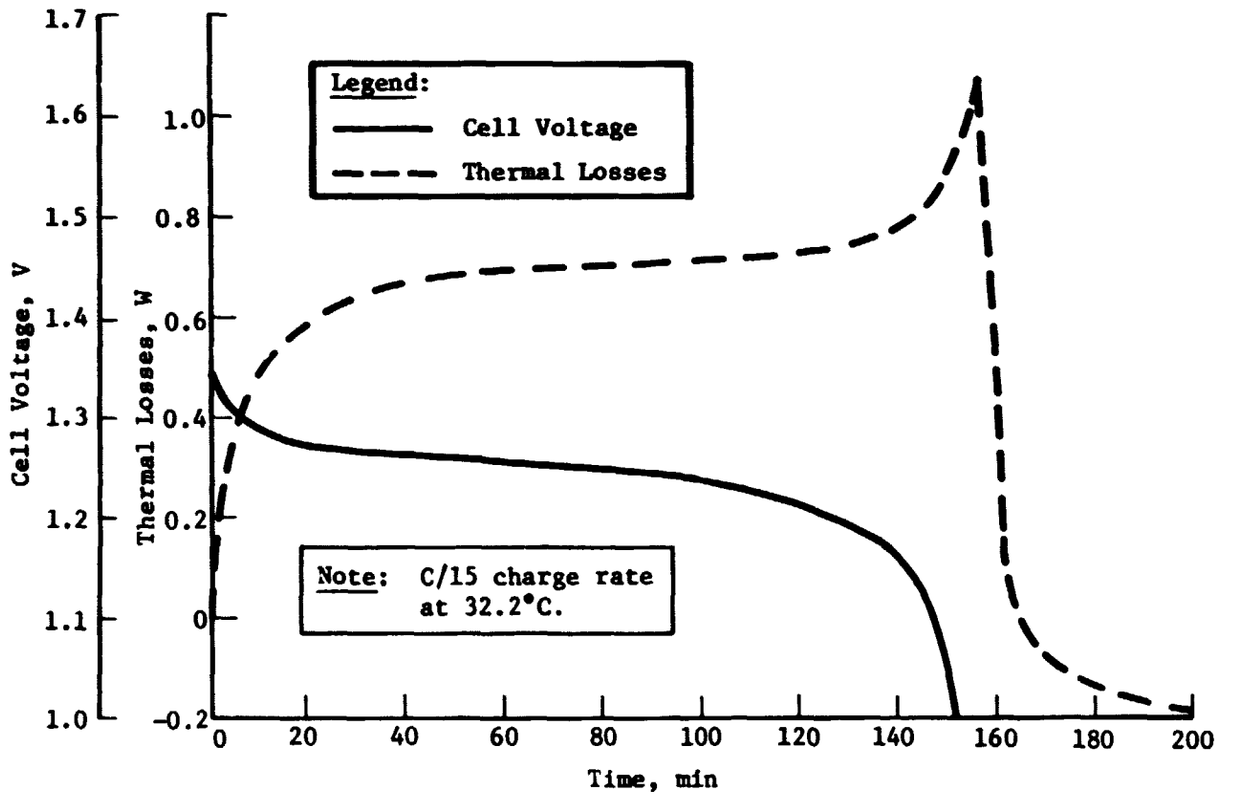

Figure V-24 Cell Voltage and Thermal Losses during Discharge at a C/2 Rate

Figures V-25 through V-27 illustrate how the thermal losses vary for several test temperatures and each of the fixed charge rates.

The computed instantaneous watt-hour charge and discharge efficiencies for each of the three charge rates are shown in Figures V-28 through V-30. Only one discharge watt-hour efficiency curve was shown for each figure since the test results showed that the discharge efficiencies varied by only 3% and most of the variation was at depths-of-discharge over 75%.

The efficiency data shown in Figures V-28 through V-30 exceed 100% for a significant portion of the charge period. This is due to the endothermic reaction of the cells during charge when heat is absorbed from the surroundings. The heat flux sensors measured this heat absorption during charge and as long as the net heat flow is negative (heat flow into the cell) the instantaneous W-H efficiency shows a value greater than 100%. As soon as the internal losses exceed the endothermic reaction, the instantaneous watt-hour efficiency will fall below 100%. In the equation shown below, the value of W_L is negative during the endothermic portion of the charge since heat is being absorbed by the cell instead of being rejected.

$$\eta_{c(W-h)} = \frac{W_c - W_L}{W_c} \times 100$$

and

$\eta_{c(W-h)}$ is the watt-hour charge efficiency in percent.

W_c is the watt-hours supplied during charge.

W_L is the watt-hours dissipated or absorbed during charge.

8. Cell Environmental Testing

Four of the General Electric prototype cells were subjected to dynamic environmental tests to evaluate their capability to function in the predicted environments. The three classes of tests performed were shock, sine vibration, and random vibration. The shock tests consisted of both a pyrotechnic induced shock and a Mars landing simulated shock. The shock frequency response

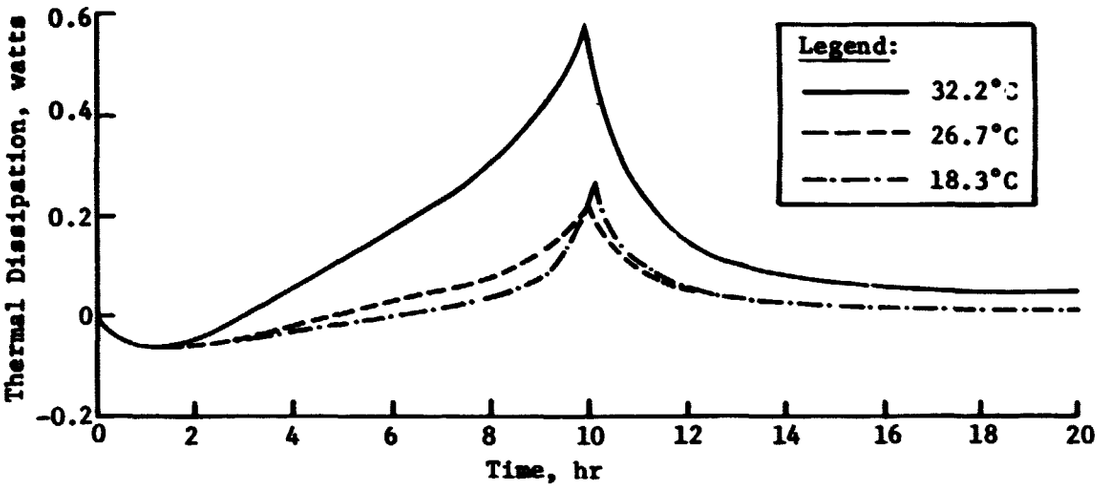

Figure V-25
Thermal Loss during Charge at C/7.5 Rate for Temperatures of 18.3, 26.7, and 32.2°C

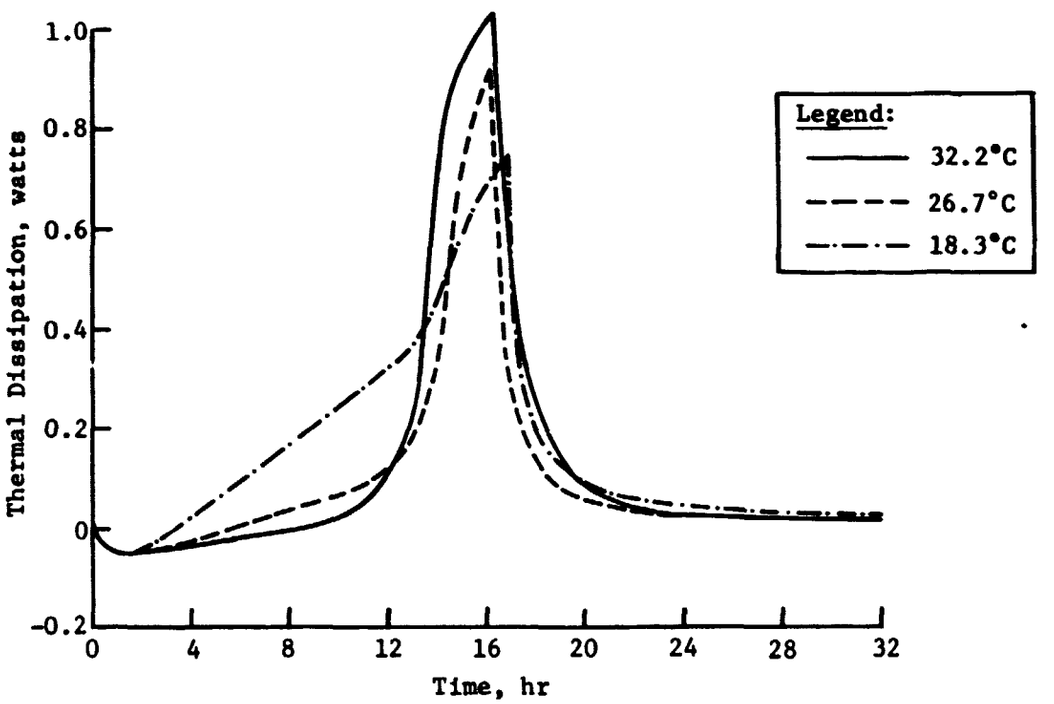

Figure V-26
Thermal Losses for a C/10 Charge Rate at Temperatures of 18.3, 26.7, and 32.2°C

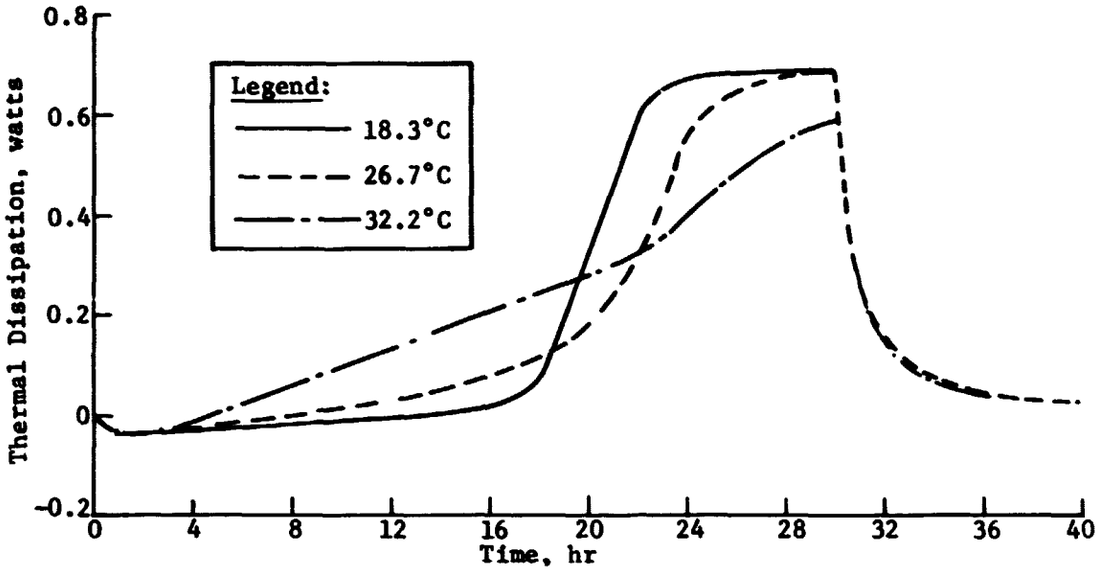

Figure V-27
Thermal Losses for a C/15 Charge Rate at 18.3, 26.7, and 32.2°C

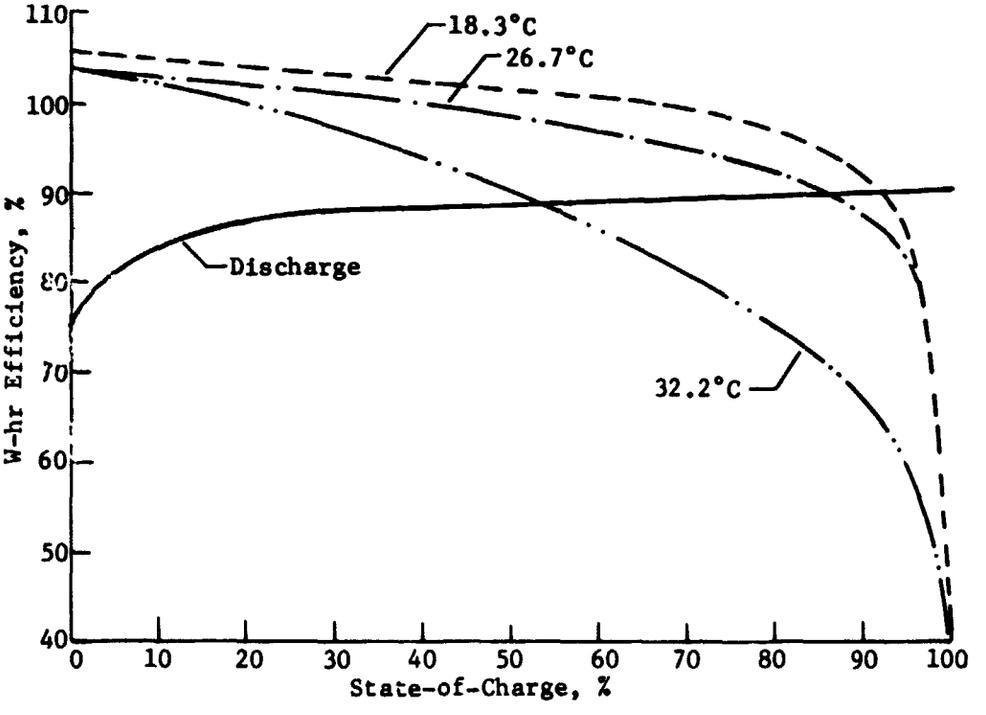

Figure V-28
Instantaneous W-hr Charge and Discharge Efficiency for C/7.5 Charge Rate at Temperatures of 18.3, 26.7, and 32.2°C

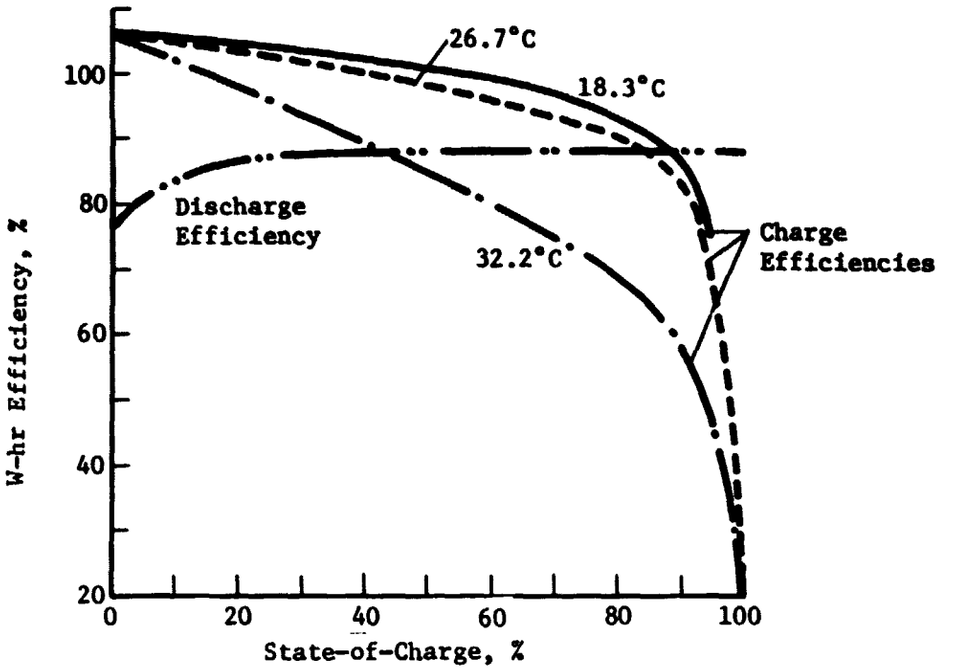

Figure V-29
Instantaneous W-hr Charge and Discharge Efficiency for C/10 Charge Rate at Temperatures of 18.3, 26.7, and 32.2°C

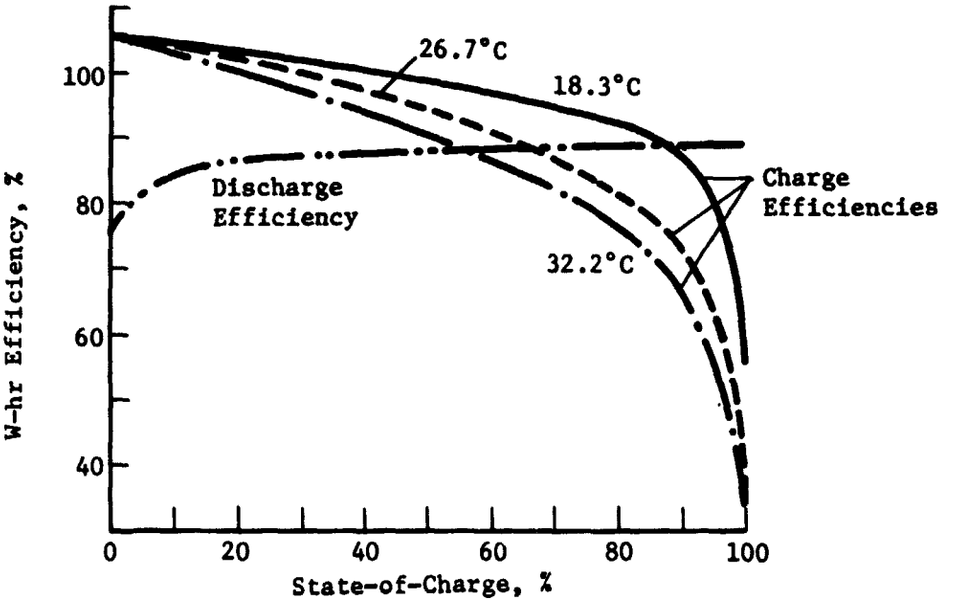

Figure V-30
Instantaneous W-hr Charge and Discharge Efficiency for a C/15 Charge Rate at Temperatures of 18.3, 26.7, and 32.2°C

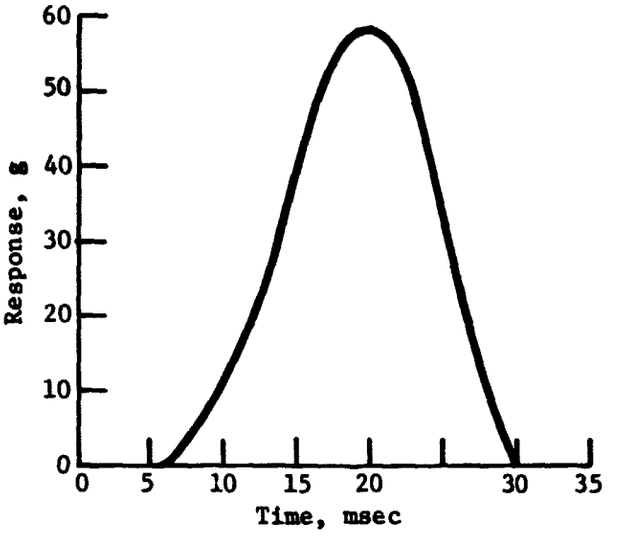

Figure V-31 Landing Shock Response Curve

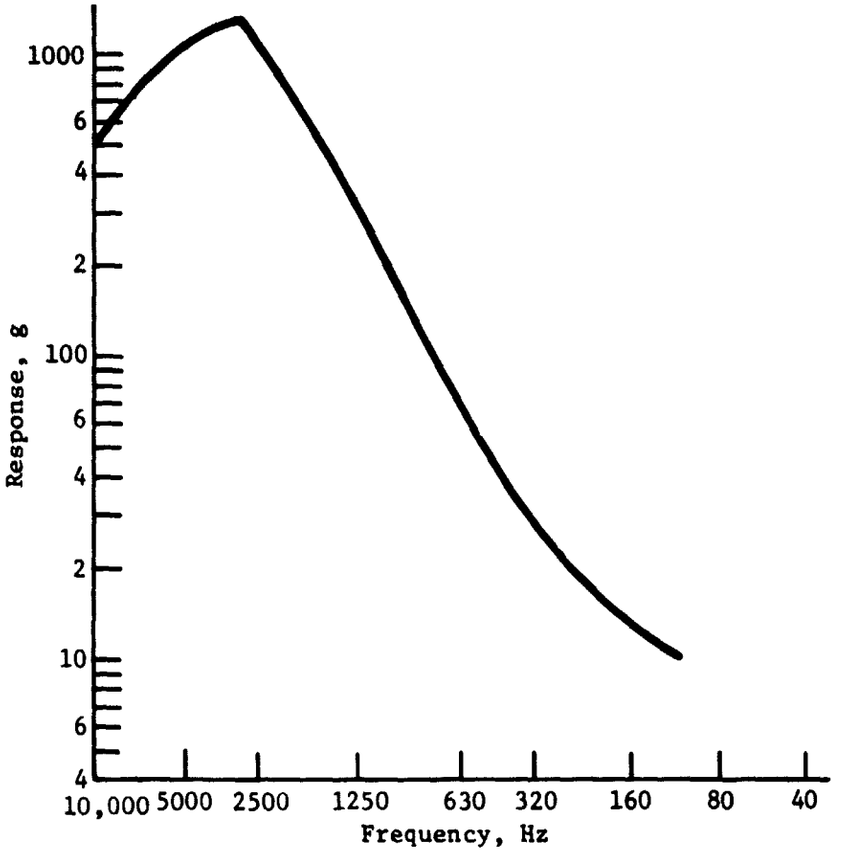

Figure V-32 Pyroshock Response Curve

curves are shown in Figures V-31 and V-32. The shock impulses were applied three times for each of the positive and negative axes and repeated for each of the three axis. Table V-3 contains a breakdown of the sinusoidal vibration spectrums that were used. The first tests used a high level of 75 g while the second level was at 15 g. The random vibration spectrum is shown in Figure V-33. This vibration spectrum was also applied to each of the three axis of the cell.

Table V-3 Sinusoidal Vibration Test Levels

Initial Test Level	
Displacement	Frequency Range
1.016 cm DA*	5 to 50 Hz
0.712 cm DA*	50 to 70 Hz
Level: 75 g	70 to 250 Hz
Duration: 11 min/axis	
Sweep Rate: 1 octave/min	
Retest Test Level	
Displacement: 1.016 cm DA*	5 to 27 Hz
Level: 15 g	27 to 250 Hz
Duration:	11 min/axis
Sweeprate: 1 octave/min	
*DA = Double Amplitude	

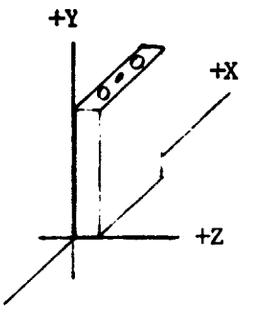

Sinusoidal Vibration - A cell failure occurred during the high level (75 g) sinusoidal test. Both cell terminals failed on the downsweep of the Y axis (3rd axis tested) at a frequency of about 120 Hz. Both terminals broke loose from the cell cover and plate weld tabs. The sinusoidal vibration test was repeated on another cell using a reduced (15 g) level from 27 to 250 Hz with no failure. The 15-g vibration level was based on a vibration amplification of 2 Q while the 75-g level represented an amplification of 10 Q. The failure at the 75-g level indicated that a significant vibration level reduction was necessary to insure the integrity of the cell. Vibration testing at the battery level showed that the predicted amplification of 10 Q was excessive and the 15 g vibration test level was adequate. The Q factor discussed herein is the amount of amplification to the environment test level due to the resonant effects of the cell components.

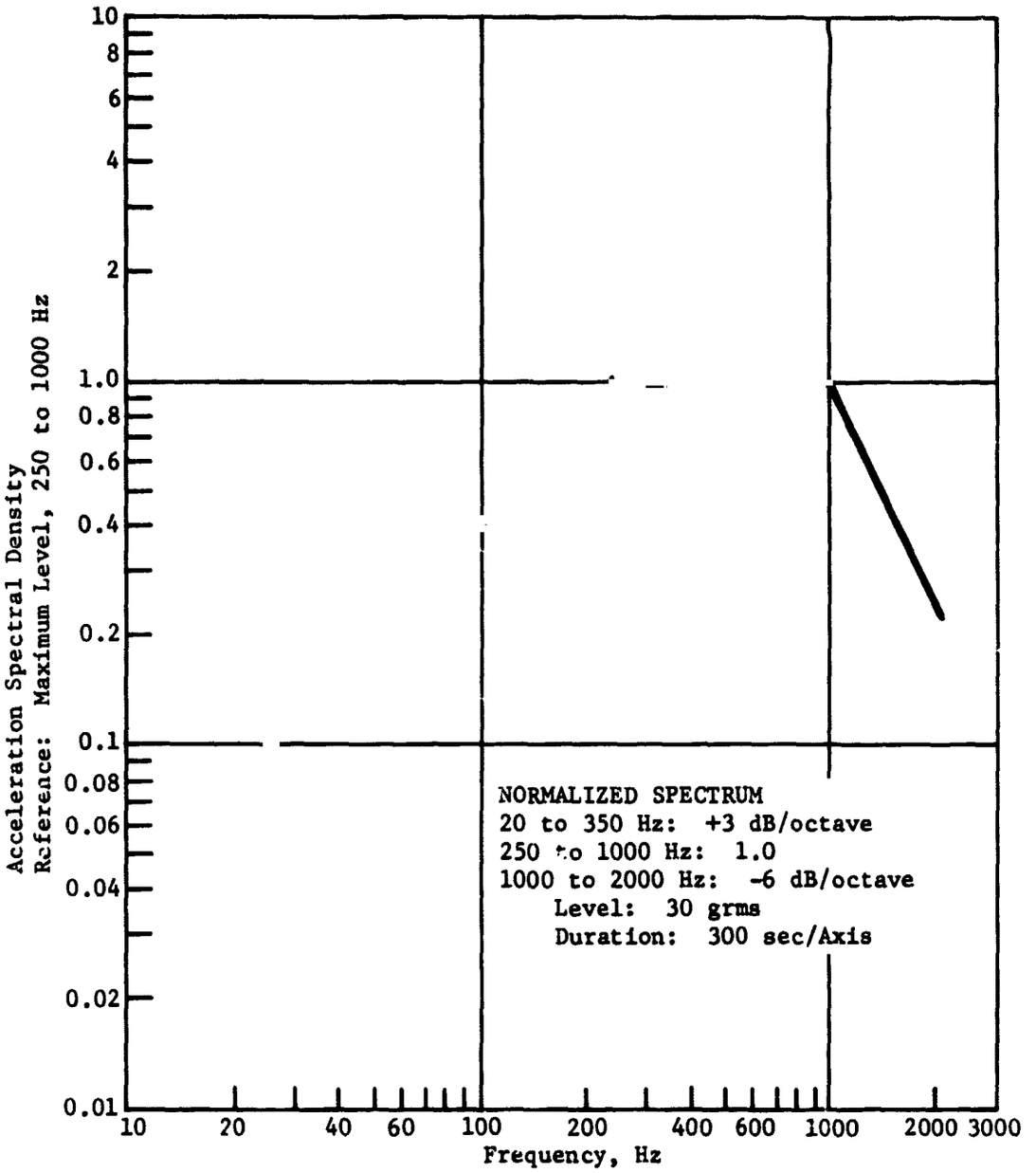

Figure V-33 Normalized Random Vibration Spectrum

Random Vibration - Several failures occurred to the cell that was subjected to the random vibration testing. These failures included: (1) an electrolyte leak developed at the ceramic-metal interface of the negative terminal, (2) a high impedance short developed in the cell, and (3) cell teardown showed 12 plate tabs had broken away from the terminals and the remaining tabs were severely stressed. The tab breakage occurred at the beginning of the Y-axis test (3rd axis tested).

Figures V-34 through V-36 show the cell damage as a result of the failures.

During the environmental testing, the cells were monitored using the circuit configuration shown in Figure V-37. Before the start of a test, the cells were charged and discharged to establish their performance characteristic. They were then recharged for the test.

Shock - No problems were discovered during the shock testing and no failures were detected.

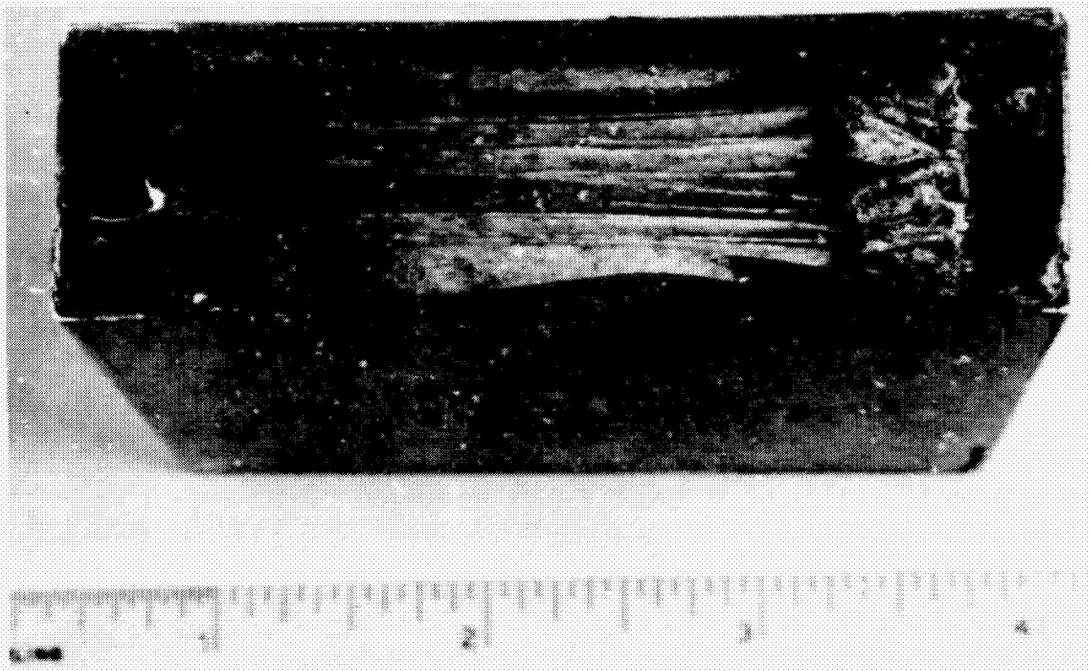

Figure V-34 Cell Plates with Broken Weld Tabs

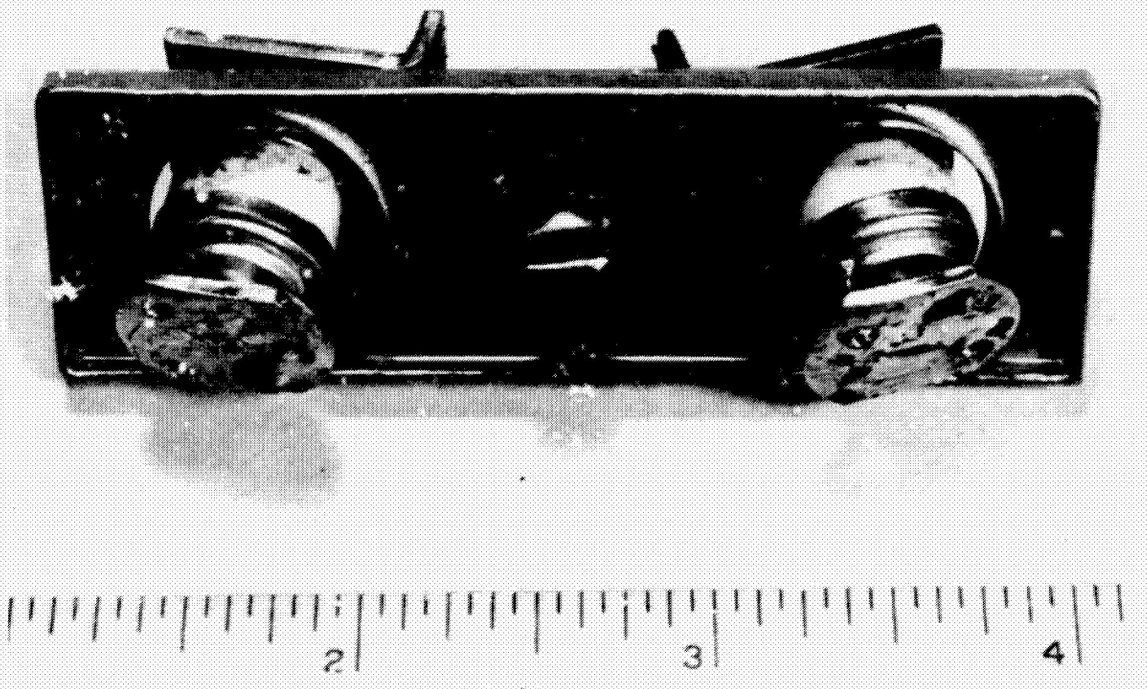

Figure V-35 Cell Terminal Failure

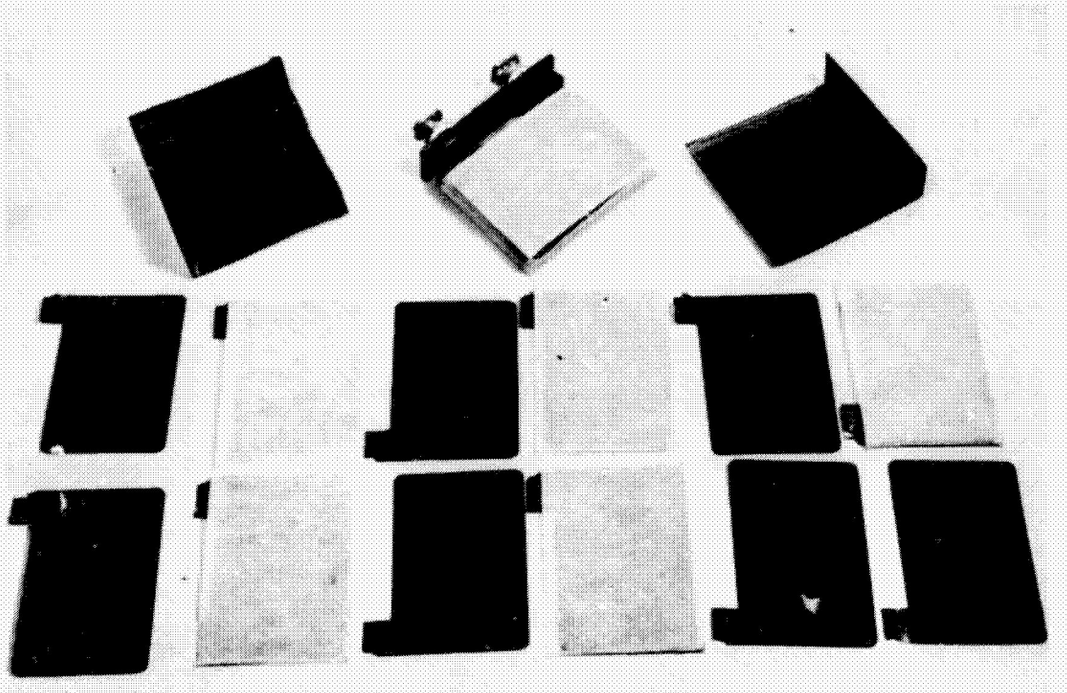

Figure V-36 Cell Plate Pack with Broken Plate Weld Tabs

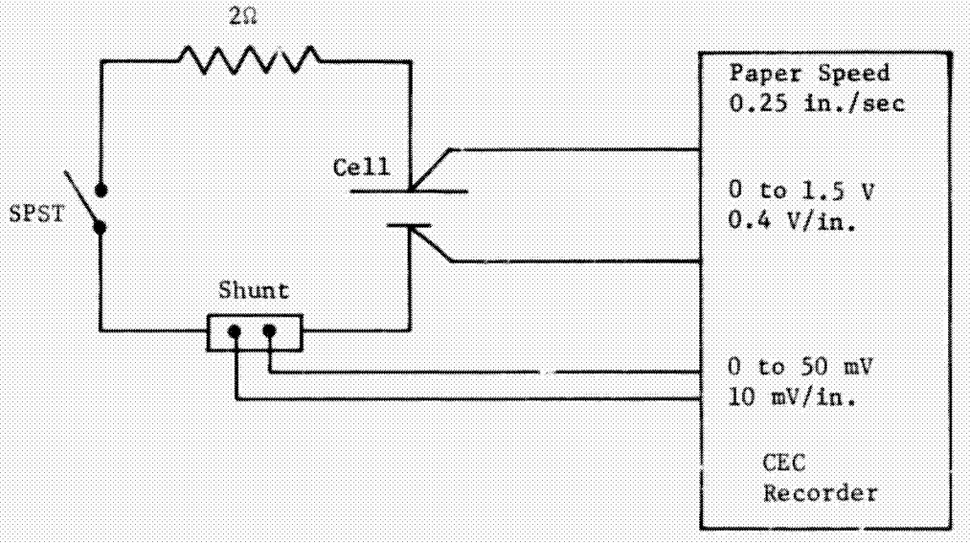

Figure V-37
Electrical Test Configuration during Environmental Testing

Table V-4 presents a summary of the environmental tests performed on the prototype batteries as well as the various other categories of batteries built. The random vibration, landing shock, and pyrotechnic shock spectrums and levels are shown in Figures V-38 through V-40.

During the initial resonant survey test on the two prototype batteries to determine their amplification factor (Q), it was discovered that the battery base plate had warped causing a permanent deflection of 0.127 to 0.152 cm. Brass shims were used to bolt the battery to the test fixtures to circumvent this problem and allow testing to continue. Analysis and tests indicated that the warpage was due to a loss in strength by the base plate material due to the high temperature experienced during sterilization. A change in material from AZ31B-H24 to HK31A-H24 magnesium alloy was made and the thickness increased from 1.11 to 1.27 cm. This material change was incorporated into the design beginning with the design development test batteries. No further problems were encountered with the battery case materials after this design change.

During the environment tests, the batteries were in a partially charged nonoperating mode. After each type of environment the batteries were given a charge/discharge cycle to determine if the electrical performance had degraded. Figure V-41 shows the General Electric battery electrical discharge characteristics as the various prototype tests were completed.

Battery Thermal Testing

The thermal characteristics of the battery assembly were evaluated by means of a test in which the battery was wrapped with 15.2 cm of fiberglas insulation and placed in a thermally controlled chamber to simulate the space environment. Once the battery temperature had stabilized at the desired test temperature, the chamber temperature controls were turned off and the battery

Table V-4 Summary of Battery Environmental Test Levels

Test Type	Prototype Test	Design Development Test (Qualification)	Environmental Acceptance Test
Sine Vibration	1.016 cm DA*, 5 to 19 Hz; 7.5 g, 19 to 250 Hz and back at 2 octaves/min	1.016 cm DA*, 5 to 19 Hz; 7.5 g, 19 to 250 Hz and back at 2 octaves/min	1.016 cm DA*, 5 to 15.5 Hz; 5-g peak, 15.5 to 250 Hz and back at 4 octaves/min
Randon Vibration	Level: 10 grms, +3 dB/octave rise from 20 to 250 Hz. Flat from 250 to 1000 Hz, -6 dB/ octave decay from 1000 to 2000 Hz. Duration: 5 min/ axis	Level: 10 grms, +3 dB/octave rise from 20 to 250 Hz. Flat from 250 to 1000 Hz, -6 dB/ octave decay from 1000 to 2000 Hz. Duration: 5 min/ axis	Level: 6 grms, +3 dB/octave rise from 20 to 250 Hz. Flat from 250 to 1000 Hz, -6 dB/octave from 1000 to 2000 Hz. Duration: 1 min/axis
Landing Shock	30-g peak, ½ sine pulse, 22 msec duration	30-g peak, ½ sine pulse, 22 msec duration	None
*DA - Double Amplitude			

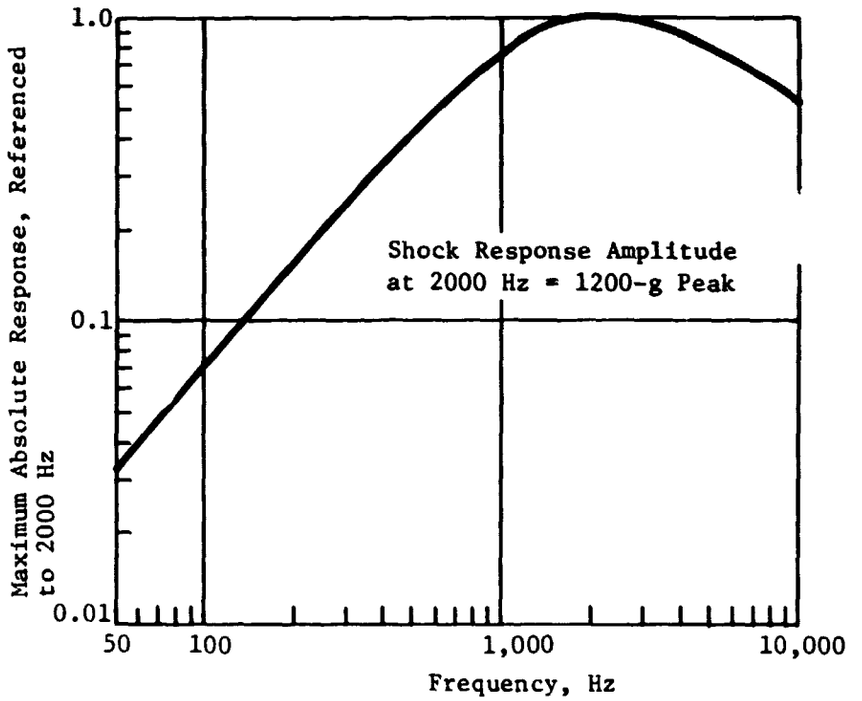

Figure V-38 Shock Test Spectrum

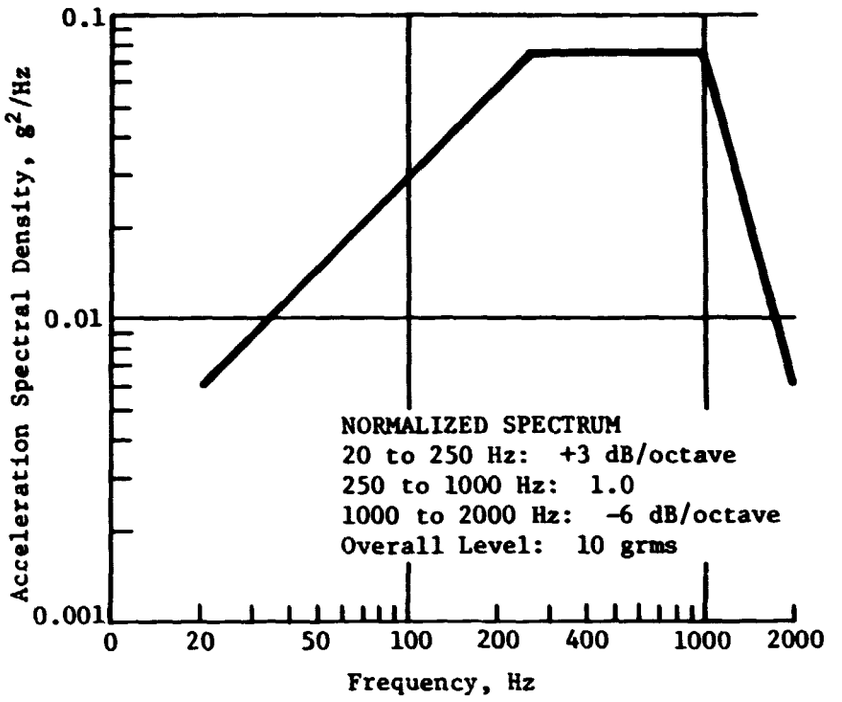

Figure V-39 Random Vibration Spectrum

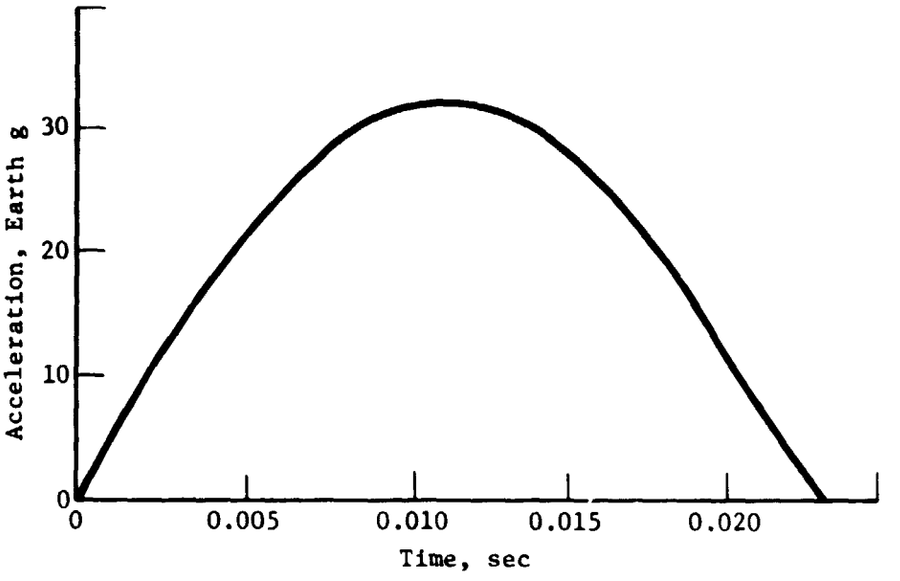

Figure V-40 Landing Shock Acceleration Pulse

charged and discharged. Battery temperatures were recorded throughout the test. Figures V-43 and V-44 show the battery temperature profile for each of the test conditions. The data showed that at the higher charge rate the temperature rise was very small. This was attributed to the highe. charge efficiency and the fact that the battery was only charged for nine hours which did not result in any significant amount of overcharge.

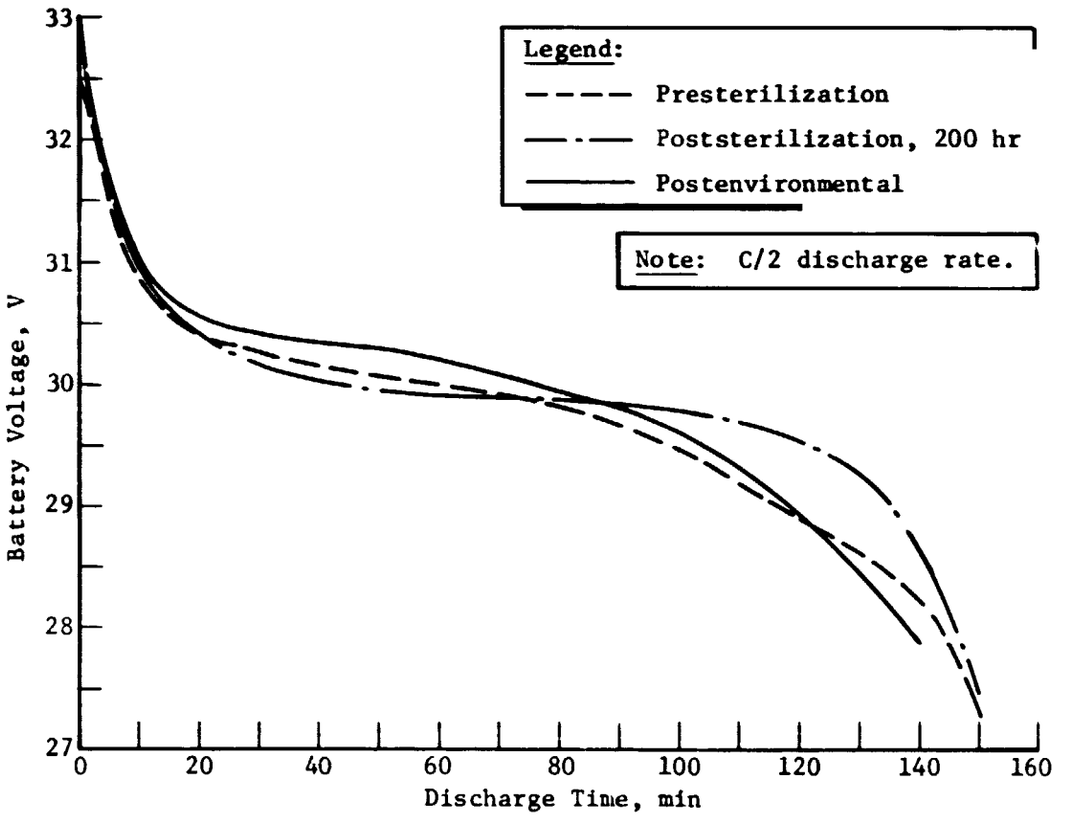

Figure V-41 Prototype Battery Discharge Characteristics

The low rate charge (C/15 rate) produced a significant temperature rise near the end of the charge. The charge that was started in an ambient temperature of 21.1°C was continued for an additional four hours beyond the normal charge termination time (24 hr) and resulted in a battery temperature approaching 49°C.

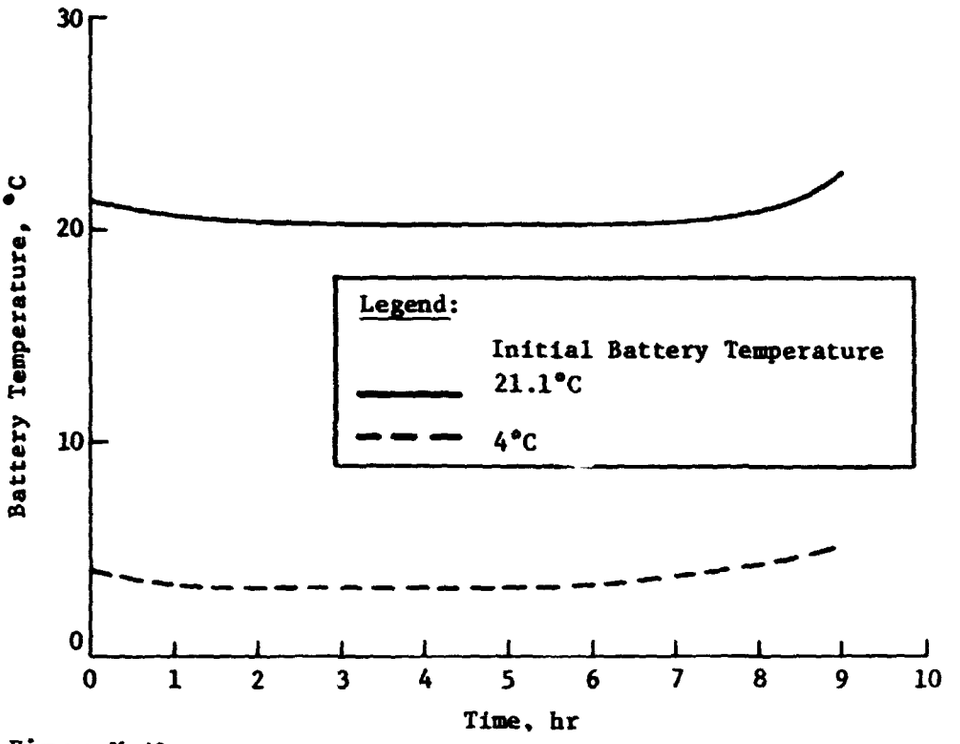

Figure V-42
Battery Temperature Profile during C/7.5 Charge at Initial Temperatures of 4 and 21.1°C

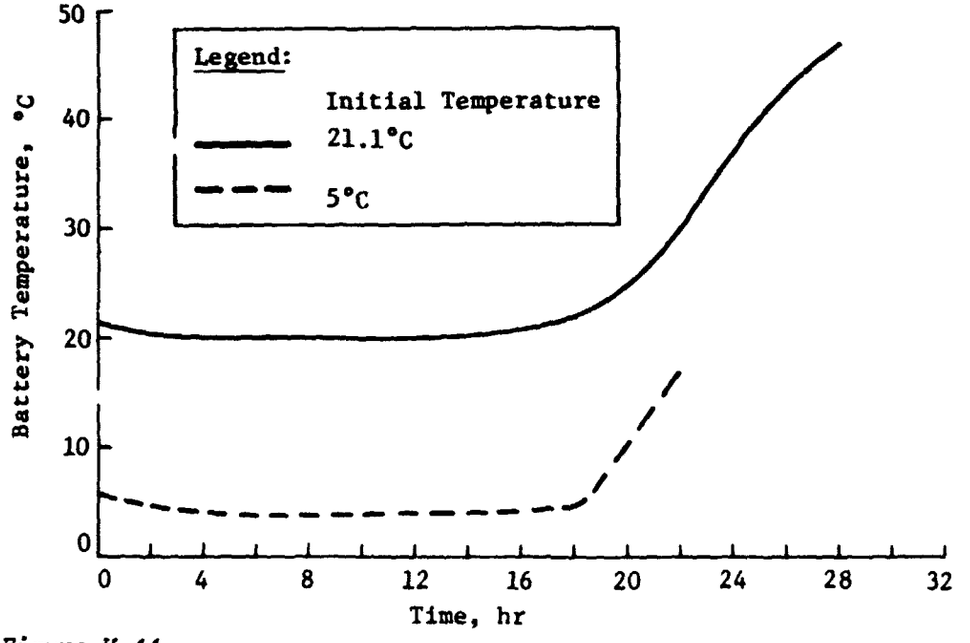

Figure V-44
Battery Temperature Profile during C/15 Charge at Initial Temperatures of 5 and 21.1°C

It was concluded as a result of this test that the battery temperature (when installed in the lander) will not rise appreciably during charge until the battery approaches a full state-of-charge. At that time, the charge efficiency begins to drop and a larger percentage of the charging energy goes into losses.

C. DESIGN DEVELOPMENT TEST PROGRAM

The purpose of the design development test program was to confirm the results obtained from the prototype test program using cells that were built to the requirements of the Procurement Specification.

In most cases, the tests performed were a repetition of the prototype tests and consequently the same results and data were obtained. Table V-5 presents the test program for both the cells and batteries. The levels for each of the environment tests are shown in Table V-4.

The following paragraphs summarize the features of the design development test program.

11. Sterilization

One battery was subjected to three sterilization heat cycles. The first exposure was at a temperature of 111°C for 54 hr. This test was designated as the component level sterilization. The second sterilization was at a temperature of 123°C for 40 hr and was designated as the Lander vehicle sterilization. The Lander sterilization was repeated once to verify the capability of being resterilized in case of a problem on the Lander after the initial sterilization. The electrical cycles following sterilization showed the typical elevated voltage during the first charge. There was a reduction in capacity of 0.24 A-h as a result of the qualification level sterilization tests.

Table V-5 Design Development Cell and Battery Test Summary

Test Quantities	Test Type	Test Description	Operational Conditions
60 Cells	Life	Heat Compatibility	Discharged
		Seal Test	Discharged
		4 months Prelaunch	OCV Stand (Discharged)
		13 months Interplanetary Cruise	OCV Stand (Discharged)
		80 days Mars Orbit	Trickle Charge 50 mA
		90 days Landed Operation	2 cycles/day - 30% DOD
1 Battery Assembly	Environmental	Seal Test	Nonoperating
		Heat Compatibility	↕
		Entry Acceleration	
		Descent Vibration	
		Landing Shock	Nonoperating

OCV - Open Circuit Voltage

DOD - Depth of Discharge

2. Life Testing

The life testing was intended to prove that the nickel-cadmium cells would survive the long duration cruise to Mars in a discharged condition and then meet the entry landing and postlanding cycle requirements. Since an actual simulation would take nearly a year, the program evolved into a short term discharge stand test of four months which ran concurrently with a long term (8-month discharged stand) test. The short term test was included to provide interim data of a qualitative nature since the program schedule could not stand the delay of an eight-month test. The life test and the subsequent 180 cycles at a 30% depth-of-discharge were completed with all test objectives met.

The extent of the testing performed to verify that the battery and cells meet the qualification and the mission requirements is shown in Table V-6. This matrix (including the system level tests) shows the degree to which the battery usage on the Lander was evaluated.

3. Dynamic Environment Testing

One of the objectives of the Design Development program was to subject a battery built to engineering drawings and processes and procedures, to the dynamic environments required for qualification. These tests were intended to identify any problems early enough in the program to permit any required redesign and retest without a schedule impact.

The dynamic environmental tests required for qualification included sine vibration, random vibration, and landing shock. The levels were the same as used during the prototype battery environmental tests as shown in Table V-4. This entire design development environmental test program was completed with no test failures. A recommendation was made to NASA to delete the formal battery qualification test program based on the results of the development test program. NASA accepted this recommendation and the qualification test program was deleted.

Table V-6 Design Verification Test Matrix

Test Requirement	Cell Tests		Battery Tests			Engineering Tests System Tests				
	Prototype Cell	Qualification & Development Cell	Prototype Battery	Qualification & Development Cell	Flight Battery Acceptance Test Procedure	Cell Tests	Battery Tests	Proof Test Capsule Vehicle	System Test Bed Vehicle	Flight Vehicle
Seal (Leakage)*	X	X	X	X	X			X	X	X
Sterilization*	X	X	X	X	X	X	X	X		X
Pyroshock*	X							X		
Landing Shock*	X		X	X				X		
Sinusidal Vibration*	X		X	X	X			X		X
Random Vibration*	X		X	X	X			X		X
Cruise Thermal Vacuum*			X					Partial		Partial
Float Test (C/160)*	X	X								
Float Test (C/40)							X			
Thermal Efficiency	X									
Thermal Characterization							X			
Self Discharge						X				
Electrical Characterization	X	X	X	X	X	X	X	X	X	X
Cycle Life*	X	X	X			X	X	X	X	
Cruise Simulation	X	X					X	Partial		

*Required for Battery Qualification

Table V-6

VI. CELL DESIGN, ASSEMBLY AND TEST

A. CELL DESCRIPTION

In outward appearance, the eight-A-h nickel-cadmium cell selected for the Viking Lander batteries is similar to many other cells manufactured by General Electric for aerospace applications. The significant differences lie internal to the cell and include:

1) Use of polypropylene separator material;
2) Incorporate heat treatment to improve separator wettability;
3) Perform final electrolyte quantity adjustment after heat treatment;
4) Plate carbonate reduction process.

The distinguishing features of the cell and the acceptance testing are described in the following paragraphs. A description of the cell manufacturing sequences, processes, and testing used by General Electric during the production of the flight cells is included in Appendix C.

1. Capacity

The program requirements dictated the design of a cell with an end-of-mission capacity of eight ampere-hours. This led to the requirement for an acceptance test or beginning of life capacity of 9.5 A-h. However, the cell is identified as an eight-ampere-hour (nameplate capacity) cell.

2. Case

A conventional stainless steel prismatic case was selected for the Viking cell. The dimensions of the case, including terminals, are shown in Figure VI-1. Both the case and cover are fabricated from 304L stainless steel with a wall thickness of 0.043 to 0.053 cm The side, bottom and cover seams are heliarc welded. Early prototype cells were fabricated using Cerameaseal cell terminals; however,

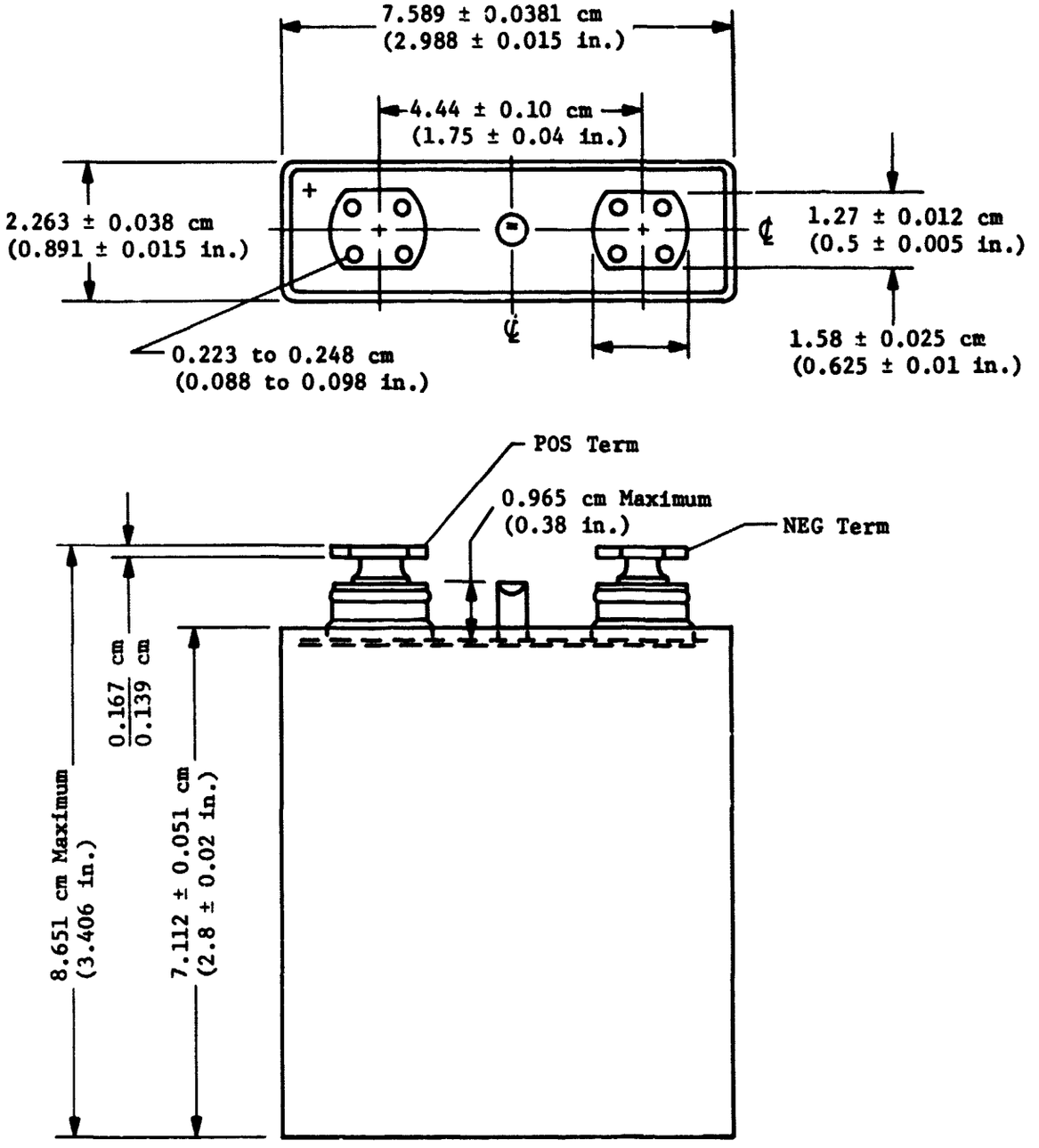

Weight: 273 gm Nominal, 280 gm Maximum.
Wall Thickness: 0.432 to 0.533 mm (0.017 to 0.021 in.).

Figure VI-1 8-A-h Nickel-Cadmium Cell Dimension

the cells built to the procurement specification requirements used insulated terminals with an all nickel-braze ceramic to metal seal. This change was made due to reports of leakage problems by various military and NASA agencies. The terminals were rated at 40 A (5 C rate). These terminals increased the cell weight by 5.7 grams; however, an improvement in reliability was achieved since no leaks were detected in testing over 1200 cells.

3. Plates

The substrate selected for the plates consists of a 0.101 mm steel sheet. This substrate is perforated with 2.03 mm holes and nickel plated before plaque production. The plates are coined after sintering along the four edges before blanking to minimize the possibility of the sinter cracking and flaking. The coining width was set to 0.20 cm and the depth to 15% of the minimum plate thickness. The same size dies are used to blank out the positive and negative; however, the weld tab configuration on the negative plates were altered by trimming the width on the early cells and cutting a corner at an angle on flight cells to provide a means of identifying the positives from the negatives. The plate dimensions are given in Figure VI-2.

Beginning with the lot 6 production (cells used to fabricate the flight hardware) the cell plates were given a carbonate reduction process*. Cells built with this process exhibited both a lower end of charge voltage (10 to 15 mV) and a reduced voltage spread. These cells also delivered approximately 0.5 A-h more than the previously accepted cells. Since these changes occurred during the final production phase, no attempt was made to determine if the carbonate reduction process was the cause for the increased capacity and improved characteristics.

---

*General Electric Proprietory Process

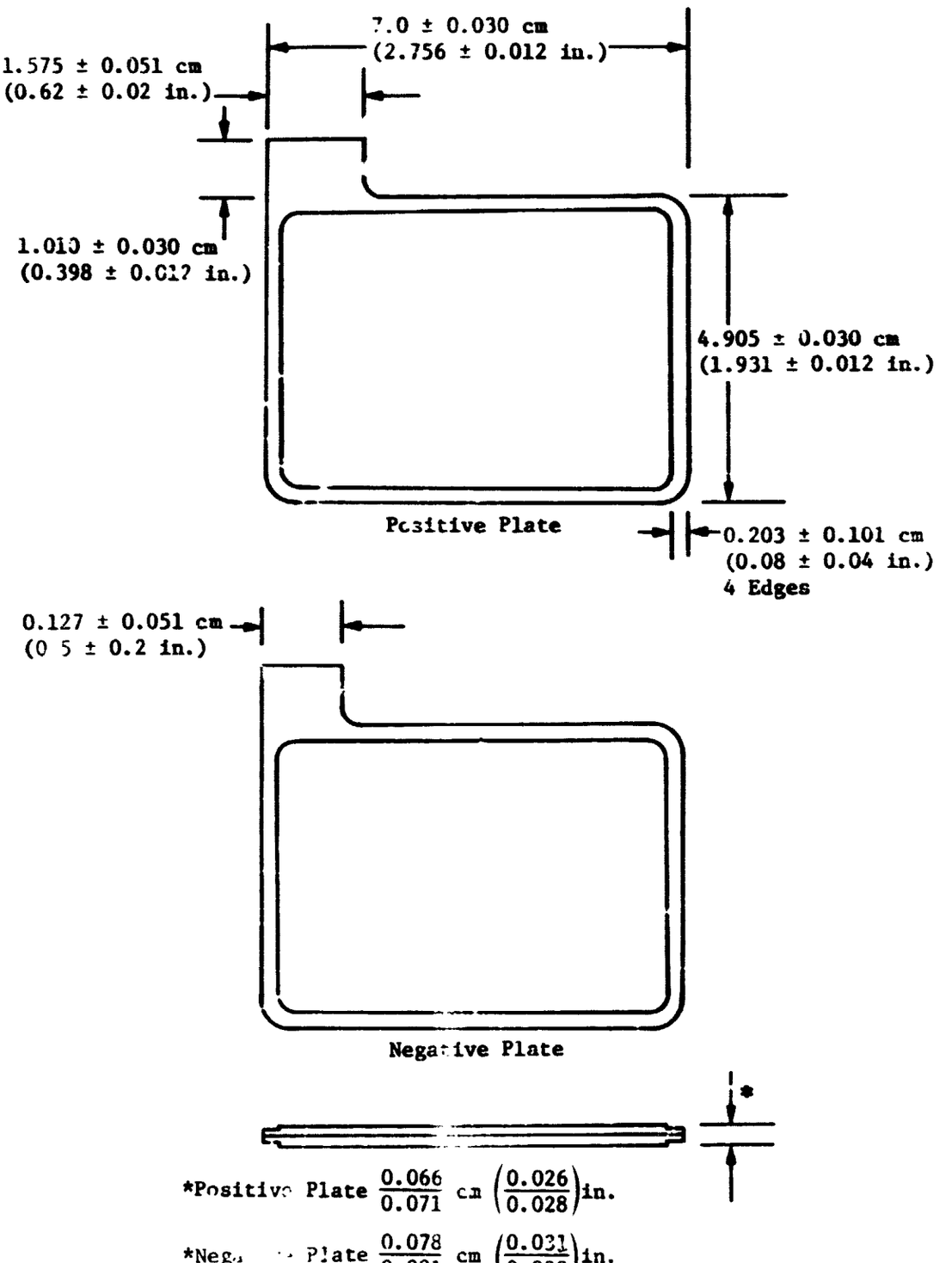

Figure VI-2 Cell Plate Dimensions

Eleven positive and 12 negative plates were used in the cell to provide the desired capacity and plate current density.

4. Separator

The positive and negative plates are insulated from each other using a nominal (0.216 mm) thick nonwoven polypropylene separator which was fabricated into bags and slipped over each positive plate. An additional layer of polypropylene separator was placed around the outside of the plate pack to prevent the outside negative plates from drying out. The plate pack is insulated from the case by means of a 0.127 mm solid sheet of polypropylene.

Separator characterization tests were required by the cell procurement specification. These tests included: (a) electrolyte absorption, (b) electrolyte retention, (c) porosity, (d) dimensional changes when wet, (e) wettability, (f) tensile strength, (g) extractable organic content, (h) inorganic content, and (i) thickness variations. The method used in performing each test is described in the procurement specification data included in Appendix A. These data are summarized in Table VI-1.

5. Electrolyte

The quantity of electrolyte used in each cell ranged from 21.5 to 23.5 and was closely controlled to prevent premature cell dryout due to inadequate electrolyte or conversely to prevent an inadequate oxygen recombination rate due to excessive electrolyte.

The concentration of potassium hydroxide (KOH) electrolyte is 34% by weight. Rigid controls were imposed to limit the introduction of impurities. The quantity of potassium carbonate (K_2CO_3) allowed in the electrolyte, before filling, is limited to two grams per liter. Burets were used to fill the cells thus further limiting the exposure of the electrolyte to the atmosphere and contamination by carbon dioxide (CO_2).

Due to the incorporation of a heat treatment during the final manufacturing tests (just before the acceptance tests) which improved the separator wettability, a change was made to the procedure to add

Table VI-1 Separator Material Characteristics

Supplier: Pellon Corporation, Lowell, Massachusettes
Material: Polypropylene
Supplier's Part No.: 162A8080AB-153
Supplier's Lot No.: 2140-00

Wetting Agents: None

Impurities after Wash
Inorganics 0.35% ASH
Organics 0.24% Methylene Chloride Extract

Thickness:
Nominal: 0.0216 cm
Maximum: 0.0254 cm
Minimum: 0.0178 cm

Sample Size:
2.5 by 6.5 cm

Weight, gm/m^2:
Sample 1: 61.54
Sample 2: 62.15
Sample 3: 55.38

Dimensional Change

	Length, cm		Width, cm		Thickness, cm	
Sample	Dry	Wet	Dry	Wet	Dry	Wet
1	6.53	6.52	2.50	2.50	0.0136	0.0142
2	6.53	6.52	2.50	2.50	0.0144	0.0144
3	6.53	6.53	2.50	2.50	0.0119	0.0125

Electrolyte Absorption, 16.25 cm^2 area

Sample	Electrolyte Absorbed, gm
1	0.801
2	0.768
3	0.653
4	0.748
5	0.707
6	0.767

Table VI-1 (cont)

Electrolyte Retained

Sample	Electrolyte Retained, %
1	92.6
2	99.0
3	98.6
4	98.4
5	98.0
6	97.0

Porosity:

Sample	Percent Porosity
1	59.2
2	59.0
3	59.0

Definition: $\% \text{ porosity} = \frac{W_W - W_D}{V_W \times P}$

W_W = Wet Weight of Separator, gm

W_D = Dry Weight of Separator, gm

V_W = Wet Volume of Separator, cc

P = Density of Absorbed Electrolyte

Separator Resistance:

Sample	Specific Resistivity, Ω cm
1	27.48
2	35.48
3	30.08

Tensile Strength:

Sample	Tensile Strength at Break, N/cm^2
1	192.5
2	280.5
3	207.3
4	186.8
5	186.8
6	185.0

Table VI-1 (concl)

Thickness Variations:

Thickness variations taken from 10 readings on 5 separate samples gave a variation of 0.0889 mm (0.0035 in.).

Inorganic Contents:

Element	Sample 1%	Sample 2, %	Sample 3, %
SiO_2	0.031	0.032	0.041
Zn	0.029	0.032	0.034
Ni	0.0004	0.0017	0.0029
Ti	0.0058	0.0142	0.0155
CL	0.015	0.002	0.002
CO_3*	10^{-6}	10^{-6}	10^{-6}
NO_3†	0.001	0.001	0.001

*Grams of K_2CO_3/dm^2

†Mgm KNO_3/dm^2

additional electrolyte over the initial quantity supplied. This was accomplished during a 48 hr C/10 overcharge test. Sufficient electrolyte was added to reach a nominal pressure of 137.9 kPa (20 psig). This test is a part of the final manufacturing tests which are performed just prior to the final acceptance tests.

6. Cell Assembly

A description of the cell assembly is given in Appendix C. A summary of the cell characteristics and parts description is shown in Table VI-2 herein.

B. MANUFACTURING DATA

Typical vendor test data for the cells used in the manufacturing of the flight batteries is included in Tables VI-3 through VI-6. Table VI-3 presents the results of the electrochemical cleaning and testing (ECT) of the plates for lots 7 and 8 from which the cells for some of the flight batteries were fabricated. The ECT test is a flooded test of temporary cells. These data show an average negative-to-positive capacity ratio of 1.54 for lot 7 and 1.53 for lot 8. The nitrate and carbonate content of these plates is given in Table VI-4. The electrode capacity data for sample cells from each lot are shown in Table VI-5. The acceptance test capacity range for each lot is shown in Table VI-6.

Table VI-2 Cell Characteristics and Parts Description

Cell Capacity	8 A-h (Rated)
Cell Weight	273 gm - Lot Average
Cell Size	7.589 cm x 2.27 cm x 8.651 cm (including terminals)
Case Material	304L Stainless Steel
Case Wall Thickness	0.48 ± 0.05 mm
Insulated Terminals	Positive and Negative
Terminal Type	Nickel Post with Ceramic Insulator GE - all Nickel-Braze
Auxiliary Electrode	None
Separator Material	Pellon FT2140 Nonwoven Polypropylene
Separator Thickness	0.216 mm
Plate Pack Wrap	Pellon FT2140 Nonwoven Polypropylene
Case Liner	0.127 mm Solid Polypropylene Sheet
Electrolyte	KOH
Electrolyte Concentration	34%
Electrolyte Quantity	21.5 to 23.5 cc
Plate Substrate	0.101 mm Perforated Steel Sheet
Sinter Porosity	80% Nominal
Number of Plates	POS 11
	NEG 12
Plate Size	7.0 ± 0.03 x 4.9 ± 0.03 cm
Plate Thickness	POS 0.066 to 0.071 cm
	NEG 0.078 to 0.081 cm

Table VI-3 ECT Results for Lots 7 and 8

Lot	Positive Capacity	Negative Capacity
7	10.5 A-h average 10.1 A-h minimum 10.8 A-h maximum	16.2 A-h average 15.8 A-h minimum 16.7 A-h maximum
8	10.7 A-h average 10.2 A-h minimum 11.7 A-h maximum	16.4 A-h average 15.3 A-h minimum 17.1 A-h maximum

Table VI-4
Nitrate and Carbonate Content for Plate Lots 7, 8, and 10

	Lot 7		Lot 8		Lot 10	
	Neg	Pos	Neg	Pos	Neg	Pos
Nitrate Content mg/g*	<10	34	<10	26	<10	96
Carbonate Content mg/g*	2345	4769	2345	3568	2662	4954

*Average of three samples

Table VI-5
Electrode Capacity Test Data for Samples from Lots 7 and 8

Lot	Precharge, A-h	Full Positive, A-h	Full Negative, A-h	Discharged Excess Negative, A-h
7	1.81	11.47	17.60	4.32
8	1.34 2.44 2.29	10.93 10.67 11.27	17.67 20.60 16.67	5.40 7.49 3.11

Table VI-6 Lots 7, 8, and 10 Acceptance Test Capacity

Lot	No Cells	Minimum A-h	Average A-h	Maximum A-h
7	60	10.1	10.7	11.0
8	268	9.86	10.3	11.0
9	123	9.5	10 5	10.9

C. RECEIVING INSPECTION

Receiving inspection was performed as the cells were received from the supplier and before cell matching tests. These tests included a physical inspection and weighing of each cell, an electrolyte leakage test, measuring the ac impedance of the cell, and finally performing a high impedance leakage test. Once these tests were completed, the cells were subjected to characterization and capacity tests for matching and assembly into batteries. Surplus cells bypassed the receiving inspection and were placed directly into storage.

1. Inspection and Weighing

Each cell as it was removed from the shipping container was inspected for bent terminals, dents, nicks, and scratches. The shorting wire was removed and the cell was weighed on a Mettler laboratory scale to the nearest 0.1 gram. These data were compared to the data supplied by the vendor.

2. Electrolyte Leakage

Before performing the chemical leak test, the cells were washed in deionized water and dried by immersion in acetone to remove any external contamination. The cells were then placed in a vacuum chamber and subjected to a vacuum of 635 ± 127 mm of mercury for 10 min. The cells were then immersed in a solution of phenolphthalein for a minimum of 15 sec and observed for traces of pink color around the cell terminals, fill tube, and welded seams. Over 1200 cells, built with the General Electric-designed cell terminals, were tested for leaks without a failure.

3. AC Impedance

An ac impedance test was performed by applying a 60-cycle current of 100 ± 5 mA for 60 sec to the cell terminals. A schematic of the test circuit is shown in Figure VI-3. The maximum cell voltage allowed was 0.0013 V. Typical values recorded were 0.0004 V which is four millohms. No cell failures were found during this test.

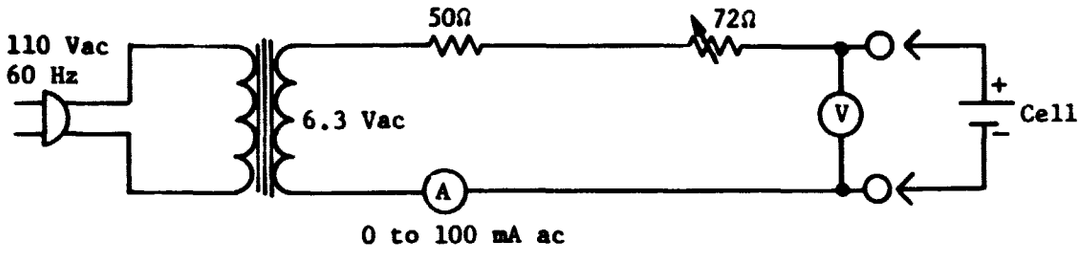

Figure VI-3 Cell ac Impedance Test Circuit

4. High Impedance Leakage Test

Rather than repeat the same voltage retention test the supplie: performed during acceptance tests, a variation in the test method was selected to evaluate the insulation or impedance between the cell plates. The test procedure used consisted of charging the cells at a C/10 rate for five minutes from the fully discharged condition as received from the vendor. The cells were then allowed to stand in an open circuit condition for 24 hr at which time the cell voltage was measured. The cell voltages were required to be 1.16 V or greater. No test failures were recorded as a result of this test.

CELL MATCHING

The Viking battery mission profile involves numerous modes of operation including open circuit charged stand, open circuit discharged stand, trickle charging and cycling to a 70% and then 50% depth-of-discharge during Mars atmospheric penetration and planetary operation. Because of these requirements and combined with the use of polypropylene separator material, which has a low wettability characteristic, and the high temperature sterilization requirement, cells in a battery were matched to within ± 1% of the average cell capacity.

The possibility that a dispersion in cell capacities due to usage, which could result in completely discharging and reversing some cells, would then be minimized.

1. Cell Matching Program

Rather than select cells with the same A-h capacity from cell acceptance test data obtained at the cell manufacturer's facility, a test program was devised which would subject the cells to a number of charge discharge cycles at various rates to induce the capacity dispersion which occurs during the initial phases of cyclic usage. The cells would then be matched based on the capacity that existed after the cell characteristics had stabilized. Cells with abnormal electrical characteristics and low capacity would be identifiable during these cyclic tests and rejected.

Testing performed during the development phase had shown that the rate of change of the cell electrical characteristics and capacities decreases significantly by the time the cells have been exposed to 60 to 70 charge-discharge cycles (see Fig. VI-4). Capacity loss after these cycles would be minimal and would occur over several hundred cyclic operations.

Based on the test duration required and the anticipated stability in cell characteristics, 64 charge discharge cycles were selected for the cell matching program. Since the cells would experience charge rates that could vary from a C/40 up to a C/7.5 rate, the 64 cycles were divided up into several separate tests using C/15, C/10 and C/7.5 charge rates to evaluate their characteristics. Constant current charging to a time cutoff was used for all the charge phases. A standard C/2 discharge to a cell voltage of 1 0 V was selected for all the discharges to provide uniformity in evaluating the cell capacities and discharge voltage characteristics. The cells were power discharged at the C/2 rate with a regulated power supply operating in a constant current mode. The various test conditions for the matching tests are summarized in Table VI-7.

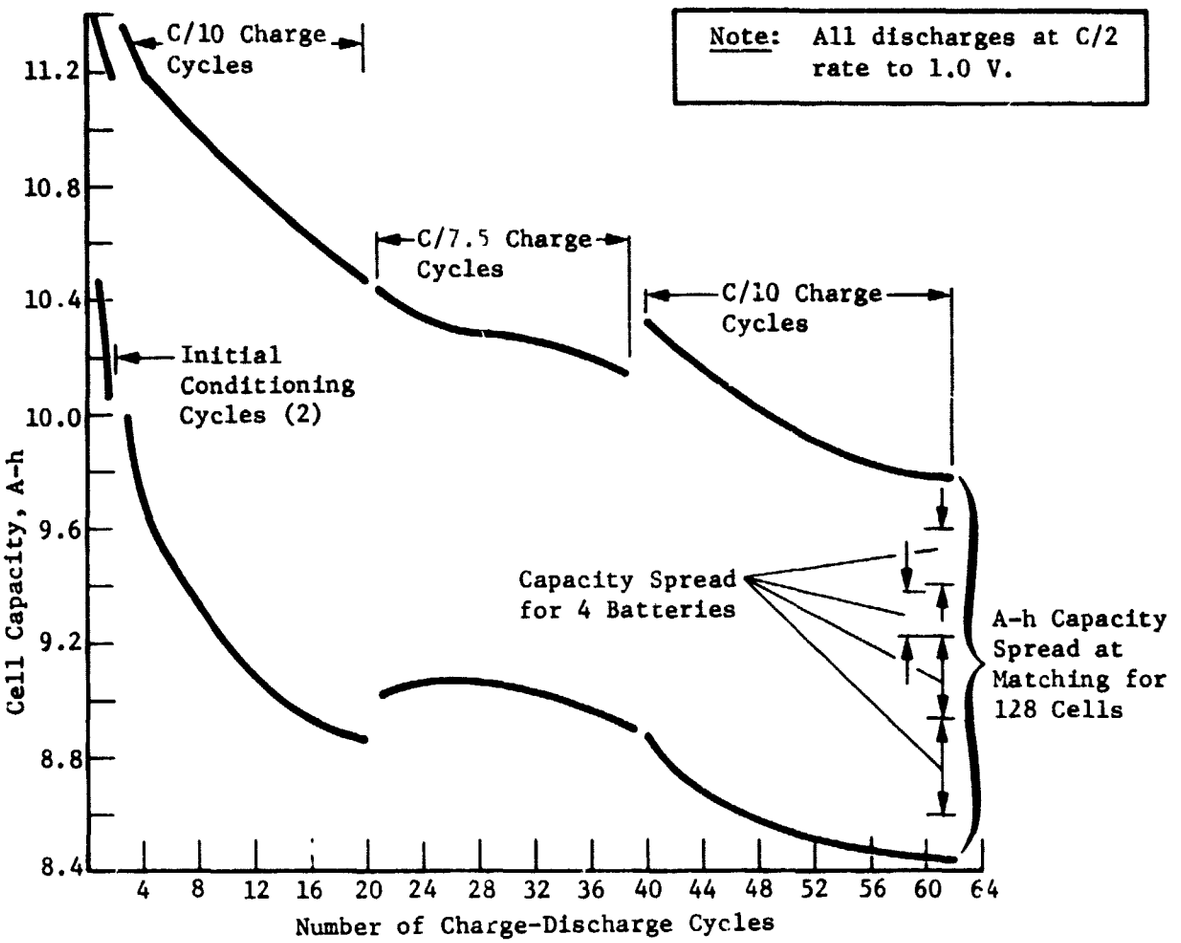

Figure VI-4 Capacity Variation During Cell Matching Cycle Testing

The test sequences (see Table VI-7) subjected the cells to both overcharging and deep discharging to induce a significant level of stress and degradation. Cell temperatures were controlled by performing the testing in temperature controlled chambers with forced air circulation which was maintained at 21.1 ± 1.6°C.

Table VI-7 Cell Matching Test Matrix

Test Step	No. Cycles	Charge Rate, A	Charge Duration, hr	Discharge Rate, A	End of Discharge Voltage, V
1	2	C/15	30	4.0	1.0
2	20	C/10	16	4.0	1.0
3	20	C/7.5	10.5	4.0	1.0
4	24	C/10	16	4.0	1.0
5	3	C/10	13.5	4.0	1.0
6 1-Ω Discharge for 24 to 48 hr					
7	1	C/15	24	4.0	1.0
8	2	C/7.5	10	4.0	1.0
9 1-Ω Discharge for 24 to 48 hr					

Thermal analysis had predicted that the batteries would operate for the majority of the time at around 21°C. Therefore, this temperature was selected for performing the cell matching cycle tests.

The first two charges were made at a C/15 charge rate (0.53 A) which was the in-flight conditioning charge rate provided from the Orbiter power system. This low rate of charge was selected because of the long term (9 to 10 months) storage in a totally discharged condition. Previous tests showed that cells in an inactive state for long periods of time tend to operate at higher voltages than normal during the first charge. Using a low charge rate for the first charge prevents the development of high voltages.

The data obtained from the last three cycles of step 4 was used in matching the cells.

Three charge-discharge cycles (test step 5) were performed to evaluate the charge acceptance dispersion among the cells. A partial charge at a C/10 rate for 13.5 hr was followed by a C/2 discharge to one volt. Cells that had a lower charge acceptance for a partial recharge would have a lower capacity when charged; however, results of this test showed that the charge efficiency variations, when comparing the partial charge capacity of the cells to the capacity obtained with overcharging, was insignificant.

In numerous instances during these tests, a group of cells would reach the 1.0 V end-of-charge cutoff simultaneously and overload the computer. This resulted in the discharge being terminated to prevent cell reversal. Little variation in cell capacity ranking was observed when the cells were sorted in order of decreasing capacity for both the partial charge and overcharge cases.

2. Cell Matching Procedure

The cell matching parameters were based on watt-hour capacity, ampere-hour capacity, and cell voltage characteristics at the end-of-charge and during discharge in that order. Watt-hour capacity was selected as the primary evaluation parameter for cell matching since the cell voltage characteristics are included in its calculation. Cells selected using this parameter would have the highest energy density. The computer-controlled data acquisition and test system (see Appendix B) used during the cell matching test program provided the capability for data reduction using computer programs to calculate the watt-hour capacities during both charge and discharge. The computer program also sorted the capacity data and ranked each cell in order of either decreasing watt-hour or ampere-hour capacity.

The cells were matched by preparing lists of cells in order of decreasing watt-hour and ampere-hour capacity and then comparing the relative location of cells on each ranking. Cells that had

significant ranking differences between the ampere-hour and watt-hour listings were subjected to further analysis by examining the charge and discharge voltage profiles. Cells whose characteristics varied from the typical cell characteristics were removed from the matching lists.

Actual cell selection consisted of the selected 24 cells from the watt-hour capacity list with a minimum spread in watt-hour capacity.

A quantity of 32 cells was procured for each battery. Since two batteries were packaged in one assembly, a minimum of 64 cells were placed on test at any one time. From these 64 cells, two groups of 24 cells were selected. The actual matching criteria was to obtain the lowest spread in watt-hour capacity for the cell group from the quantity of cells available. In many cases, higher capacity cells were rejected because a closer matching capacity could be achieved by using cells with a lower capacity.

Figure VI-4 shows the spread in capacity of 128 cells that were placed in the cell matching test program at the same time. Cells for four 24 cell batteries were selected from this group of cells. The initial cell capacities ranged from a low to 10.46 A-h to a high of 11.38 A-h. At the end of the matching cycles, the capacity had decayed to a low of 8.4 and a high of 9.8 A-h. The spread in capacity had increased from 0.92 A-h to 1.4 A-h and the capacity had decayed by approximately 1.6 A-h. It was observed that the low capacity cells had a high rate of capacity loss over the first twenty cycles while the high capacity cells had a lower rate of capacity loss.

The actual spread in ampere-hour capacity for each of the four batteries is shown in Figure VI-4 for the last matching cycle. The cells at the upper and lower ends of the capacity distribution were rejected since they were at the extremes of the distribution. Their use would have resulted in a higher capacity matching percentage.

Figures VI-5 and VI-6 show the spread in ampere-hour capacity at the last cycle for four battery groups as plotted on probability graph paper. This method of presentation provides information as to the spread in cell capacities and the percentage of cells within certain capacity ranges. The data on the two figures were obtained by selecting four groups of 24 cells from the 128 cells processed beginning at the high end of the cell capacities and working to the low end. Several selection iterations were made to optimize the cell matching percentage which resulted in rejecting cells at the high and low ends of the capacity spread. As an example, Figure VI-6 shows that for battery group number 4, the lower 50% of the cells were between 8.7 and 8.79 A-h with a spread of 0.09 A-h while the upper 50% were between 8.8 and 8.85 A-h with a spread of 0.05 A-h.

Variations between the cell ampere-hour and watt-hour rankings were minimal. Either method of selecting the cells could have been used with the same results; however, the watt-hour method was preferred since it takes into account the cell voltage characteristics. Table VI-8 shows the spread in watt-hours and ampere-hours capacity for 30 of the cells that were tested in one group. These cells were combined with 98 other cells at matching.

The capacity distribution plots shown in Figures VI-5 and VI-6 were obtained using cells matched to between 1.57 to 2.14% in A-h capacity. The cell capacity matching accuracy was found to be related to the number of cells available to choose from. When groups of 128 cells were processed at the same time, matching accuracies of between 1.5 to 2.5% were obtainable; however, when groups of 64 cells were processed the cell matching ranged between 2.0 to 3.5%.

After completing the matching cycles (step 4) and charge acceptance test (step 5), the cells were each deep discharged with a one-ohm load for 24 to 48 hr. An evaluation test was then performed to obtain performance data using the conditioning charge-discharge cycle and the recharge that was scheduled during the interplanetary cruise phase of the mission. This information was placed

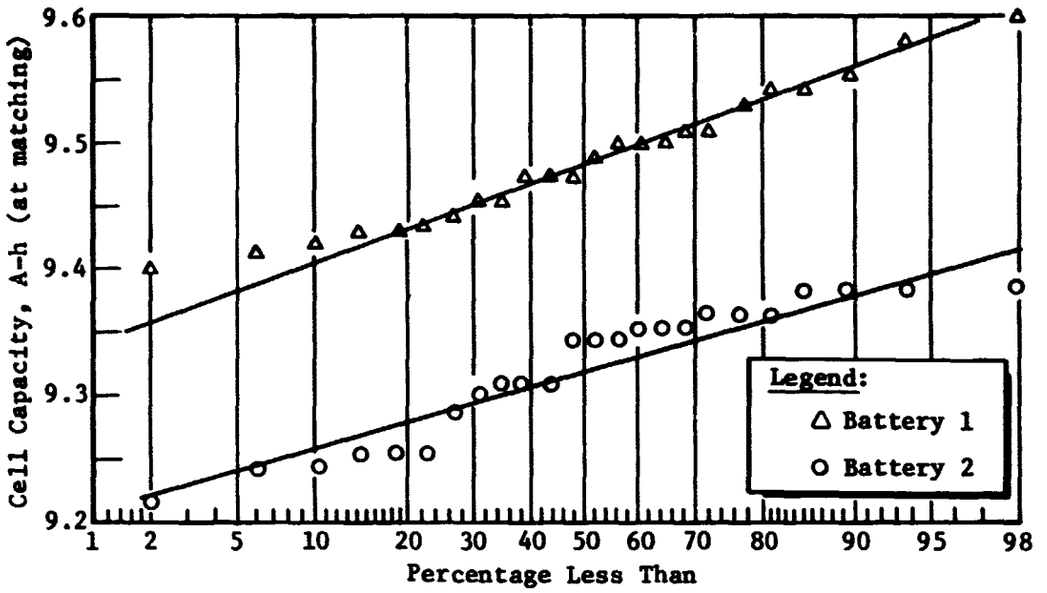

Figure VI-5 Cell Matching Capacity Spread (Batteries 1 and 2)

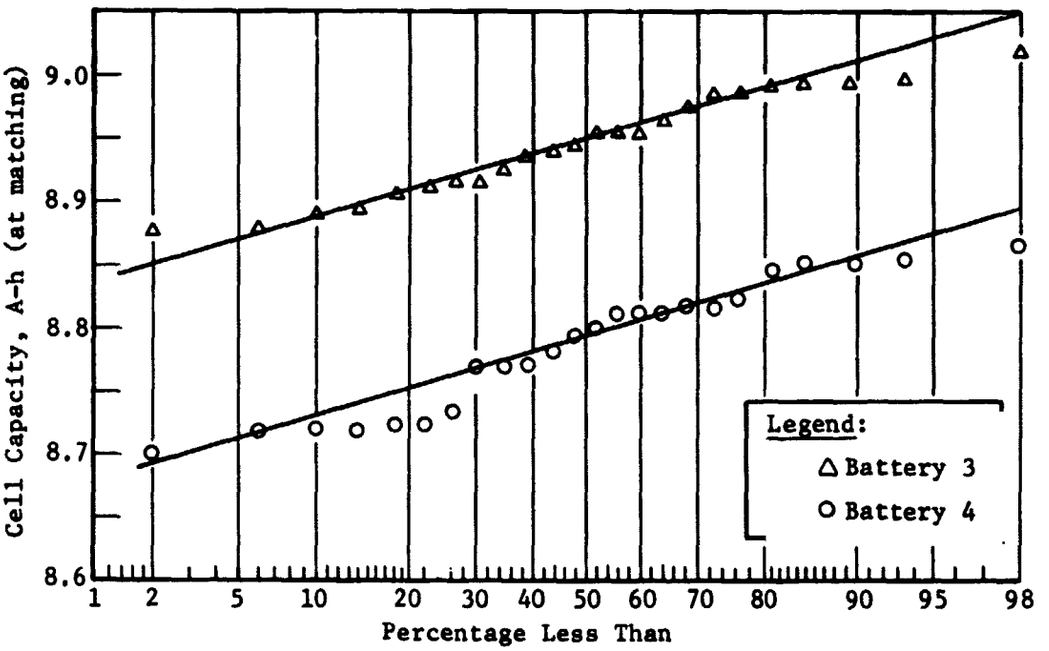

Figure VI-6 Cell Matching Capacity Spread (Batteries 3 and 4)

Table VI-8
W-h and A-h Capacity Spread for 30 Cells at the Time of Cell Matching from Computer Data Reduction Program

W-h	A-h
12.495	9.912
12.493	9.912
12.437	9.868
12.414	9.857
12.374	9.824
12.323	9.780
12.321	9.780
12.288	9.757
12.279	9.745
12.271	9.734
12.259	9.723
12.195	9.689
12.192	9.678
12.160	9.648
12.147	9.634
12.098	9.600
12.094	9.600
12.049	9.567
12.048	9.556
12.041	9.545
12.037	9.545
12.009	9.534
11.973	9.500
11.922	9.467
11.838	9.400
11.807	9.366
11.800	9.366
11.798	9.379
11.786	9.344
11.467	9.087

Average Cell Capacity

12.114 W-h
(Standard Deviation = 0.245 W-h)
9.613 A-h
(Standard Deviation = 0.195 A-h)

in a data bank for later analysis if the need arose. This test was inserted in the cell matching procedure to take advantage of the existing test setup which could readily accommodate the test requirements. The cells were discharged with a one-ohm load for 24 hr after the testing, and removed from the test setup in preparation for assembly into batteries. During battery assembly operations, the cells were in an open circuit condition.

The results of the cell matching program were considered excellent based on the performance of the battery during postmanufacturing assembly tests and again after the battery component sterilization. Discharge at a C/2 rate could easily be accomplished to a 27 V cutoff with some capacity remaining before a cell reversal would occur. During partial charging and discharging, the cells exhibited a very close capacity range. All flight batteries were delivered with a capacity exceeding 10.0 A-h at the beginning of life. Battery capacity exceeded the cell matching capacity due to several reconditioning cycles the cells received before assembly in a battery and as a prerequisite to sterilization.

VII. BATTERY DESIGN, FABRICATION, AND TESTING

A. BATTERY DESCRIPTION

The Viking battery uses 24 eight-ampere-hour cells to provide a bus voltage range from 27 to 34 V.

Two batteries were packaged into one assembly primarily due to the limited space available in the Lander. The battery assembly configuration is shown in Figure VII-1. The bottom, top, side plates, restraining bars, and connector bracket of the assembly were fabricated from HK31A-H24 magnesium alloy. This material was selected based on its weight and capability to withstand high temperature sterilization. Figure VII-2 shows an exploded view of the battery case.

Figure VII-3 shows a partially assembled prototype battery with a few cells in place. The 24 cells per battery were arranged in three stacks of eight cells each. The three stacks that comprised the cells for one battery were placed on one side of the divider shelf. The second battery was assembled on the opposite side of the shelf.

Thermal control was achieved by using the center shelf as the heat flow path to conduct the heat from the cell bases to the assembly base plate from which it was conducted into the Lander structure.

Three platinum resistance temperature sensors were provided for each battery. They were installed between the fourth and fifth cell in each of the eight-cell stacks. Two of the sensors had 1500-Ω elements and were used to supply a temperature compensation voltage for use by the charger control logic. The

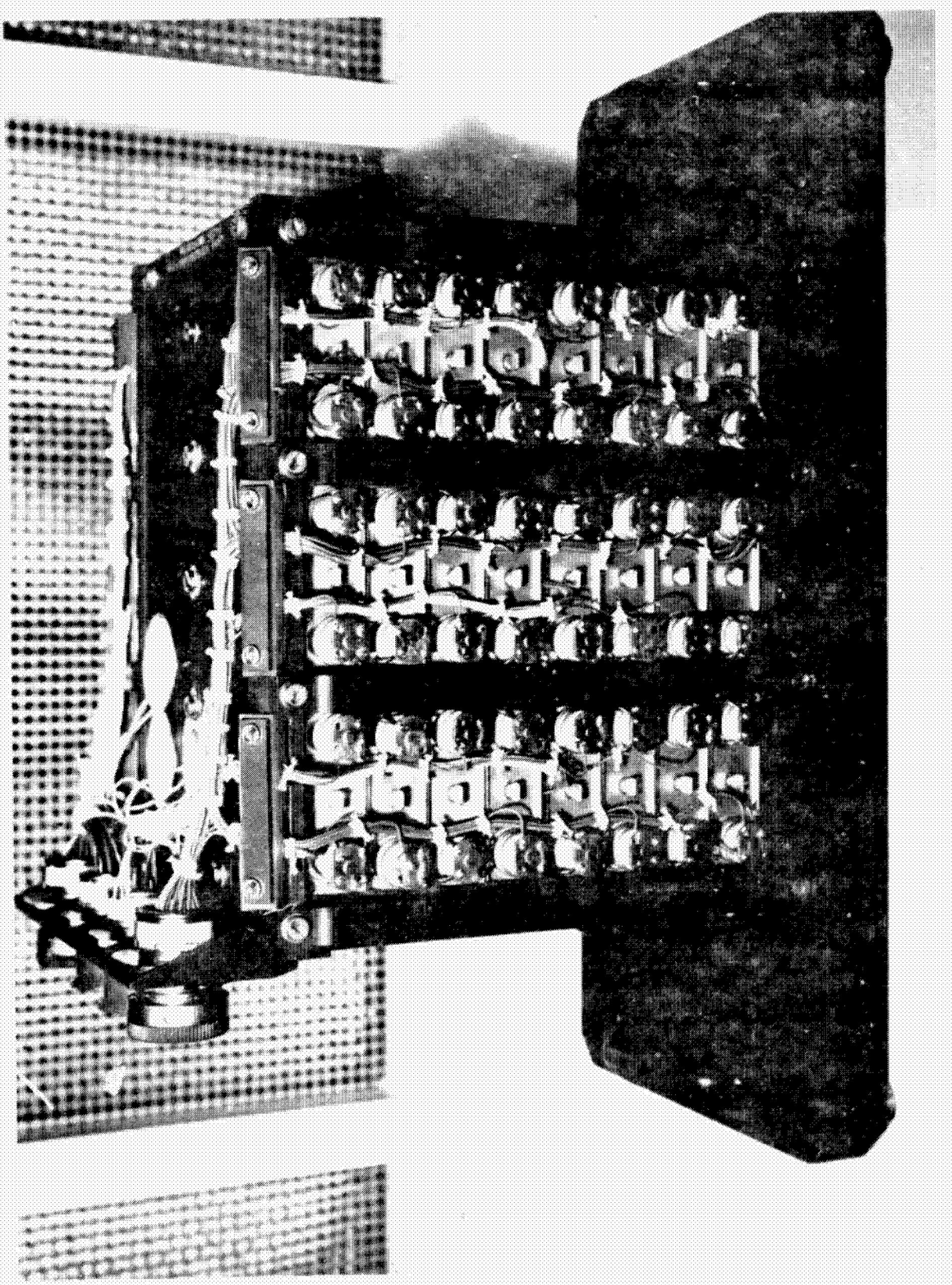

Figure VII-1 Battery Assembly Consisting of Two 24-Cell Battery Packs

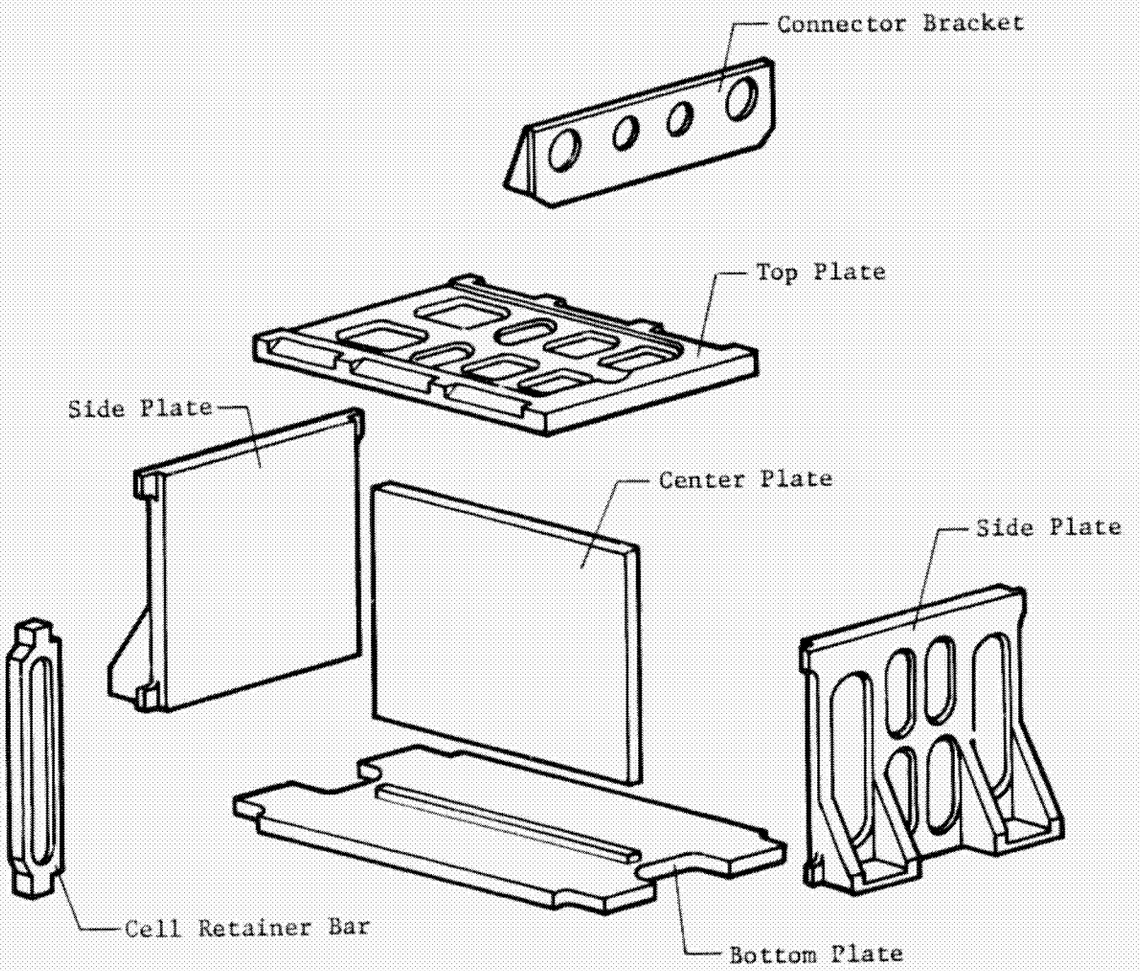

Figure VII-2 Battery Case (Exploded View)

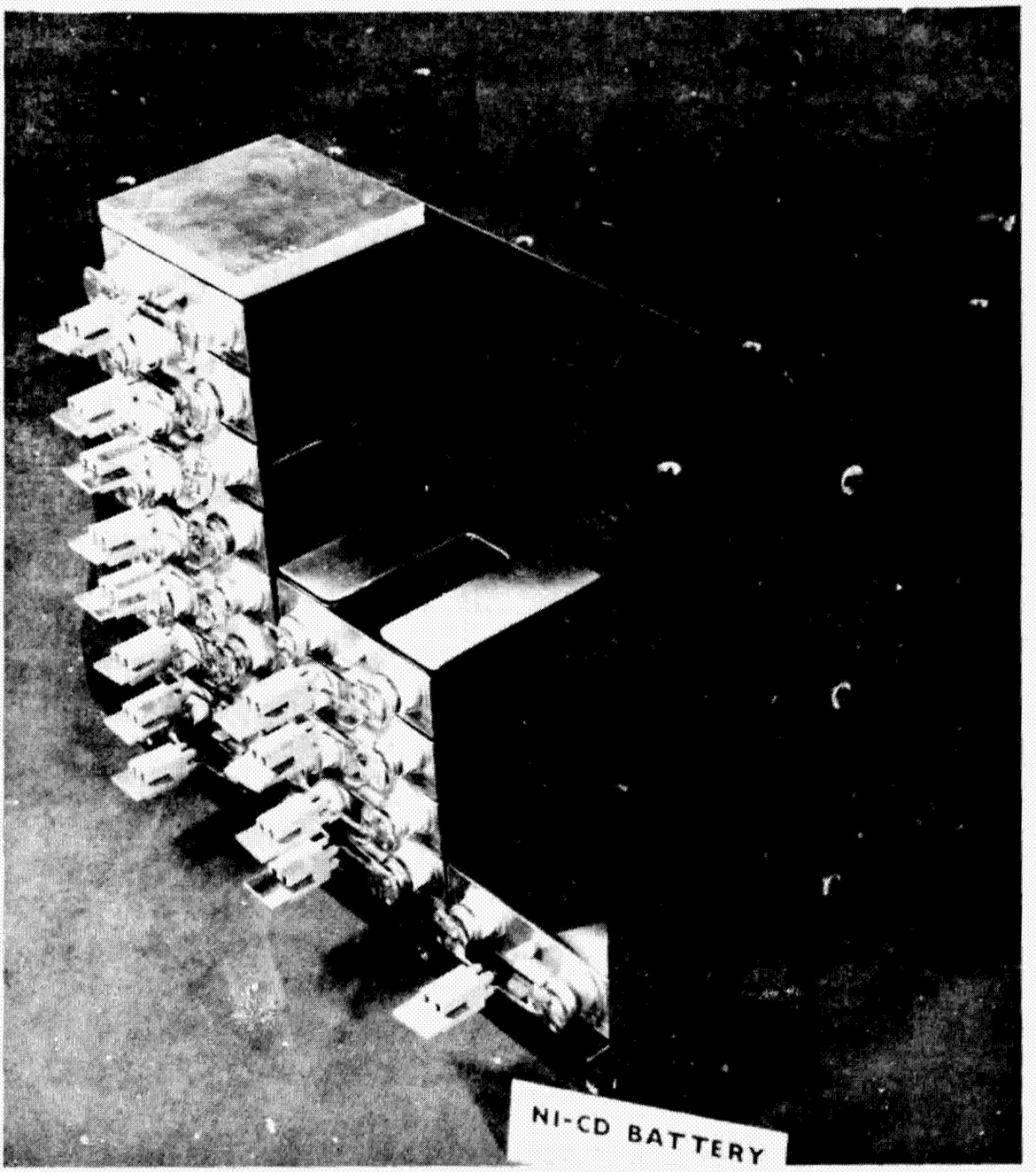

Figure VII-3 Prototype Battery Assembly Showing Cell Arrangement

charge control logic used the temperature data to generate a temperature-compensated end-of-charge voltage for the charge termination. The third sensor (a 150-Ω unit,) was used by the data acquisition system to acquire battery temperature data for transmittal back to the ground station via the telemetry system.

Separate power and checkout connectors were provided for each battery in the assembly. Redundant positive and negative power-carrying conductors were connected from the battery terminals to the power connectors; however, only one was used because a later requirement minimized weight on the landers. The power connectors also provided access to the platinum temperature sensors.

Individual cell voltage monitor circuits were provided to the connector. The connector was used by the computer-controlled test and data acquisition system to monitor the cell voltages during the postmanufacturing acceptance tests. This connector was also used for access to the cells to discharge them with one-ohm loads as required during the battery testing. During flight, this connector was not used and only the battery voltage and temperature were available for monitoring.

A structural analysis was performed on the redesigned battery assembly because the prototype hardware failed to withstand the sterilization temperature and the material was subsequently changed from AZ31B to a HK31A magnesium alloy. This analysis was made to identify the margin-of-safety in the design. During this analysis, it was determined that the worst-case conditions were:

1) Pressure loads during sterilization that are accompanied by a degradation in material properties at the elevated temperatures; and
2) Combined dynamic and preloading during Martian entry when the battery temperature is between 32.2 to 37.8°C.

Based on these conditions, a 413.7 kPa cell pressure and 75 g (75 g, Q = 10) inertial loading were used for the design loads.

The three factors we analyzed during the study are:

1) Material properties at sterilization temperatures;
2) Adequacy of load paths; and
3) Ability of fasteners to transmit induced loading.

B. BATTERY ASSEMBLY AND HANDLING

The sequence of operations for assembling the battery begins after the cell matching process is complete and 48 cells (24 cells per battery) have been selected.

Before assembly operation, an aluminum shim was epoxied in the cavity at the base of each cell using Dow Corning DC93-076 epoxy. This shim provided a heat transfer path through the cell base into the battery assembly structure. A 0.127-mm thick sheet of Kapton was cut to size and wrapped around the cell side walls to provide electrical isolation between adjacent cells and from the assembly structure. Dow Corning DC93-076 was used to glue the Kapton to the cell at the overlapping seam along one of the narrow edges.

Once the kapton insulation was installed, the eight cells in each stack along with the temperature sensor spacer were stacked in a pressure preload tool and preloaded to a pressure of 241 kPa (35 psi). This pressure was based on the results of a test to measure the deflection of a stack of eight cells when subjected to pressures from 0 to 482.6 kPa (0 to 70 psi). Figure VII-4 shows how the deflection varied as a function of the pressure. The 244 kPa (35 psi) pressure was selected based on the cell stack deflection and the battery chassis design considerations. Figure VII-5 shows the tool with eight cells in position ready for the preload. The dial indicator on the tool provides a direct readout of the shim thickness required. The distance that the cell stack moved from a reference height (the height of the bat-

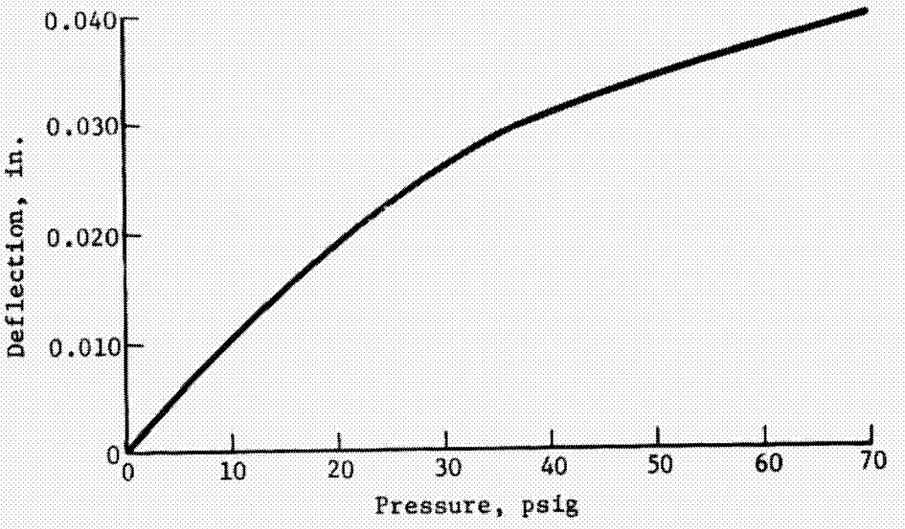

Figure VII-4 8-Cell Stack Preload Deflection

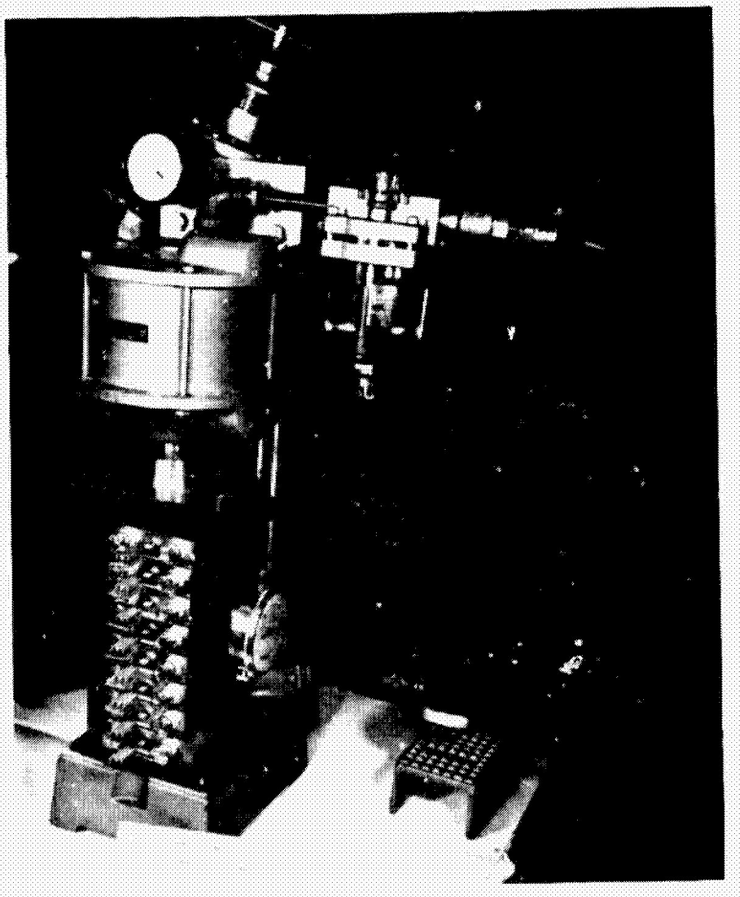

Figure VII-5 Cell Preload Tool

tery assembly shelf) was measured and used to select the thickness for an aluminum shim. This shim was placed on the cell stack before torquing the cover bolts and resulted in each cell stack being preloaded to the required pressure.

The assembly sequence consisted of: (1) bolting the center shelf to the base plate, (2) loosely bolting the two end plates to the base plate and center shelf, (3) coating one side of the center shelf with a thin layer of Dow Corning DC6-1104 epoxy. (This epoxy provided both electrical insulation and a heat transfer path from the cells to the shelf.) and (4) placing the cells from one of the three stacks in position and seating them against the epoxy and center shelf.

This process was repeated for the remaining cell stacks until all six stacks were in place. Teflon spacer strips were placed between the adjacent cell stacks and between the cell stack and side plates. At this point, the bolts holding the side plates to the center shelf were tightened. Before installing the top plate, the cell orientation was inspected to insure that the correct polarity sequence between adjacent cells had been observed. The six shims were then placed on their respective cell stacks, the cover placed in position, and the bolts sequentially torqued to the specified values. The assembly was visually inspected to insure that the cells were seated against the center shelf.

After the mechanical operations were complete, the epoxy was cured by exposing the battery assembly to a temperature of 18 to 24°C for 24 hr followed by a temperature of 54 to 66°C for six hours

Redundant intercell connectors and wiring were placed in position and soldered in accordance with soldering specification NHB 5300.4(3A). Electrical checks were performed throughout the assembly process to insure that 100 MΩ cell-to-cell and cell-to-battery chassis isolation was achieved using a 50-V meggohmmeter. A schematic of the 22-cell battery wiring is shown in Figure VII-6. This schematic is typical for both batteries in the assembly since the only difference is the connector clocking.

Eacn battery was returned to the battery and cell test facility after the manufacturing operations were completed for the electrical, sterilization, environmental exposure, and final electrical acceptance tests.

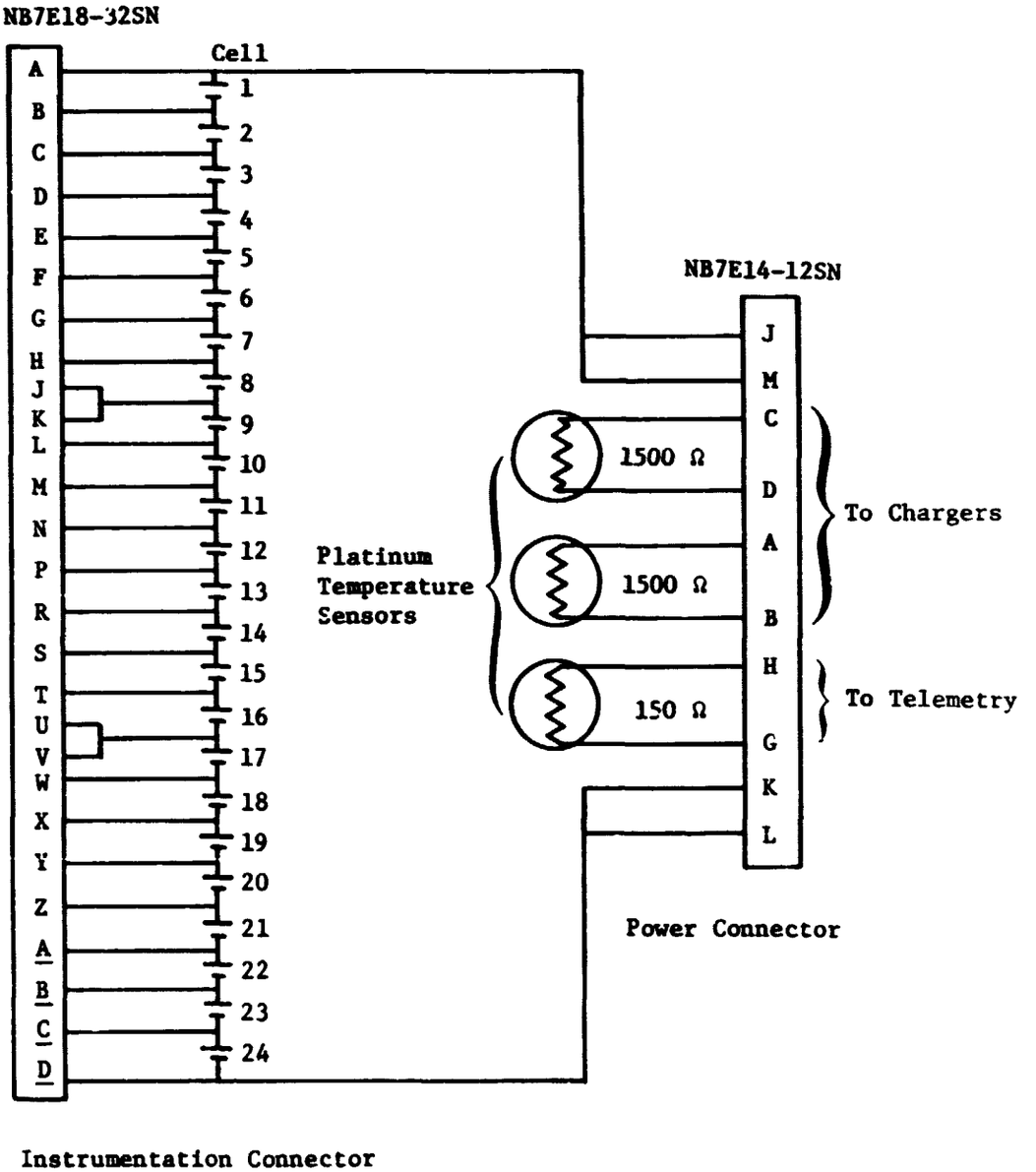

Figure VII-6 Battery Electrical Schematic

ACCEPTANCE TESTS AND PROBLEM SUMMARY

Martin Marietta separated the battery acceptance tests into five categories and performed them in the sequence listed:

1) Electrical performance,
2) Sterilization,
3) Poststerilization electrical performance,
4) Environmental acceptance tests, and
5) Final electrical performance test.

1. Postmanufacturing Electrical Tests

The postmanufacturing electrical tests consisted of a charge retention test followed by 10 charge/discharge cycles using a C/10 charge rate for 16 hr and a C/2 discharge.

The purpose of these tests was to (1) establish that the battery assembly techniques were satisfactory, and (2) establish electrical performance acceptance before performing the battery sterilization procedure.

The charge retention test was initially performed as the first step of the procedure; however, because a cell failed this test, we decided to subject the cells to one charge/discharge cycle before performing the test. This change was made to compensate for the variable discharged stand experienced by the cells during the battery assembly operations. This could range from several weeks up to two months depending upon the build schedule. The charge retention test is described in Section VI.

2. Sterilization

Sterilization of the flight hardware was accomplished in a thermally controlled test chamber under a dry nitrogen atmosphere. Temperature changes during start-up and cool-down were

limited to 29 to 32°C per hour. The batteries were maintained at the sterilization temperature of 111°C for 54 hr. Before the start of sterilization, the individual battery cells were discharged with one-ohm resistors for 24 hr by means of the checkout connector. The battery and cell terminals were in an open circuit condition during sterilization.

A leak test was performed after sterilization to determine if the high temperatures had introduced failures to the insulated terminals seals. A Q-tip was dipped in the phenophthalein solution and wiped around each terminal and stress relief collar. No leaks were detected on any of the 19 batteries tested.

Five charge-discharge cycles using the standard C/10 charge for 16 hr followed by a C/2 discharge to a battery voltage of 27 Vdc were performed to evaluate the electrical characteristic change induced by sterilization and the degree-of-recovery obtained by cycling. The elevated voltage during charge and the suppressed voltage during discharge that were observed during the prototype and development tests were present during the first charge-discharge cycle; however, the voltage deviation from the typical values was less for the flight batteries. This was due in part by incorporating a process to reduce the amount of potassium-carbonate introduced into the flight cell during manufacturing. This potassium-carbonate reduction also resulted in an increase (an average of 1 cc) in the quantity of electrolyte added to the cell. This also contributed to the improvement in the cell characteristics as evidenced by a lower charge voltage and higher discharge voltage after sterilization as compared to cells built before lot 6.

Only one electrical problem was encountered during the performance of the sterilization tests. One cell had an abnormally low voltage after sterilization cool-down was completed and the battery was ready for the cycle tests. All of the cell voltages recovered to approximately 0.2 V except for one which

remained at a few millivolts. A charge retention test was performed to determine if the cell had developed an internal leakage path; however, the cell passed this test. Subsequent cycling tests did not indicate any loss in performance or variation in electrical characteristics.

Table VII-1 shows the watt-hour and ampere-hour capabilities of a typical battery and its cells. These data are representative of a C/10 charge for 16 hr and a C/2 discharge to 27 V in a 21.1°C environment.

3. Environmental Acceptance Tests

Each battery was subjected (in a nonoperating discharged mode) to both a random and a sinusoidal vibration spectrum in each of three axes.

The sinusoidal vibration criteria were as follows:

Level: 5 to 15.5 Hz at 1.016 cm double amplitude,
15.5 to 250 Hz at 5.0-g peak;

Frequency: 5 to 250-5 Hz;

Sweep Rate: Four octaves/min, log sweep;

Over Acceleration Limiter: 6.5-g peak;

The random vibration spectrum used is shown in Figure V-40.

During the initial vibration testing on the flight batteries, a washer was discovered to be loose. An inspection of the assembly bolts revealed that the bolts holding the top and base plate to the center shelf and end plates had loosened. The remainder of the batteries were checked and it was found that the loss in torque occurred during the sterilization procedure.

As a result of this investigation, a change was made to the sterilization procedure to incorporate a test to check and readjust the bolt torques on all the assembly bolts after the sterilization process and before any charge/discharge cycle tests. It was noted that the battery capacity increased by several tenths of an ampere-hour after the environmental testing which was assumed to be caused by electrolyte redistribution during vibration.

Table VII-1 Battery and Cell Electrical Capabilities

	Charge C/10 for 16 hr at 21.1°C		Discharge C/2 to 27 V at 21.1°C	
	W-h	A-h	W-h	A-h
Battery	428.918	12.851	324.891	10.753
Cell	17.858	12.851	13.561	10.753
	17.857	12.851	13.558	10.753
	17.856	12.851	13.555	10.753
	17.850	12.851	13.555	10.753
	17.850	12.851	13.553	10.753
	17.850	12.851	13.552	10.753
	17.849	12.851	13.550	10.753
	17.848	12.851	13.547	10.753
	17.847	12.851	13.546	10.753
	17.847	12.851	13.546	10.753
	17.845	12.851	13.545	10.753
	17.844	12.851	13.542	10.753
	17.844	12.851	13.541	10.753
	17.842	12.851	13.532	10.753
	17.842	12.851	13.532	10.753
	17.841	12.851	13.531	10.753
	17.839	12.851	13.530	10.753
	17.839	12.851	13.526	10.753
	17.838	12.851	13.525	10.753
	17.838	12.851	13.517	10.753
	17.835	12.851	13.511	10.753
	17.835	12.851	13.505	10.753
	17.832	12.851	13.489	10.753
	17.831	12.851	13.470	10.753
	Average Cell Capacity		Average Cell Capacity	
	17.844 W-h (Standard Deviation = 0.007 W-h)		13.534 W-h (Standard Deviation = 0.023 W-h)	

4. Final Electrical Acceptance Tests

The final electrical acceptance test consisted of (1) a charge/discharge cycle to measure the battery capacity, (2) a simulated in-flight conditioning charge/discharge and (3) a recharge at a high rate (C/7.5). The batteries were required to deliver 9.0 A-h and 265-W-h as a condition for acceptance.

The standard C/10 charge for 16 hr followed by a C/2 discharge to 27.0 V was used to measure the battery capacity. This test was performed in a temperature-controlled chamber set at 21.1°C. Table VII-2 presents the capacities for the flight batteries and spares. The voltage profiles are shown in Figures VII-7 and VII-8.

Table VII-2
Flight Battery Acceptance Test Capacities

Battery Serial No.	Side A		Side B	
	A-h	W-h	A-h	W-h
20*	10.96	331.8	10.96	331.5
21	10.65	322.78	10.74	323.1
22†	10.78	329.07	10.54	319.36
23†	10.88	327.8	10.29	309.0
24	10.72	324.4	10.8	325.4
25*	10.78	328.05	10.77	324.87
26	10.58	319.94	10.36	312.4
27	10.46	316.73	10.25	308.5

*Installed on VLC-1.

†Installed on VLC-2.

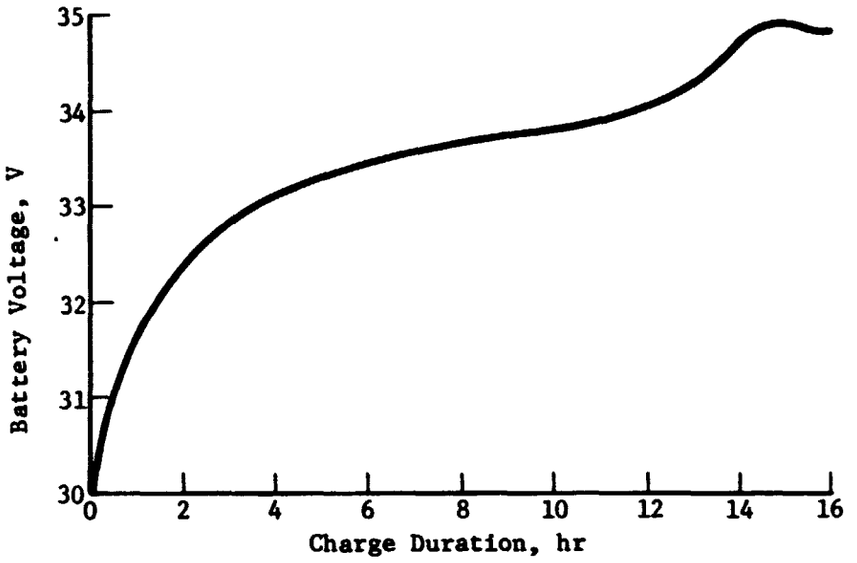

Figure VII-7
Typical Battery Acceptance Test Charge Voltage at a C/10 Charge Rate

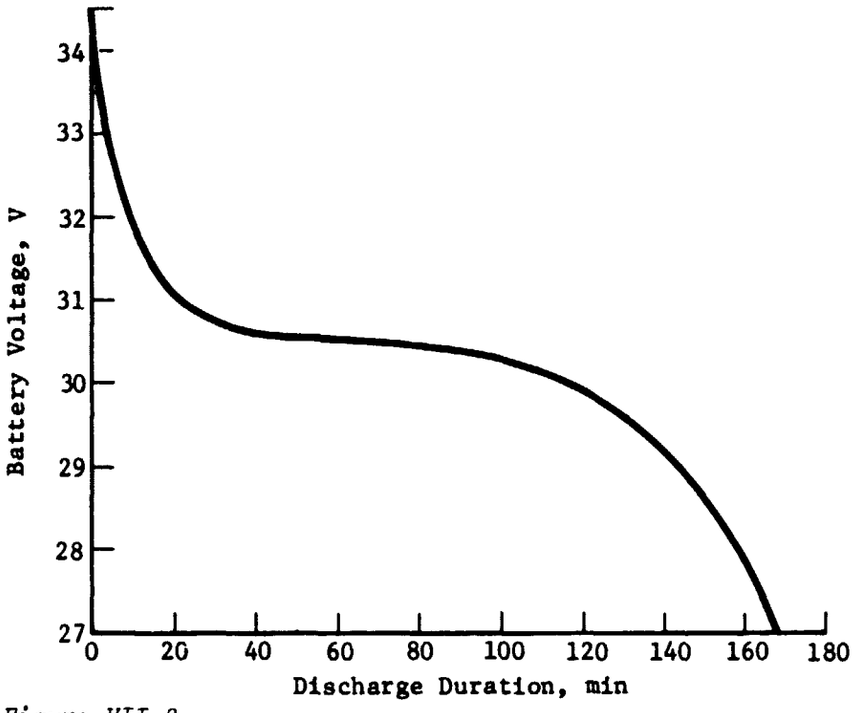

Figure VII-8
Typical Battery Acceptance Test Discharge Voltage at a C/2 Discharge Rate

The conditioning charge compatibility test was performed after the battery cells had been totally discharged with one-ohm resistors for 24 hr. A C/15 rate for 24 hr was used to charge the batteries. Each battery was then discharged at a C/6 rate for six hours to approximate the removal of eight ampere-hours. This simulated the anticipated depth-of-discharge that would be experienced during the in-flight conditioning. The battery was then recharged at a C/7.5 rate to a voltage cutoff of 35 V or a time limit of 10.5 hr to evaluate the high charge rate performance. The batteries were discharged at a C/2 rate to 27 V followed by a one-ohm per cell discharge for 24 hr in preparation for final cleaning and inspection before packaging the battery for shipment to the launch site. The batteries were shipped in a discharged open circuit condition in specially designed shipping containers.

At the time that the batteries were delivered and accepted as flight hardware, a total of 90 charge/discharge cycles had been accumulated. The cells were deep-discharged (less than 0.05 V) six times either to recondition the cells as a condition for handling or for sterilization. At the time of acceptance, the batteries delivered over 10 A-h.

VIII. SYSTEM INTEGRATION AND TESTING

This section describes tests performed at the system level, including tests conducted following the Lander assembly at Martin Marietta's Denver facilities using nonflight batteries. It also traces the history of the flight batteries from their arrival at Kennedy Space Center (KSC) through installation, sterilization, system test, and launch. Figure VIII-1 shows the flow sequence from cell manufacture through launch.

The Viking Lander batteries were required to be in a complete discharged state to withstand the heat sterilization cycle. Since this requires access to individual cells, which is not available once the battery is installed into the spacecraft, the batteries were discharged before shipment to KSC. They were then installed into the spacecraft in the completely discharged condition. Flight batteries were installed on each vehicle before final encapsulation and sterilization. System testing involving the flight batteries included battery conditioning, a power subsystem verification test, and a power transfer test.

A. SYSTEM TEST

Extensive system level testing was conducted throughout the program on the Viking Lander test and flight vehicles. This testing covered a period from 1973 through 1976. The majority of this system level testing was accomplished following the assembly of the Lander at Denver facilities using development and flight-type test batteries. Although the majority of these tests were oriented toward evaluating system and electronic component performance and interfaces, several significant factors were observed which affected the design and utilization of the batteries.

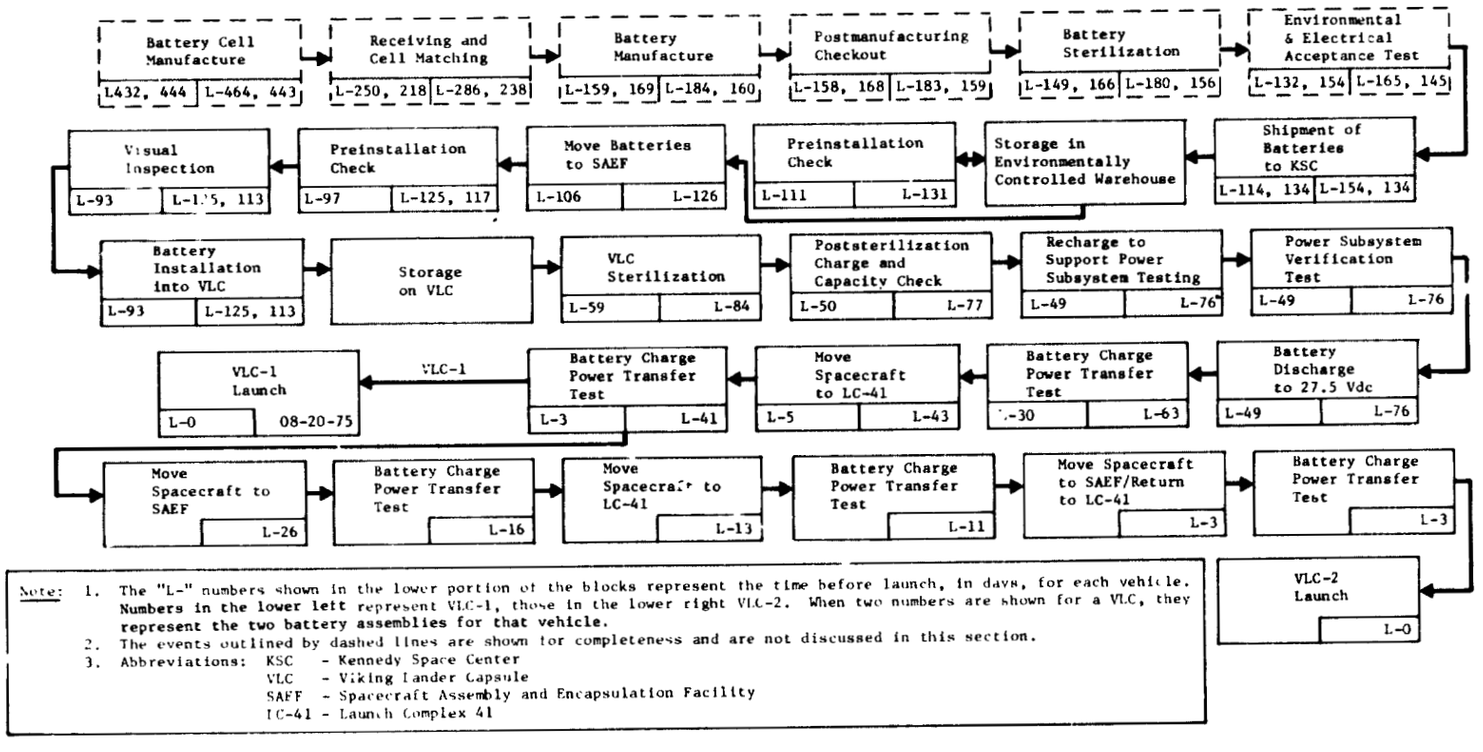

Figure VIII-1 VLC Flight Battery Flow Diagram

1. Ground Testing Problems

Batteries were used to support tests on the proof test capsule (PTC). This test vehicle was used for mission simulation testing and to evaluate the various test areas and configurations such as the thermal vacuum and environmental test facilities before usage by the flight vehicles. Before performing a mission simulation test, the batteries were removed for reconditioning and a capacity test. Reconditioning consisted of a discharge using one-ohm loads for each cell for a period of 24 hr or more. After reconditioning, it was found that one battery could not be charged due to the development of a high impedance. Cell voltages as high as seven volts were obtained at C/15 charge rates. A review of the battery usage history indicated that the battery had received very little cyclic use. The battery was left in a charged, open circuit condition for long periods of time (1 to 6 weeks or more). Infrequent recharging replaced energy lost due to self-discharge and the drain due to either a 19,300 Ω telemetry load or 7000-Ω combined telemetry and ground support instrumentation isolation resistors.

A failure analysis was performed on several of the high impedance cells to verify this conclusion. The results of the failure analysis activity are discussed in Section IX. As a result of this analysis, we concluded that the cell separators had dried out due to the electrical inactivity and the deep discharge which consumes water and produces the highest electrolyte concentration.

During the checkout and acceptance testing of VLC-2, there were several months when there was very little battery usage activity. During this period, the batteries were installed in the vehicle and connected to the electrical subsystems. The only load on the batteries during this time was the 19,300-Ω telemetry isolation resistor. At the conclusion of this period,

the batteries were placed in use with only one battery exhibiting a low voltage on discharge. The battery was removed from the vehicle and sent to the battery lab for analysis where it was found that cell number 24 was nearly discharged while the remaining cells were at a full state-of-charge. Failure analysis showed that the probable cause for the discharged condition was due to the presence of a piece of contaminant between a separator bag and a positive plate. This introduced a high impedance leakage path causing the cell to discharge during the long period of inactivity. Further evidence indicated that the cell was probably reversed when the battery was used after testing resumed. Details of the battery laboratory investigation and failure analysis are presented in Section IX.

It should be noted that the cell had received a charge retention test at receiving inspection and again after the cell matching program was completed during battery fabrication without detecting the presence of this leakage path. This test was repeated as a part of the failure analysis and again the cell passed the 1.16 V criteria after a 24-hr open circuit stand.

Battery Design Change

A design change was made to the batteries to provide protection against shorts to the exposed terminals due to inadequate space for installing components and the possibility of thermal insulation coming loose. This change was made because a connector was dropped by a technician and allowed to contact the exposed terminals. This momentarily created a short circuit on a test support battery. The change consisted of applying 0.0127-cm sheet of Kapton between the cell restraining bars to protect the terminals. The Kapton sheet was clamped under the cable clamp at one end and taped to the battery base plate on the other end.

B. FLIGHT BATTERY HANDLING, INSTALLATION, AND TEST

Four flight battery assemblies and two spares arrived at KSC during April and May of 1975. The batteries, in their shipping containers, were stored at room temperature in a temperature- and humidity-controlled storage area. Storage life was limited to 24 months from the time of acceptance. In early May, the batteries were removed from their shipping containers on a laminer flo clean bench for a preinstallation check. This check consisted of a room temperature verification of both the telemetry and charge control temperature sensors and a check of the open circuit battery and cell voltages.* The check showed battery voltages ranging from 28.3 to 29.0 Vdc and a maximum spread of 17 mV between the cells of any given battery. The batteries were reinstalled in their shipping containers and in mid-May were shipped to the Spacecraft Assembly and Encapsulation Facilities (SAEF) for installation into the two Viking spacecraft.

1. Inspection, Test and Installation

Once in the SAEF cleanrooms, the batteries were again removed from their shipping containers. A final open circuit voltage check and visual inspection was conducted just before installation. In all cases, the open circuit voltages were consistent with the previous check. The batteries were then installed into the Viking Landers according to the mechanical installation procedure. The Viking Lander battery assemblies were installed into the Lander body from below with the aid of a hydraulically operated platform which was used to raise and position the assemblies until the mounting bolts were positioned and secured. Figure VIII-2 shows two battery assemblies as installed in a Viking Lander. When the mechanical installation was completed, the Lander wiring

*The time interval between the removal of the cell shorts before packing and shipping and the performance of this check ranged from 30 to 60 days.

Figure VIII-2
Flight Battery assembled as Installed in the Viking Lander (Other Side Inboard)

harness was mated to the battery assemblies. Electrical connection of the batteries were verified by a check of the battery temperature and open circuit voltage through the Viking Lander telemetry system. Figure VIII-3 shows a simplified schematic of the Viking Lander power system. The 19.3-kΩ resistors connected between each battery output and ground are used to provide a battery voltage signal to the telemetry system. These resistors also provide a means for maintaining a quasi-short condition on the batteries during Lander sterilization and during the cruise phase of the mission.

2. Poststerilization Capacity Test

Following sterilization of the Viking Lander Capsules (VLC) for 30 to 36 hr at 111.6°C, the batteries were charged (using ground charging equipment) for 24 hr at 0.533 A (C/15). The batteries were then discharged at 4.0 A (C/2) to a voltage of approximately 27.5 to 27.8 Vdc. The capacities delivered by the eight flight batteries on this discharge ranged from 9.4 A-h to 10.04 A-h. Considering the battery sterilization, low charge rate, and battery charge temperatures these capacities compared favorably with the battery acceptance capacities. The batteries were recharged, again with the ground equipment, at 0.8 A (C/10) to a temperature compensated cutoff voltage and discharged at 4.0 A (C/2) for five minutes in preparation for the power subsystem verification test.

3. Power Subsystem Verification Test

The power subsystem verification test, (conducted in late June and early July, 1975) was a part of the VLC poststerilization testing. The portion of this test involving the batteries was verification of the battery charger interface and a functional check of the charge control logic. The [illegible] of charging each battery at 1.06 A (C/2.5) to [illegible] temperature compensated

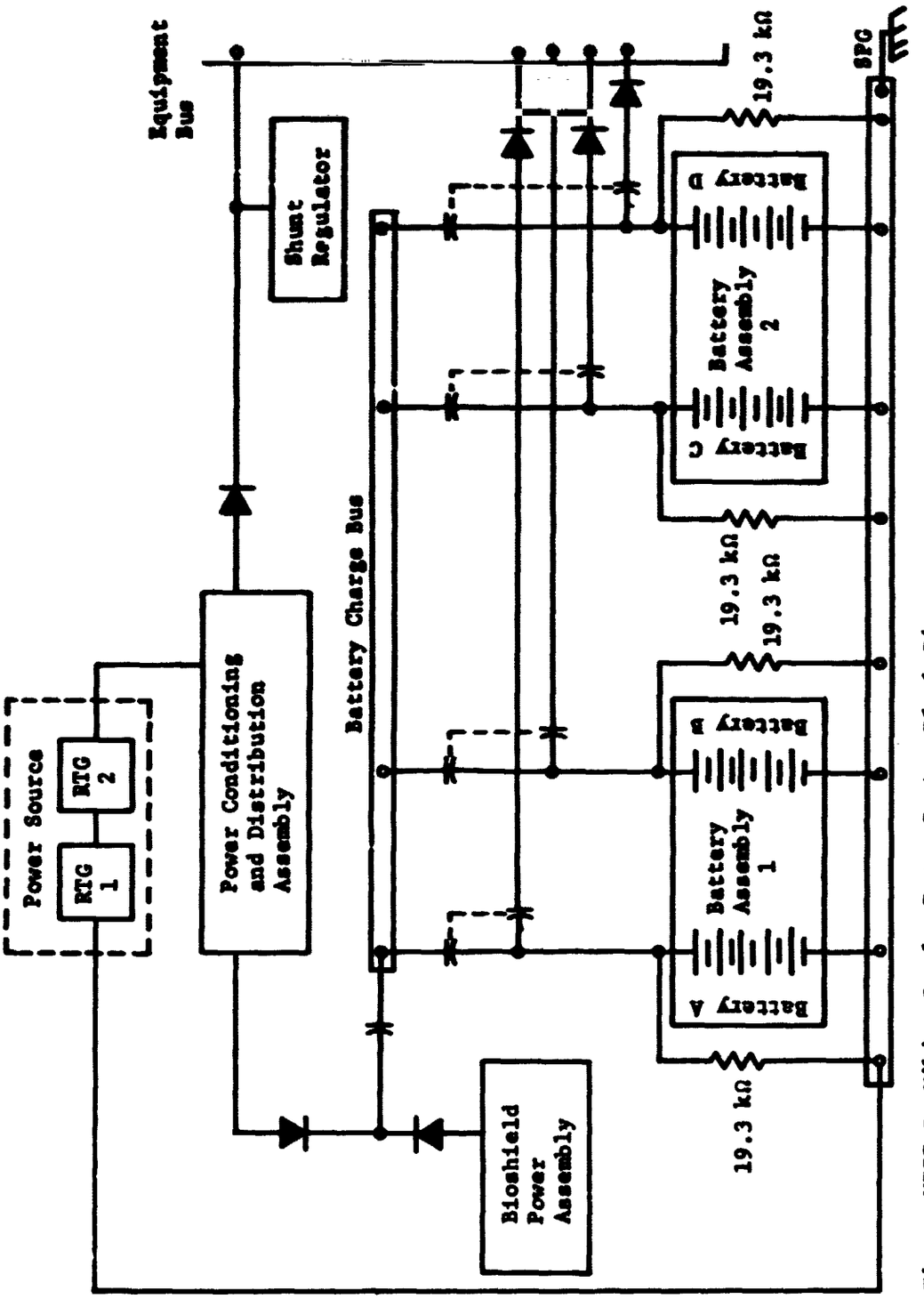

Figure VIII-3 Viking Lander Power System Block Diagram

Figure VIII-3

cutoff voltage. The test was performed twice on each battery to verify the redundant charger circuits. During this test, a failure was discovered in the charge control temperature sensor circuit of a battery in VLC 2. Since replacement of the battery would have required resterilization and retest of the Viking Lander, the decision was made to modify the flight software to use the redundant charge control circuitry and temperature sensor for control of that battery rather than replacing the battery. No other power system anomalies were discovered. Following this power system verification, all the batteries were discharged (using ground equipment) at 4.0 A (C/2) to approximately 27.5 Vdc. Two of the batteries on VLC-1 delivered 9.29 and 9.93 A-h on discharge. The remaining two batteries on VLC 1 delivered 8.8 A-h and 8.6 A-h. This lowered capacity was attributed to the fact that all four VLC 1 batteries were inadvertently placed on the charge bus in parallel for approximately 10 hr after the first two had been discharged. This caused the two remaining charged batteries to discharge into the previously discharged batteries.

4. Battery Charge and Power Transfer Test

The last battery-related test performed before launch was the battery charge/power transfer test. This test provided a final verification of the power system operation and involved a transfer to the internal Lander power source (the RTGs) and a short battery charge/discharge/charge sequence. The test used only two of the four batteries on each VLC. It consisted of a 15-min charge at 1.063 A (C/7.5), a 30-sec discharge at approximately 1.0 A and a 10-min charge at approximately 1.0 A. This test was conducted twice on VLC 1 and five times on VLC 2 due to launch delays.

The battery states-of-charge at launch, assuming zero state-of-charge for a battery discharged to 27.5 Vdc, are summarized in Table VIII-1.

Table VIII-1 Battery, State-of-Charge at Launch

Spacecraft	Battery A	Battery B	Battery C	Battery D
VLC-1	0.34 A-h	0.33 A-h	0 A-h	0 A-h
VLC-2	0.70 A-h	0.76 A-h	0 A-h	0 A-h

This estimate does not include losses due to self-discharge but does include the estimated losses due to discharge through the telemetry resistor. The discharge through the telemetry resistor will continue after launch until all batteries are completely discharged.

IX. ENGINEERING EVALUATION TESTING

A. ENGINEERING TESTS

As is the case with most battery development programs, a number of tests are performed which fall outside the formal test requirements for qualification. These tests supply valuable information as to the cell and/or battery performance for specific usage conditions. A summary of these tests and test results is included in this section. Several problems were encountered throughout the program which resulted in failure analysis activity. The results of these investigations are discussed herein.

1. Thermal Characterization

A series of thermal evaluation tests were performed using simulated batteries (cells installed in restraining fixtures) to develop analytical data for preparing a computer model of the batteries. This model was used as part of a larger computer program which modeled the thermal response of the lander vehicle.

During the tests, the battery was installed in a temperature-controlled chamber with forced air circulation. Baffels were used to limit the air flow over the battery to simulate the same temperature profile experienced by the batteries during the in-flight conditioning charge on the landers.

A series of charge-discharge cycles were performed on these two batteries using several charge rates, charge durations, and beginning of charge temperatures. All discharges were made at a C/2 rate to a battery cutoff voltage of 27.0 V. Tables IX-1, IX-2, IX-3, and IX-4 summarize the test results including temperature rise during charging, watt-hour efficiency, and ampere-hour capacity obtained for each test.

The efficiencies shown in Tables IX-1, IX-2, IX-3, and IX-4 were calculated using an estimated watt-hour discharge efficiency of 88%. This value was based on the results of the thermal

Table IX-1 Thermal Test Data for C/15 Charge Rate

Initial Temperature, °C	End Temperature, °C	Δ Temperature, °C	Charge Time, hr	W-h In	W-h Out	W-h Loss During Charge	W-h Charge Eff, %	A-h Out
23.3	28.9	5.6	24	422.8	304.4	77	82	10.1
28.3	33.9	5.6	24	424.8	289.1	96.4	77	9.58
29.4	37.2	7.8	24	416.2	248.7	133.7	68	8.29
34.4	41.7	7.3	24	419.7	190.7	203	52	6.41
32.2	40.6	8.4	20	344.5	187.2	131.8	62	6.28
34.4	41.1	6.7	16	273	169.2	80.7	70	5.68
21.6	28.9	7.3	24	430.4	304.1	84.8	80	10.1
21.6	26.1	4.5	22	385.9	287.1	59.7	85	9.52
21.6	25	3.4	20	350.6	279.5	33	90	9.26
21.1	23.3	2.2	18	315.9	258.9	21.7	93	8.56
27.2	33.3	6.1	24	422.9	275.1	107	75	9.0
27.7	31.1	3.4	20	347.1	250.5	61	82	8.28
27.22	30	2.78	16	277.7	218.3	33	88	7.22
4.44	7.22	2.78	20	337	264	37	89	8.56
5	7.2	2.2	16	286	242.6	10.6	96	7.15

Table IX-2 Thermal Test Data for C/10 Charge Rate

Initial Temperature, °C	End Temperature, °C	Δ Temperature, °C	Charge Time	W-h Charge	W-h Dis-charge	W-h Loss During Charge	W-h Charge Eff, %	A-h Out
4.44	6.67	2.23	12	316.2	254.6	28.0	91.2	8.35
4.44	8.33	3.89	16	310.0	254.0	24.0	92.2	8.34
15.56	18.9	3.34	12	326	261	29	91	8.6
15.56	19.4	3.84	16	357	264	57	84	8.68
23.9	25	1.1	8	211.95	182.8	--	100	6.03
23.9	27.8	3.9	12	319.9	251.8	33.8	89.4	8.31
23.9	35	11.1	16	428.2	274	117	73	9.02

Table IX-3 Thermal Test Data for C/7.5 Charge Rate

Initial Temperature, °C	End Temperature, °C	Δ Temperature, °C	Charge Time	W-h Charge	W-h Dis-charge	W-h Loss During Charge	W-h Charge Eff, %	A-h Out
23.9	31.1	7.2	10.5	376.4	277.5	61.0	83.7	9.17
23.9	25	1.1	7.5	264.1	227.1	6.0	97.7	7.51
23.9	23.9	0	5	174.6	157.7	----	100.	5.23
29.4	40	10.6	10.5	371.5	258.2	78.1	78.97	8.57
29.4	33.9	4.5	7.5	263.2	212.4	21.9	91.68	7.04

Table IX-4 Thermal Test Data for a C/5 Charge Rate

Initial Temperature, °C	End Temperature, °C	Δ Temperature, °C	Charge Time	W-h Charge	W-h Dis-charge	W-h Loss During Charge	W-h Charge Eff, %	A-h Out
23.9	26.1	2.2	8	341.5	268.3	36.7	89.2	8.84
23.9	26.1	2.2	6.5	333.5	268.1	28.8	91.35	8.83
23.9	25.5	1.6	5	265.0	227.6	6.4	97.6	7.49
29.4	40	10.6	8	430.1	271.6	121.5	71.6	9.03
29.4	36.1	6.7	6.5	346.6	260.1	50.6	85.5	8.63

efficiency tests discussed in Section V (see Figs. V-28, V-29, and V-30).

The watt-hour (W-h) efficiencies are based on the following relationships:

[1] $$\eta_C(\text{W-h}) = \frac{\text{W-h}_C - \text{W-h}_{TLC}}{\text{W-h}_C} \times 100$$

Where

$\eta_C(\text{W-h})$ = Watt-hour charge efficiency in percent.

W-h_C = Watt-hours supplied to the battery during charge.

W-h_{TLC} = Thermal losses during charge (W-h) including energy from oxygen recombination. The watt-hour discharge efficiency, $\eta_d(\text{W-h})$ is calculated using the following relationship:

[2] $$\eta_d = \frac{\text{W-h}_d}{\text{W-h}_d + \text{W-h}_{TLD}} \times 100$$

Where

W-h_d = Watt-hours supplied to the load.

W-h_{TLD} = Thermal losses in battery during discharge (W-h).

Multiplying equations 1 and 2 together gives the cycle efficiency:

$$\eta_C(\text{W-h})\,\eta_d(\text{W-h}) = \frac{\text{W-h}_d\left(\text{W-h}_c - \text{W-h}_{TLC}\right)}{\text{W-h}_c\left(\text{W-h}_d + \text{W-h}_{TLD}\right)}$$

Which reduces to

$$\eta_C(\text{W-h})\,\eta_d(\text{W-h}) = \frac{\text{W-h}_d}{\text{W-h}_c}$$

since

$$\frac{\text{W-h}_C - \text{W-h}_{TLC}}{\text{W-h}_d + \text{W-h}_{TLD}} = 1$$

The term $\frac{\text{W-h}_d}{\text{W-h}_c}$ is defined as the watt-hour cycle efficiency $\eta_{\text{W-h}}$

which gives

[3] $$\eta_{W\text{-}h} = \eta_C(W\text{-}h)\,\eta_d(W\text{-}h)$$

and

[4] $$\eta_{W\text{-}h} = \frac{W\text{-}h_d}{W\text{-}h_c}$$

During the testing, both the ampere-hours supplied during charge and discharge were recorded and the corresponding watt-hours calculated. Using these values, the watt-hour cycle efficiency is calculated using Equation 4. Finally the watt-hour charge efficiency is calculated using Equation 3. The ability to use these equations is dependent on the availability of the watt-hour discharge efficiency, which must be determined using techniques similar to those discussed in Section V.

Three temperature profiles for a C/15 charge in ambient temperatures of 23, 28 and 34°C are shown in Figure IX-1. The capacity available after a C/15 charge for 24 hr is plotted as a function of the end-of-charge temperature in Figure IX-2. Over the temperature range of 28 to 41°C, the data show a capacity reduction of 3.8 A-h.

2. Cruise Mode Test

Approximately six months before launch, a program decision was made to activate the Lander and perform an in-flight checkout of the various subsystems and experiments. This exercise was tentatively set at approximately 100 days after launch.

Up to this time, the total battery development and qualification effort was based on the premise that the batteries would remain in a totally discharged condition until just before Mars orbit insertion (MOI). This operating mode was selected based on the requirement to have the maximum amount of capacity available during the entry and landing sequence.

Since the in-flight checkout test was a departure from the established operating sequence and could introduce degradation

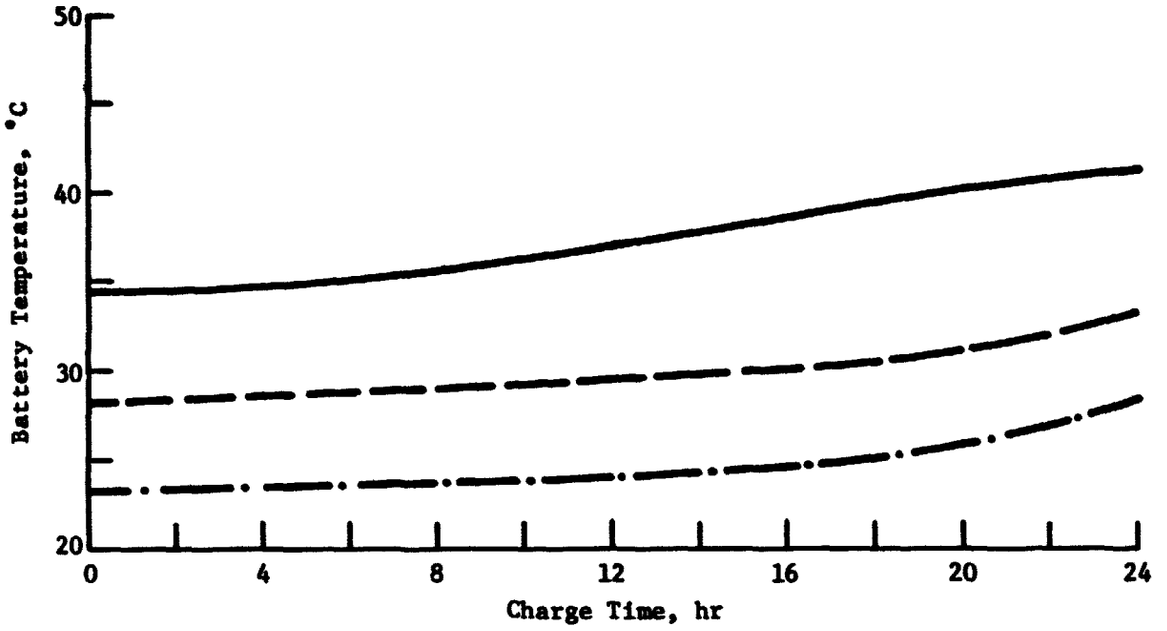

Figure IX-1
Battery Temperature Rise for Three Starting Temperatures at a C/15 Charge Rate (Simulated Viking Thermal Conditions)

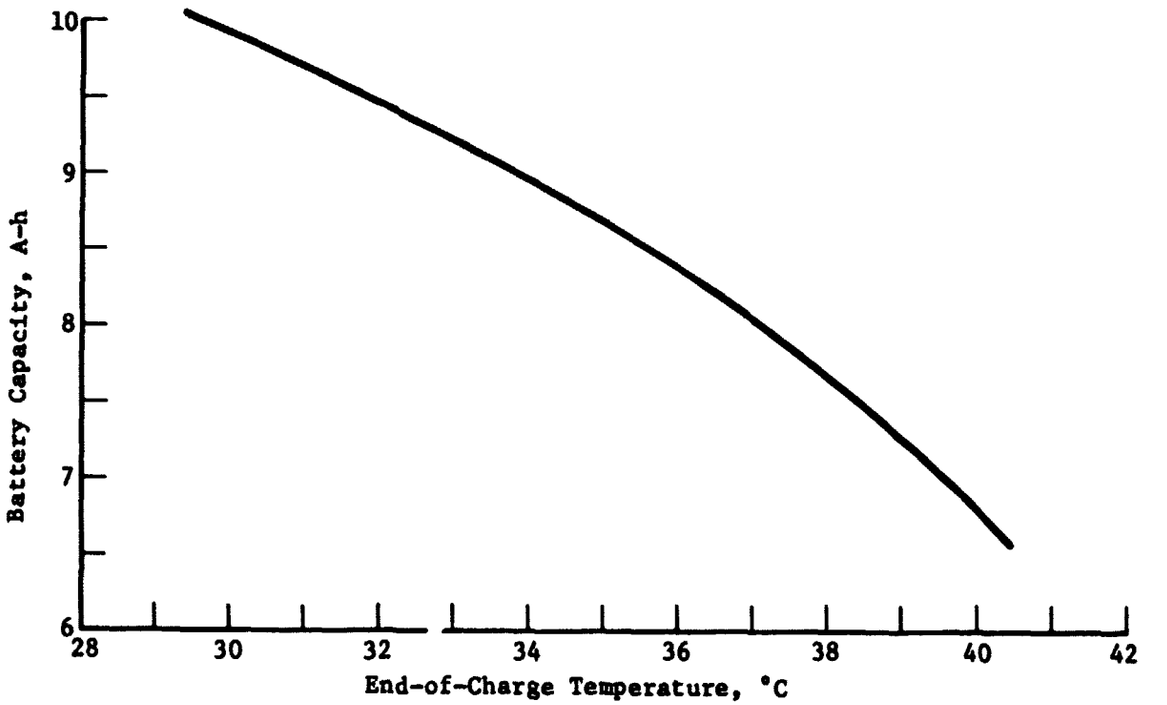

Figure IX-2
Battery Capacity Available after C/15 Charge for 24 hr for several End-of-Charge Temperatures

in subsequent battery performance, it became necessary to perform a simulation test to evaluate the degree-of-degradation introduced.

The test sequence consisted of alternating periods of discharging and charging intermixed with periods of open circuit stand which simulated the cool down periods required to maintain thermal control on the Lander. Discharge rates and depth-of-discharges were adjusted to track the projected in-flight conditions. At the conclusion of the checkout sequences, the battery was recharged and then discharged to remove eight A-h. The discharge voltage profile is shown in Figure IX-3. For 70 days following the final discharge, the battery was allowed to stand in an open circuit condition with a 19,300-Ω resistor slowly draining off the remaining energy in the battery. The intent of this last test step was to determine if the battery would be reconditioned by the slow discharge over the 70-day period to a battery voltage less than 27 V. At the end of the 70 days stand, the battery open circuit voltage was 29.18 V which indicated the stand time was not long enough to totally discharge the battery. However, the recharge and discharge (Figs. IX-4 and IX-5) performed at the end of the 70-day period did prove that the battery performance capabilities had not degraded since the battery delivered 10.2 A-h and the discharge voltage profile was not depressed. It was concluded that a major portion of the capacity remaining in the battery at the start of the 70-day stand had been discharged and the battery was effectively reconditioned even though the battery voltage did not decay below 29.18 V. No problems were encountered in supplying the energy for each of the checkout test sequences. Temperature excursions during charge and discharge were within the allowable limits.

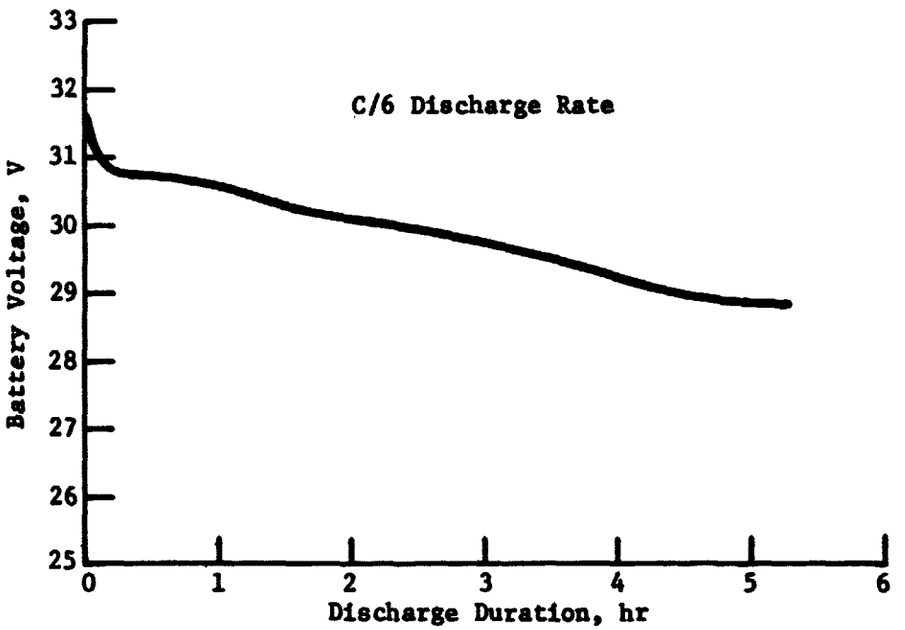

Figure IX-3 C/6 Discharge at End-of-Inflight Checkout Simulation

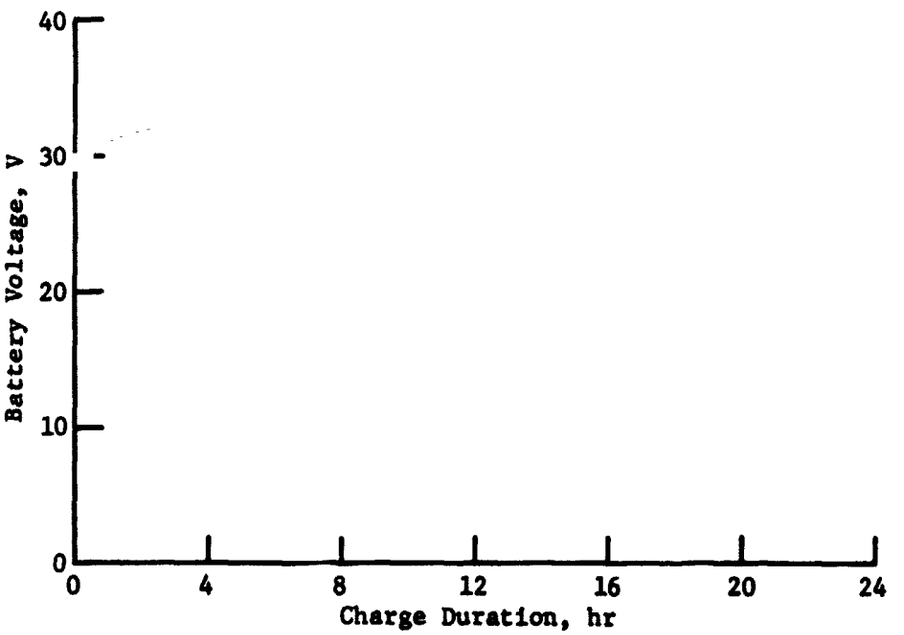

Figure IX-4
C/15 Conditioning Charge after 70-Day Discharged Open Circuit Stand

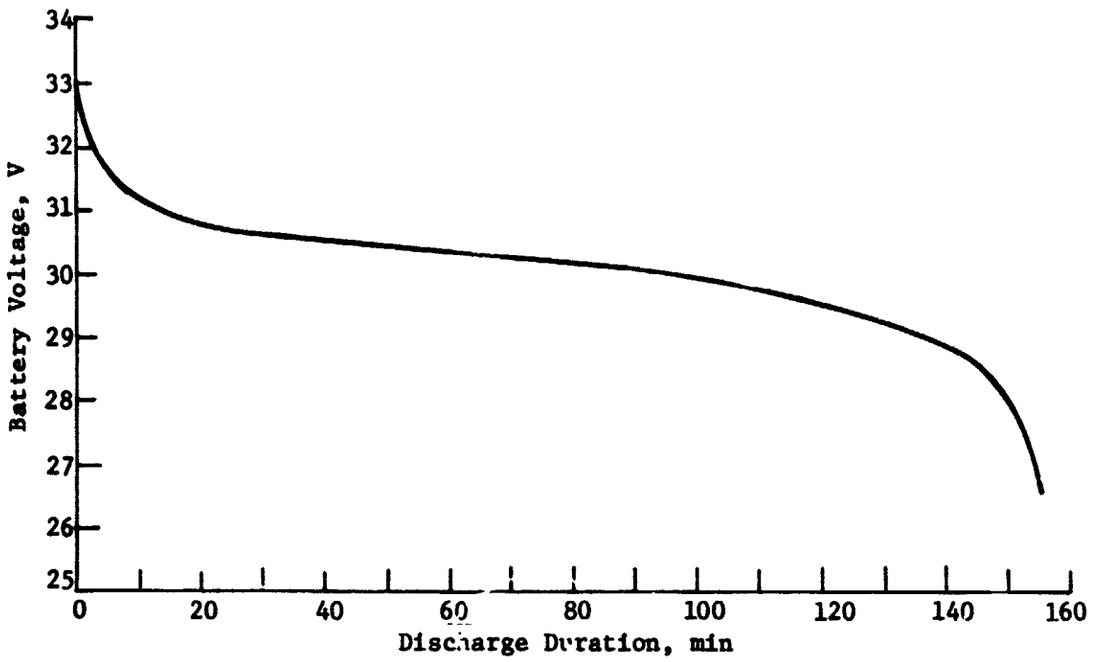

Figure IX-5 C/2 Discharge Following 70-Day Conditioning Charge

3. Self Discharge

As a result of the change in mission sequence to incorporate an in-flight checkout and experiment bakeout period, the self-discharge rate of the batteries became an important variable in determining the state-of-charge and depth-of-discharge for the various programmed sequences. Fifteen spare cells remaining from the flight battery production were placed in a self-discharge test. The cells were cycled to determine their capacity and then grouped into three 5-cell groups with similar capacity ratings. Each group was sterilized at 111°C for 54 hr. They were then placed in a charge/discharge program to determine their capacity using a C/2 charge to a 1.48 V cutoff followed by a C/2 discharge to 1.0 V per cell. After eight cycles the capacity variation between cycles had stablilized at approximately 10.3 A-h. The cells were charged at the C/2 rate to 1.48 V and then placed in an open circuit stand in a 21.1°C environment. At the end of 30 days, one 5-cell group was discharged, and the average capacity calculated. The second 5-cell group was discharged in 60 days and the last group

at 96 days. The resulting self-discharge curve for a 21.1°C environment is shown in Figure IX-6. The test data are given in Table IX-5.

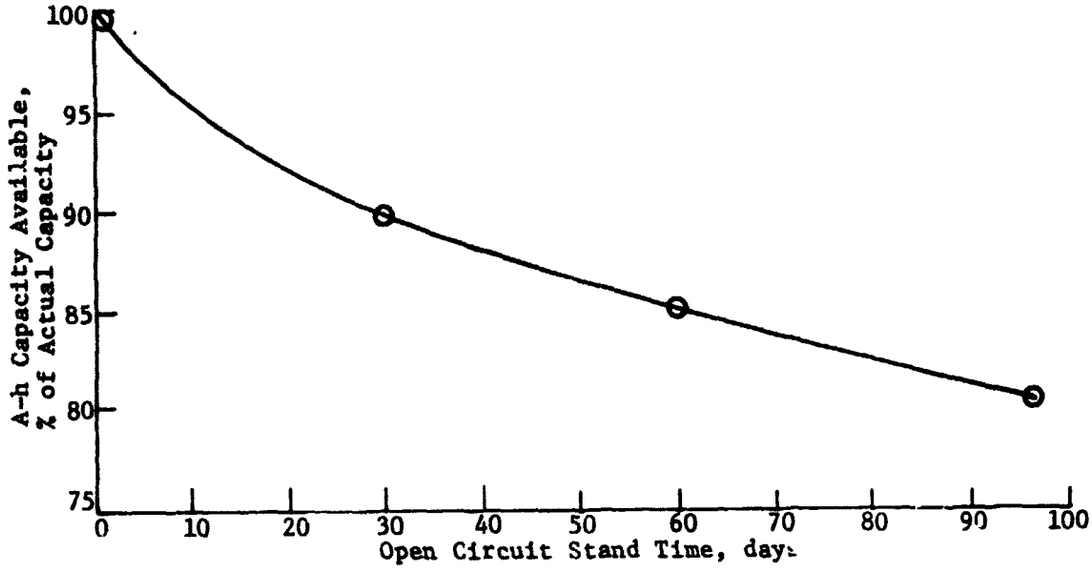

Figure IX-6 Battery Self-Discharge Characteristic at 21.1°C.

During the evaluation of the self-discharge data, it became apparent that the cell discharge voltage profile was depressed compared to the discharge voltage before starting the test. Figure IX-7 shows the average cell discharge voltages for the 30, 60, and 90 day stand cell groups. These data show that there is a significant loss in voltage as the charged stand time increases.

Figure IX-8 shows the calculated equivalent voltage of a 24-cell battery whose average cell characteristics were the same as the self-discharge test cells for the data shown in Figure IX-7. These data show that a significant loss in watt-hour capacity is to be expected in addition to the loss in ampere-hour capacity due to self-discharge when the batteries are left in an open circuit charged stand for long durations.

Table IX-5 Self-Discharge Test Data

30-Day Discharge			
Cell	Initial Capacity, A-h	Discharge Capacity, A-h	% of Initial Capacity
1	10.2	9.22	90.39
2	10.4	9.42	90.57
3	10.2	9.02	88.43
4	10.06	9.02	85.09
5	10.2	9.22	90.39
			Average 88.9
60-Day Discharge			
Cell	Initial Capacity, A-h	Discharge Capacity, A-h	% of Initial Capacity
1	10.46	8.93	85.37
2	10.26	8.8	85.76
3	10.26	8.86	86.35
4	10.4	8.86	85.2
5	10.33	8.73	84.5
			Average 85.35
96-Day Discharge			
Cell	Initial Capacity, A-h	Discharge Capacity, A-h	% of Initial Capacity
1	10.46	8.466	80.94
2	10.6	8.553	80.5
3	10.46	8.533	81.57
4	10.46	8.4	80.3
5	10.52	8.466	80.39
			Average 80.74

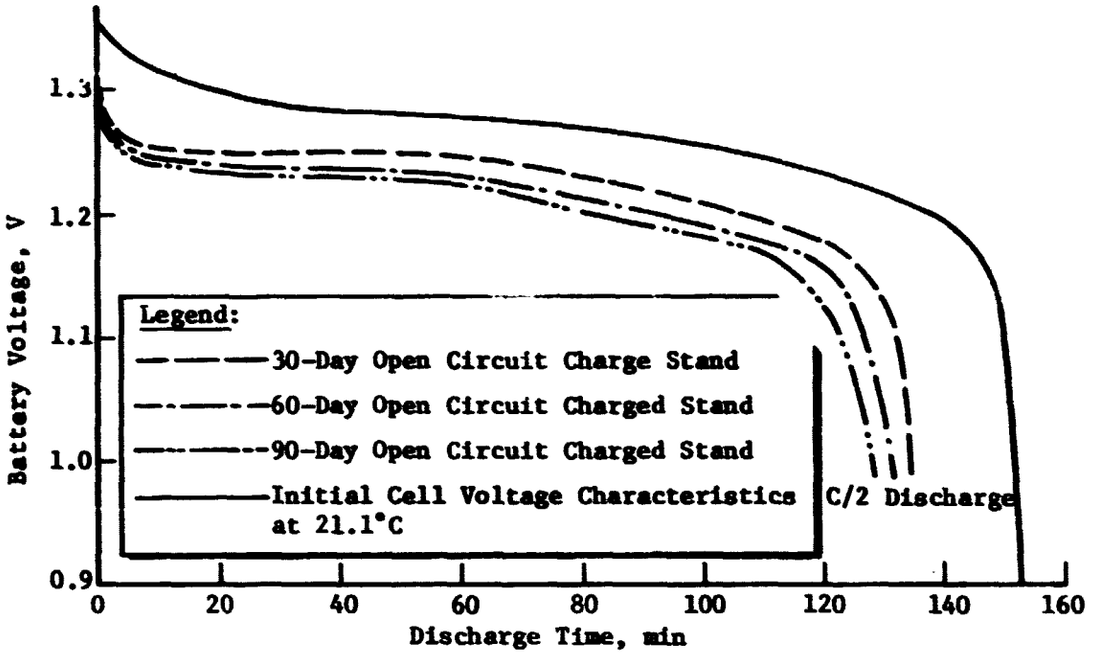

Figure IX-7
Depressed Cell Voltage Characteristic due to Charge Stand

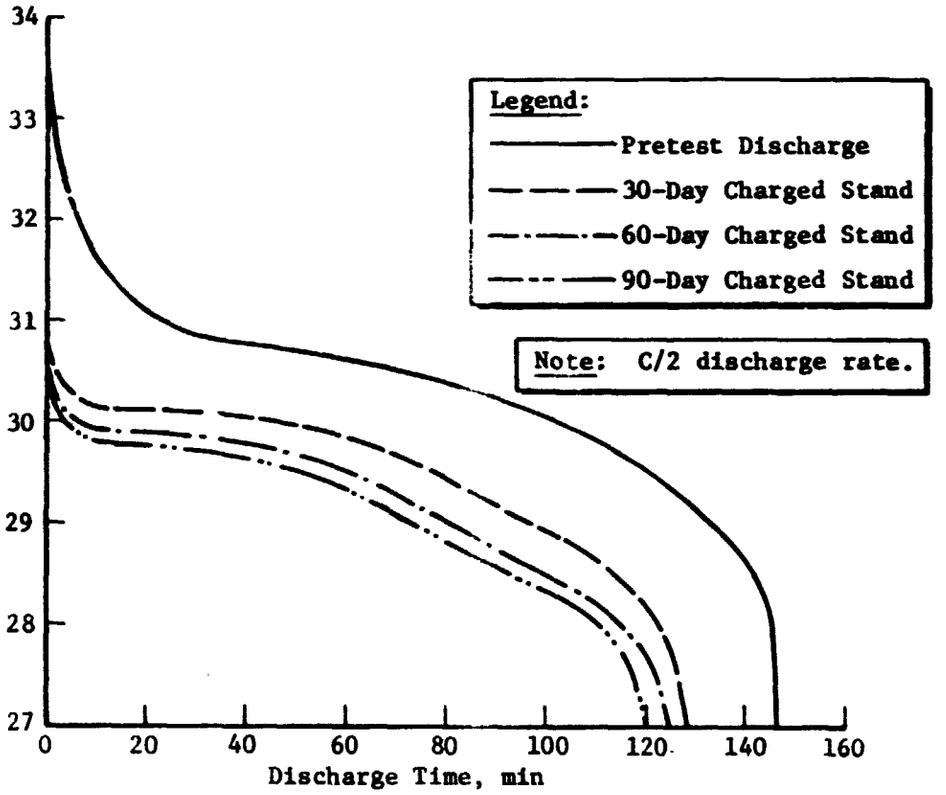

Figure IX-8 Calculated Battery Discharge Voltage

4. High Rate Trickle Charge

With the in-flight failure of one of the two redundant chargers on VLC-2, the failure of the second charger would result in the loss of the Lander. The planned operating mode required that the four batteries be fully discharged after the cruise checkout. However, if the one remaining charger should fail, the batteries could not be recharged and consequently could not be transferred over to the Lander internal power sources since the Lander batteries supply power to operate the power transfer switch. To circumvent this possibility, three of the four batteries on each vehicle were discharged as previously planned. The remaining battery on each vehicle was kept in a charged condition by trickle charging at a C/40 rate.

Since no development tests had been done to determine the battery response to this charge rate and the effect of charging for this extended period of time was unknown, a laboratory test was performed to provide the evaluation data. Two 24-cell batteries previously used for the thermal characterization tests were placed on trickle charge at the C/40 rate. Throughout the test the temperatures were adjusted to maintain the batteries at the temperature of the batteries being charged on VLC-1 and VLC-2. One battery was removed from the test after 65 days of trickle charging and allowed to cool down from 32.2 to 21.1°C over a three-day period. The battery delivered 9.51 A-h after being discharged to 27.2 V using a 19.3-Ω load bank to simulate an in-flight discharge. The discharge voltage profiles shown in Figure IX-9 compares the prefloat test data to the trickle charge test data. These data show a depressed voltage after trickle charging of about 0.5 to 0.7 Vdc.

5. Electrical Characteristics

The battery electrical characteristics were determined for the various usage conditions anticipated during the Lander program

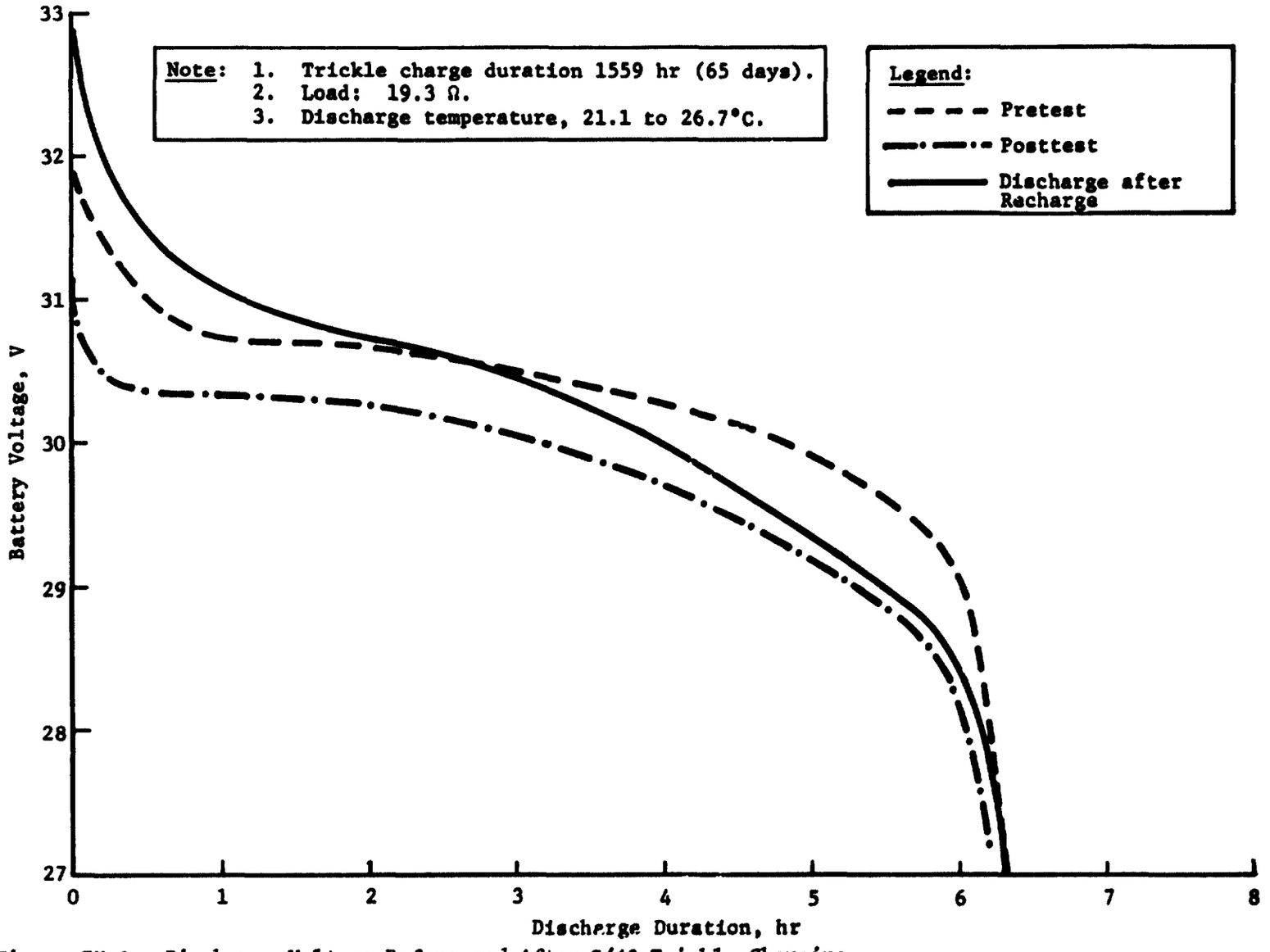

Figure IX-9 Discharge Voltage Before and After C/40 Trickle Charging

Figure IX-10 shows the discharge voltage range for several discharge rates for a battery maintained between 21.1 and 26.7°C.

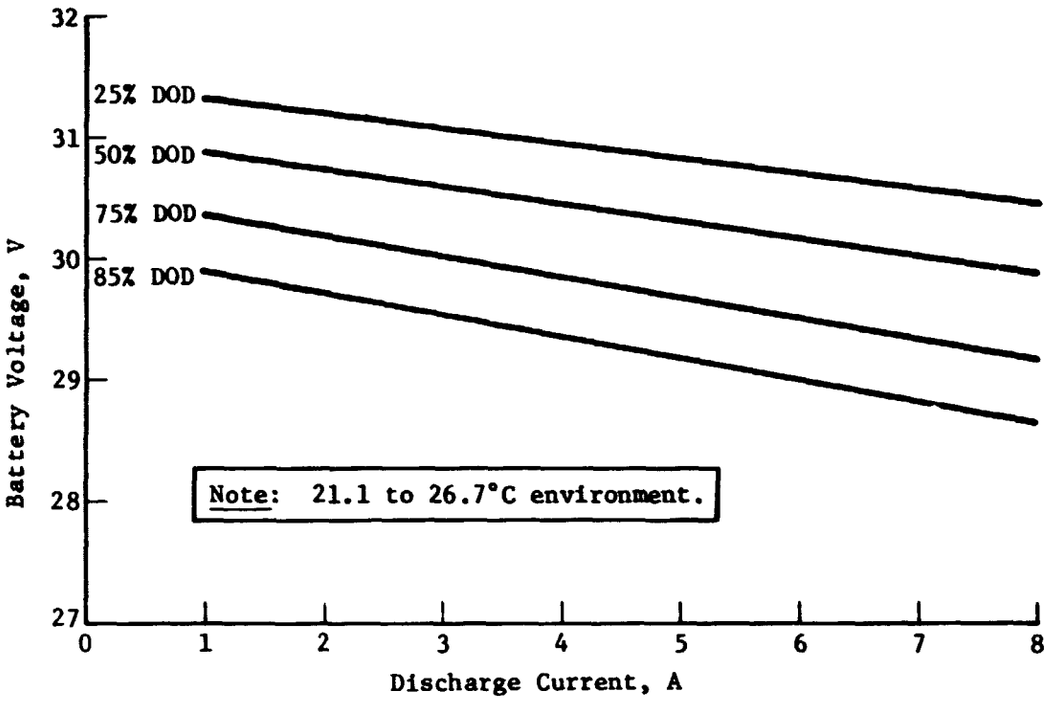

Figure IX-10
Typical Battery Voltages as a Function of Load Current at Different Depth-of-Discharges (DOD)

The watt-hour charge efficiency for three different charge rates used on the landers were calculated for a temperature range from 18 to 32°C using the techniques presented earlier in this section. These data are shown in Figure IX-11. The data calculations were based on a watt-hour discharge efficiency of 88% which was determined by the thermal efficiency tests discussed in Section V. The data are also dependent upon the characteristics of the charger which used the temperature compensated end-of-charge voltage criteria to control the charge duration instead of the typical constant current charge for a fixed time period.

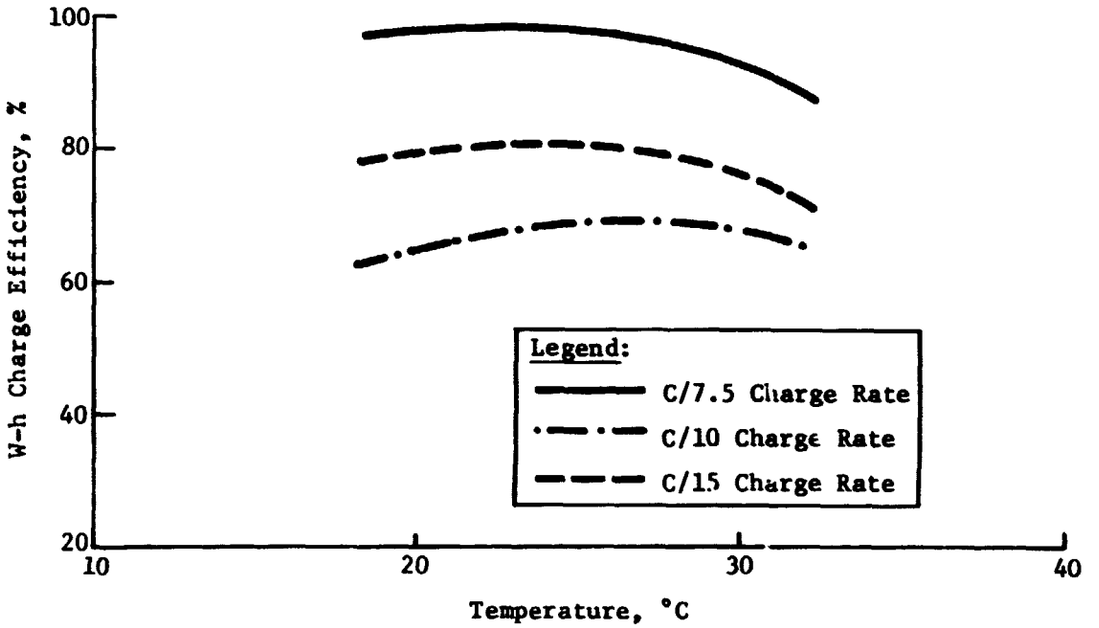

Figure IX-11 Average W-h Charge Efficiency

6. Battery Dynamic Impedance

The battery dynamic impedance and step response to load changes was measured. The dynamic impedance was measured over a frequency range of 100 Hz to 500 kHz. The technique used consisted of applying a one-ampere load to a charged battery and then varying the load current sinusoidally at the test frequencies. Battery voltage and current were recorded and used to calculate the magnitude of the impedance at each frequency. The phase angle between the voltage and current was also measured and recorded. The battery impedance and phase angle over the frequency range tested are shown in Figure IX-12.

The response to a step increase in load current of one-ampere was measured. These data were used to calculate the circuit parameters for the battery equivalent circuit shown in Figure IX-13.

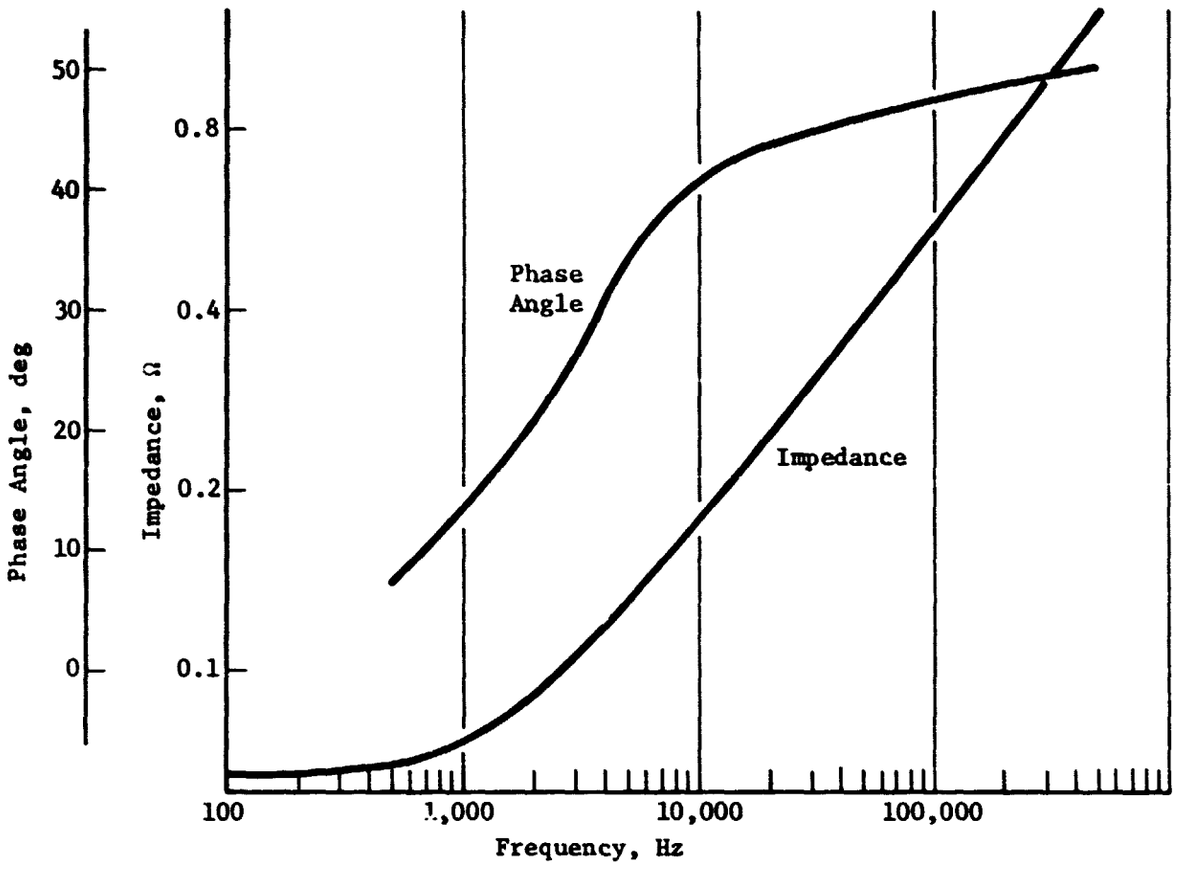

Figure IX-12 Battery Impedance and Phase Angle

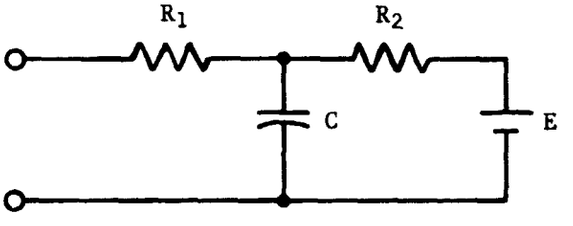

Figure IX-13
Battery Low Frequency Equivalent Circuit

The parameters calculated from the test data were:

R_1 = 0.1Ω

R_2 = 0.125Ω

C = 4.8F

E = Cell Voltage

These values were based on the data shown in Figure IX-14.

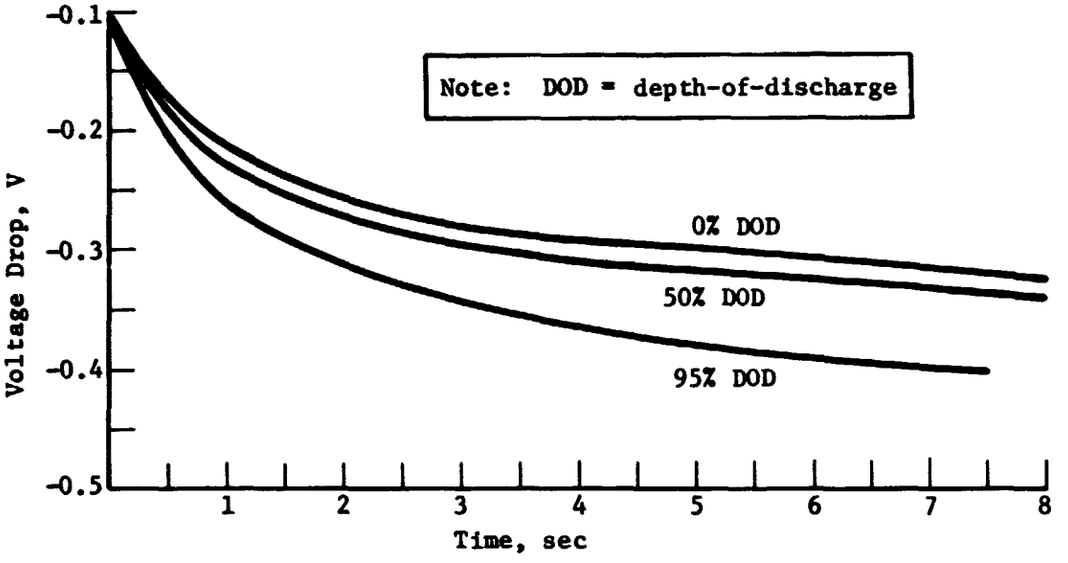

Figure IX-14
Step Response of a Battery to a 1-Ampere Load for 10, 50, and 100% State-of-Charge

LIFE CYCLE TESTS

In 1974 a test program was devised, as a research project, to evaluate the cyclic life capability of the Viking nickel-cadmium cells with polypropylene separators when subjected to repeated cycling under low earth orbit conditions. The test regime consisted of a simulated 93-min orbit of which 33 min were used to charge at a C/2 rate. The charge period was followed by a 15 min open circuit stand and then a C/2 discharge for 30 min. Another 15 min open circuit stand was imposed between the discharge and recharge after the discharge.

Two groups of cells were placed on the cyclic tests. The first group of 24 cells was controlled at the battery level. The other group of 25 cells was controlled at individual cell level. Since a low recharge fraction was used, the battery and cells operated at a low state-of-charge throughout the cycle tests. During charge, 2.2 A-h were supplied while 2.0 A-h were removed during discharge resulting in a recharge fraction of 1.1. During the cycling operation, the battery and cells were placed in a temperature-controlled chamber with forced air circulation at a temperature of 40°C.

The battery and cells successfully completed 4000 cycles under these test conditions without a failure.

The second phase of testing on the same cells consisted of varying the recharge fraction at temperatures of 0, 20, 25, and 40°C. The same C/2 charge and discharge rates were used throughout this phase. The discharge duration was set at 0.5 hr and the charge duration varied to obtain the desired recharge fraction. At the time of this writing, 10,000 cycles had been accumulated with no cell failures under these test conditions.

The battery and cell cycle tests were interrupted after the 8568 cycle in response to a request from the Viking Project to ascertain the degree-of-degradation experienced by the cyclic operation. The battery and cells were charged from a discharged condition for 24 hr at a C/15 rate. They were then discharged at a C/5.3 rate to 27 V for the battery and 0.2 V per cell for the cell group. The battery and cells were reconditioned by discharging each cell individually with one-ohm resistors for 24 hr. The capacity test was performed by charging at a C/15 rate for 24 hr and then discharging at a C/5.3 rate. The battery delivered 8.28 A-h while the cells delivered 7.8 to 7.9 A-h.

The discharge voltage data show the development of a substantial second voltage plateau as shown in Figures IX-15 and IX-16. During the discharge the cell voltages were all discharged below 1.0 V. Following the discharge, the cells were reconditioned by discharging them individually with one-ohm resistors

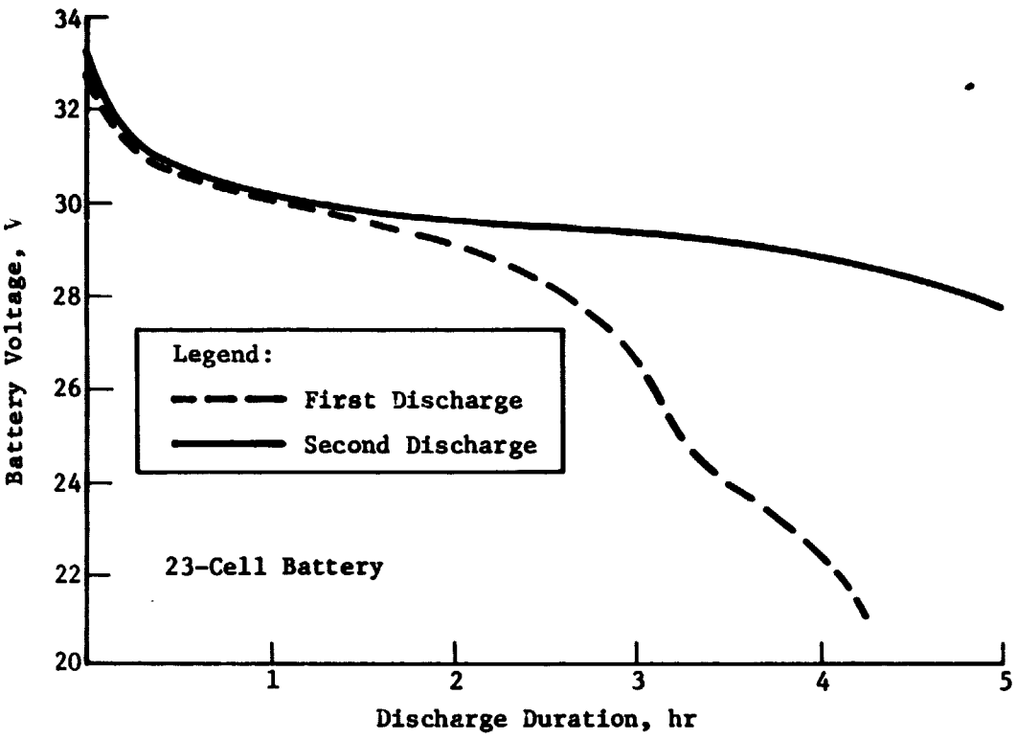

Figure IX-15
Battery Discharge Voltage at 3600 Cycles, 1.5-A Discharge Rate

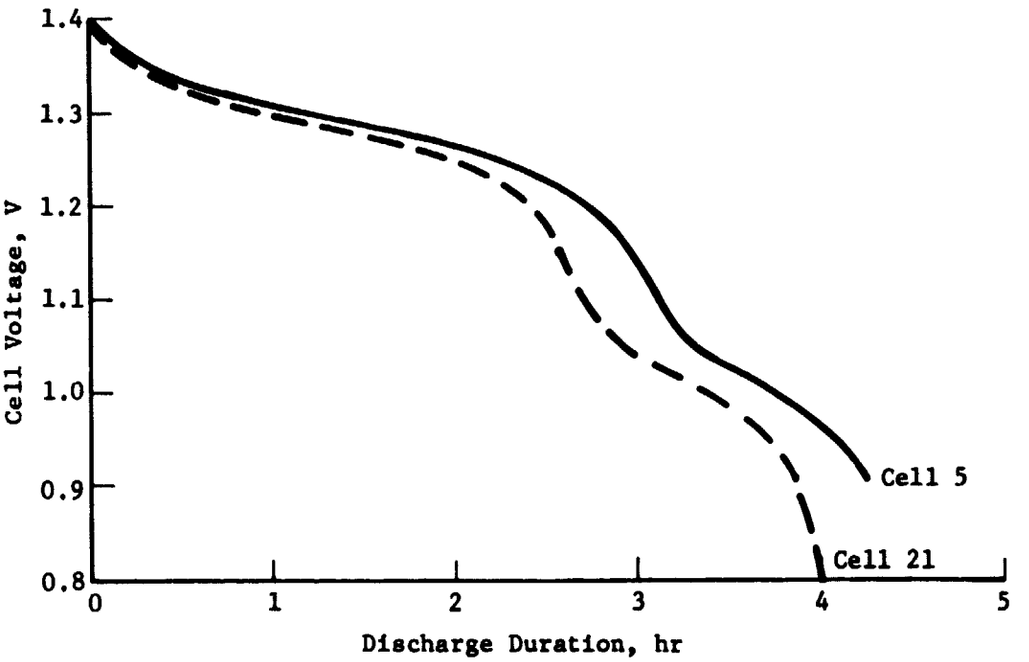

Figure IX-16
Cell Discharge Voltage at 8600 Cycles, 1.5-A Discharge Rate

for 24 hr. The second discharge shows the effect of the reconditioning since the battery delivered 7.9 A-h.

The conclusions reached are that the nickel-cadmium cells built with polypropylene separators are capable of operating at higher temperatures than conventional cells manufactured using nylon separators and that high cycle life is obtainable.

C. FAILURE ANALYSIS

Cell failures were recorded during the cell matching tests, during battery acceptance tests, and during the period when the test support batteries were used to support ground checkout and acceptance tests on the two Landers and Proof Test Capsule (PTC). The results of the laboratory tests and failure analysis performed are presented in this section. The failures are discussed according to the type of failure that occurred as shown below:

1) Charge retention test failures;
2) Self discharge; and
3) High impedance cells.

1. Failure Analysis Techniques

Chemical analysis of the cell components were performed under a nitrogen blanket to prevent the introduction of carbonates by exposure of the electrolyte to the atmosphere. Electrolyte extraction from the plates and separators was accomplished using a soxhlet extractor under a nitrogen blanket. Visual examinations were made using a 50X microscope. A scanning electron microscope (SEM) was used to evaluate separator material, plate structure, crystal size and configuration, and contaminants. Elements were identified using an atomic absorption spectrometer. Nitrates, carbonates, and total KOH were analyzed by titration methods using the procedures outlined in NASA GSFC procedure X-761-73-314, "Procedure for The Analysis of Nickel-Cadmium Cell Materials".

2. Charge Retention Test Failures

This test was designed to detect high impedance leakage paths between the cell plates which would result in excessive capacity loss over a long period of time and could eventually result in a cell becoming discharged and possibly reversed during normal battery operation. The test method used consisted of a 5-min charge at a C/10 rate from a fully discharged condition followed by a 24 hr open circuit stand. At the end of this time, the cell voltages were required to be greater than 1.16 V.

This test is initially performed as a part of the cell receiving inspection and is repeated after the cells are assembled into batteries. A cell (S.N.704) on one of the flight batteries failed during this test. A review of the test data showed that all the battery cells (except the cell that failed the test,) maintained an open circuit voltage of greater than 1.19 V during the battery assembly time. The open circuit voltage of the failed cell was 0.05 V. This prompted an investigation to determine the condition of the other 96 cells that were in various stages of the manufacturing assembly operation. Two other cells (S/N 842 and S/N 1020) were found with abnormally low voltage and were replaced with spare cells. The decision to remove these cells from production was influenced by the battery fabrication schedule and the difficulties associated with replacing a cell installed in a battery assembly.

One of the two suspect cells was subjected to the charge retention test again. It passed this test with a considerable margin; however, it was decided to include both suspect cells in the failure analysis.

In addition to the three cells removed from production, two additional control cells were included for comparison purposes. One cell was obtained from the spare cells. This cell had been subjected to the cell matching tests. The second cell was removed from a life cycle test program. It had already accumulated 4000 cycles of a C/2 charge and discharge in which two ampere-hours were removed on discharge. The cell operated on the lower end of the capacity range during this test since the cell was recharged to slightly over 25% of its capacity range. This test was performed in a 40°C environment.

The cells are identified as follows:

Serial Number	History
704	Failed charge retention test
842	Low voltage suspect cell
1020	Low voltage-suspect cell
471	Cell from life cycle test
1076	Spare cell

The cells were disassembled and subjected to chemical analysis and visual inspections. The results of these analyses are presented in the following paragraphs:

Serial No. 704 - Rust stains were found on the separators and plates both along the edges and in one case in the center of a plate. It was concluded that the rust introduced a leakage plate causing the test failure. No other abnormalities were found.

Serial No. 842 - A spot of silicone grease was found between the polypropylene liner and the case. Some small black spots were found on the separators; however, they had not penetrated the separators and no disturbances on the adjacent areas of the plates were found.

Serial No. 1020 - One plate showed evidence of blistering (Fig. IX-17). Another plate had no coining on one edge and the opposite edge had a double-width coining which indicated that the Blanking die had become mislocated. Three separators showed black spots that penetrated through the separators. The adjacent areas on the positive and negative showed discoloration and evidence of chemical and electrical activity. Figure IX-18 shows a typical black spot on the separator while Figure IX-19 shows a SEM picture of the contaminant. Figure IX-20 shows the ring of discoloration on the adjacent area on a plate indicating that a current path had existed through the separator. Traces of nickel, cadmium, and other trace materials were found in these areas.

Serial No. 1076 - No abnormalities were found in this cell and the general condition was good.

Serial No. 471 - The cell plates were hard to separate due to the separator adherence to the negative plates. The positive plates showed some evidence of sinter weakness as material flaked easily off the edges during handling. A yellow-greenish buildup of cadmium-oxide was noted on the positive comb. No evidence of black spots or cadmium penetration of the separators was found.

Conclusions - The failure on cell 704 was due to rust. The rust was believed to have occurred during the manufacturing operations since the cell was opened and disassembled under a nitrogen blanket.

The failure of cell 1020 to hold a charge was due to a contaminant which had penetrated the separator bag and introduced a high impedance leakage path.

The other abnormalities noted did not contribute to the failure to pass the charge retention tests. Their condition was directly relatable to the usage history for each cell. The cell that had received 4000 cycles at 40°C showed the most deterioration. There was no evidence observed of separator material degradation in any of the five cells tested.

Figure IX-17 Cell Plate with Blistered Sinter

Figure IX-18 Separator Bag with Black Spot

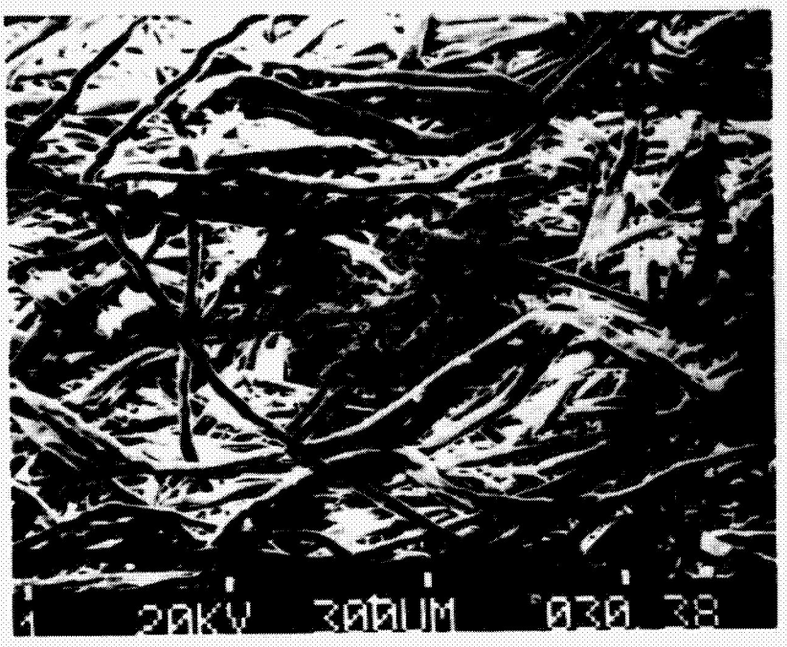

Figure IX-19
Scanning Electron Microscope Picture
of Separator and Black Spot

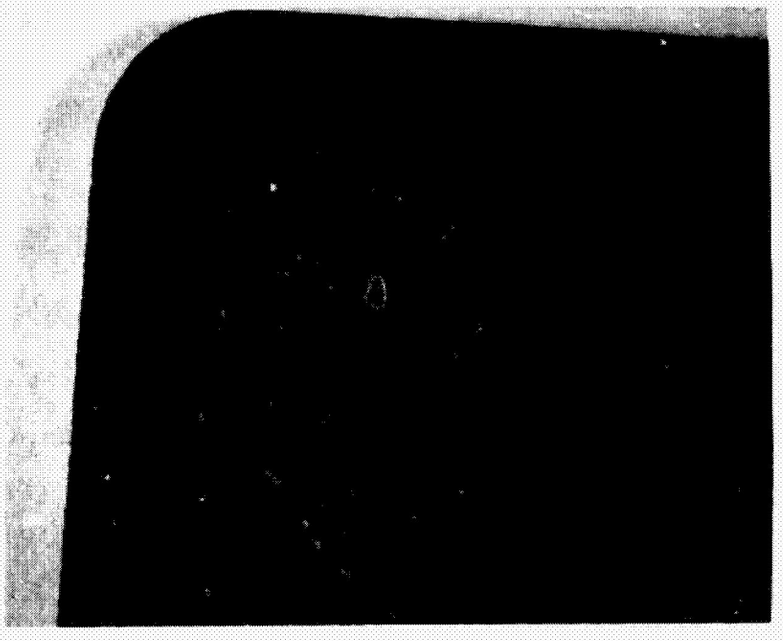

Figure IX-20
Cell Plate with Discoloration in
Area in Contact with Black Spot

3. Self Discharge

During the ground testing on VLC-2 there was a two month period when the batteries were not used. During this period, the batteries were left in a charged state with only a 19,300-Ω telemetry isolation resistor as a load. At the conclusion of this period, the batteries were placed in use; however, it was discovered that one of the four batteries exhibited a low voltage during discharge.

The battery was removed from VLC-2 and during subsequent analysis in the battery lab, cell 24 was found to be in a nearly discharged condition while the remaining cells were in a high state of charge (> 7-A). Several theories were proposed to account for the discharged condition. These theories included an internal short and the possibility that the cell terminal had been inadvertently shorted to structure during equipment removal and installation.

A review of the vehicle test data indicated that several occasions existed when the cell could possibly have been reversed. If this had occurred, the precharge on the negative plate would have been discharged and would be less than the initial 2 to 3 A-h. To confirm this suspicion, cells 23 and 24 (with a control cell) were deliberately reversed at a one-ampere rate and the cell voltage recorded. When the cell voltage was 0.5 V negative or less the negative precharge is being discharged. When the precharge is consumed the cell voltage increases to over one volt negative. The data shown in Figure IX-21 show that there was less than one ampere-hour of precharge remaining in the failed cell (No. 24), while the adjacent cell in the battery had approximately two ampere-hours, and the spare cell had over three ampere-hours. These data tend to support the supposition that cell 24 had been reversed. The data shift at 40 min was due to a test interruption to remove cell 24.

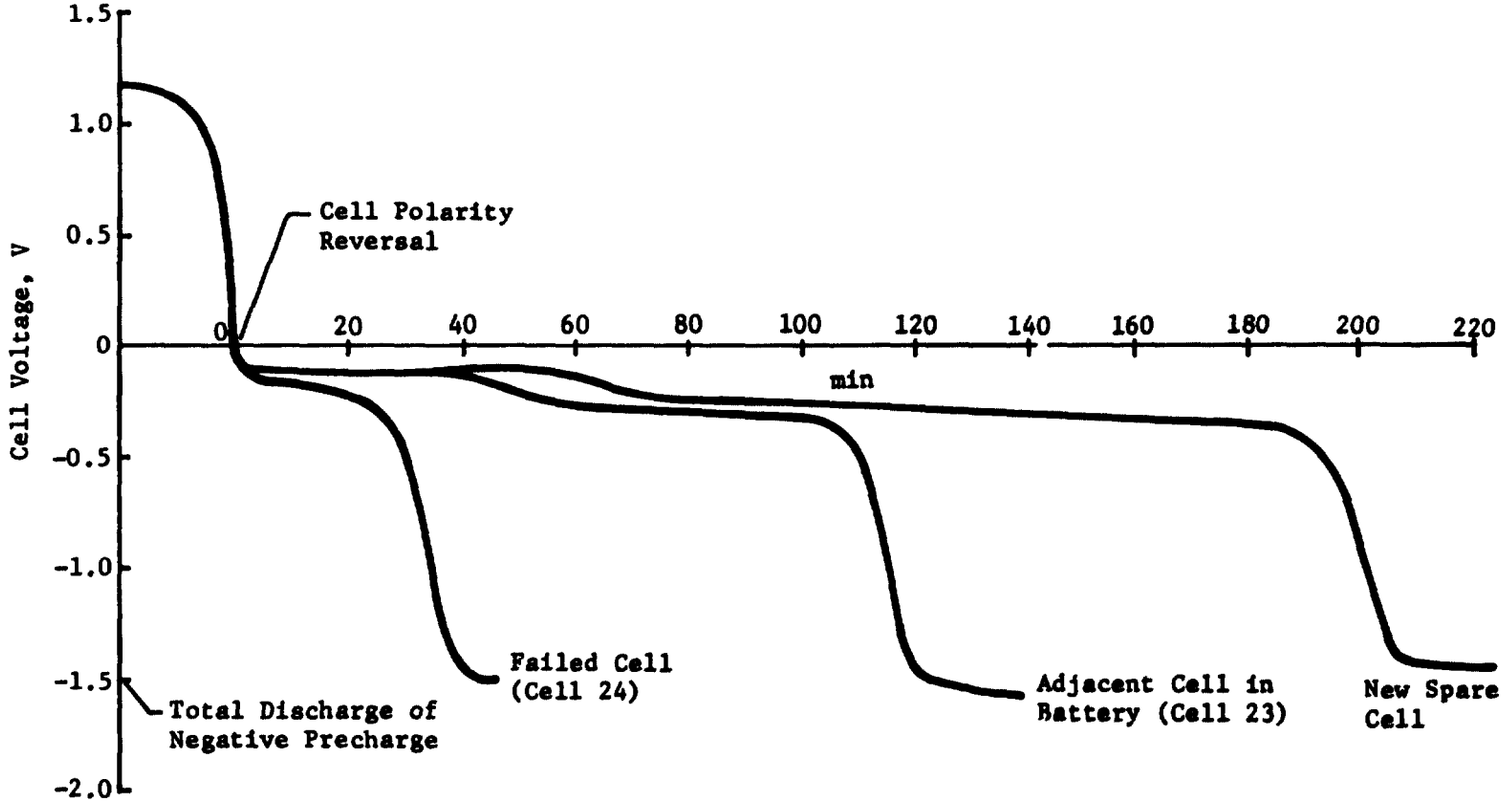

Figure IX-21 Cell Reversal Voltage Characteristic at 1-A Discharge

The cell was removed from the battery and failure analysis performed. During the separation and inspection of the plates, a large particle (0.3 by 0.5 cm) was discovered between the separator bag and positive plate. This particle had penetrated the separator material and introduced a leakage path of some unknown magnitude. This particle was found to be a cadmium metal covered with a nickel-sulfur compound. Traces of nickel-sulfur crystals were found on the adjacent area of the negative plate. Since the contaminant was found between the separator bag which is slipped over the positive plate, it was concluded that the particle was either on the separator material or fell between the bag and plate during assembly. The cell supplier was appraised of the failure and of the failure analysis results. However, a source for the sulfur contaminant could not be found in the cell manufacturing area.

A review of the cell and battery test data accumulated before delivery of the battery was made to determine if the data showed any evidence of an internal leakage path. No evidence of any abnormal characteristics was found.

It was concluded that a high impedance leakage path developed in the cell as a result of the presence of the contaminant. Consequently, the cell discharged over the time the battery was not not in use producing an unbalanced condition in which cell No. 24 operated at a low state-of-charge while the remaining cells were fully charged. It was concluded the cell was reversed which lowered the battery voltage and consequently upset the load sharing of the four batteries connected in parallel on the Lander bus. Since the batteries were discharged at low rates and operated at a low depth-of discharge during this period of testing, the reversed cell did not experience a high rate reversal current; however, the data does show that the negative precharge on the failed cell was considerably lower than the comparison cells which supports the cell reversal theory.

4. High Impedance Cells

The second battery failure occurred on the proof test capsule (PTC). This PTC was used to verify the various test facilities (vibration, thermal vacuum, etc.) before their use by flight vehicles for formal testing. During the two years that the battery had been installed on PTC, it had received two additional sterilization cycles over the normal requirements. Typical usage consisted of intermittent discharges to various depths of discharge with long periods of charged open circuit stored. Discharge rates during these open circuit stand periods were due to the self-discharge rate and the presence of an instrumentation load that (depending upon test configuration) was either 7000 or 19,300 Ω. The test support batteries on this vehicle had previously been recycled back to the battery test facility for a performance check and one of the original batteries had been replaced due to low capacity. Before placing the PTC in a mission simulation test, the batteries were again scheduled for a reconditioning discharge and a capacity verification test in the battery test facility.

The battery was reconditioned by discharging at a C/2 rate to 27 V and then each cell was loaded with a one-ohm resistor for a minimum of 24 hr. The battery was then placed on charge; however, the voltage on several cells immediately exceeded the allowable limit of 1.50 V causing the data acquisition and control system computer to generate an abort command which terminated the charge. In an attempt to determine if the high cell voltage problem was a temporary phenomenon, the abort limit was raised to several volts and the charge test restarted. This time the test was aborted due to a battery voltage greater than 35 V. The limit was again raised and the test restarted; however, it was manually terminated due to cell voltages that reached from 4 to 7 V. Several other attempts were made to charge individual cells using low rates for long

durations or constant potential charging with limited success. Two cells were opened at the fill tubes and 34% KOH was added in 2-cc increments. Partial recovery of the cell characteristics were noted and one cell delivered 10 A-h after 14 cc of electrolyte was added (cell flooded). The next step in evaluating the problem was to remove several cells and subject them to failure analysis to determine if the cells had dried out. The general condition of the separators and plates was also evaluated.

The cell cover was opened under a nitrogen blanket and the plate pack and separators placed in a soxhlet extractor to collect the electrolyte. Abnormal cell conditions were noted when the cell plates were fanned out to allow the water to penetrate between the plates. The separator fibers were trapped on the negative plate surface by a crystal growth around the fibers. The negative plates had a very granular appearance and were a silvery color (shiny and reflective). The separator bags had a dry appearance. A considerable amount of granular material flaked off the plates and collected in the bottom of the beaker holding the cell parts and wash water.

The second phase of the investigation consisted of trying to identify the electrolyte quantities on the separators, and plates. Other cells from the same battery were disassembled under a nitrogen blanket; however, the separator bags were removed from the positive plates and the negative and positive plates were segregated into separate groups. The separator bags, negative plates, and positive plates were individually subjected to an electrolyte extraction using the soxhlet extractor.

Results - The results of the chemical analysis are summarized in Table IX-6. These data show that the high impedance cells have a higher concentration of KOH and K_2CO_3 in the positive and negative plates as compared to the control cell. A significant difference in the quantity of electrolyte in the separators

exist. The two high impedance cells had 1.5 and 7.1% of the total KOH in the separators while the control cell had almost 21%.

Table IX-6 Electrolyte Quantities and Location in High Impedance Cells

Cell S/N	Component	KOH wt, gm	K_2CO_3 wt, gm	Total KOH* wt, gm	KOH Vol, ml (31% KOH)	% KOH of Total
246	(-) Plates	5.56	0.93	6.31	15.7	58.5
	(+) Plates	3.49	0.25	3.69	9.2	34.2
	Separators	0.75	0.018	0.765	1.9	7.1
	Case	0.013	0.016	0.026	0.1	0.2
	Totals	9.81	1.21	10.80	26.9	100
224	(-) Plates	5.63	0.72	6.2	15.4	58.0
	(+) Plates	3.9	0.5	4.3	10.7	40.3
	Separators	0.15	0.02	0.17	0.4	1.5
	Case	0.01	0.01	0.02	0.1	0.2
	Totals	9.69	1.25	10.69	26.6	100
1205 Control Cell	(-) Plates	4.59	0.26	4.98	12.39	48.8
	(+) Plates	2.82	0.21	2.99	7.44	29.3
	Separators	1.96	0.22	2.14	5.32	20.9
	Case	0.06	0.06	0.10	0.26	1.0
	Totals	9.43	0.75	10.21	25.41	100

*Grams K_2CO_3 converted to grams KOH and added to KOH weight for total weight.

It is evident that the electrolyte in the high impedance cells was absorbed by the positive and negative plates which left an inadequate amount for the separators. Consequently, separator dryout occurred and the cell developed a high impedance.

Three factors contributed to the failure:

1) Positive plate thickness increased due to cyclic usage which increased the porosity and allowed more electrolyte to be absorbed.
2) Negative plate thickness increased due to cadmium-hydroxide

crystal growth due to discharging at low rates (less than 0.01 A) for long periods of time. This was due to the type of usage experienced during the test program.

3) Reconditioning totally discharges the cells which leads to the highest KOH concentration since water is consumed during discharge.

The results of the visual examination support the conclusions reached as a result of the chemical analysis. These observations are as follows:

1) Shiny deposits of cadmium were observed on some of the positive plates. These areas were generally on the upper areas of the plate near the weld tab.
2) The separator bags contained white powder deposits.
3) Negative plates exhibited a rough granular spongy appearance. The plates had a silvery appearance as compared to a gray color observed on other plates.
4) The plates and separators had an extremely dry appearance while electrolyte could be seen on the separators and plates from the good cell.

NOTE: Cell 1205 was built using the low carbonate process.

Conclusion - The battery failure was induced by a nonmission oriented operating mode which caused the growth of large cadmium crystals on the negative plates. The negative plate porosity and thickness increased and additional electrolyte was absorbed in both the negative and positive plates. The deep discharge during reconditioning induced the final failure since water is consumed during discharge which results in the highest concentration of electrolyte.

X. FLIGHT PERFORMANCE

The two Viking spacecraft were launched from Cape Kennedy on Titan III-Centaur Launch vehicles. The first spacecraft was launched August 20, 1975 and the second spacecraft was launched September 9, 1975. At the time of launch, the battery conditions were as described in Section VIII.

Figure X-1 summarizes the battery usage activity during the first part of the cruise phase on VLC-1 and VLC-2. Throughout the initial period of the mission, the batteries were in a discharged condition with the 19.3 k telemetry isolation resistance slowly draining any residual energy from each battery. A typical discharge voltage profile during this period is shown in Figure X-2. By the time of the first in-flight charge (55 days after the first launch), the battery voltages had decayed to below five volts on the first Lander (VLC-1).

The batteries were charged at a C/15 rate starting on the 55th day of flight in preparation for the in-flight checkout test. The end-of-charge was determined by the battery voltage and temperature using the power distribution assembly (PCDA) voltage-temperature charge cutoff logic. The charge duration on VLC-1 varied from 21.7 to 22.8 hr. for the four batteries. The calculated capacity stored ranged from 9.1 to 9.4 A-h. At various times during the in-flight checkout tests, the batteries supplied energy at a low rate to supplement the energy supplied by the RTGs. During nonusage periods, the batteries were each being discharged via the 19.3 kΩ telemetry isolation resistor. Each battery was recharged at a C/5 rate 85 days after the launch and again used to support additional Lander subsystem tests. Between tests the batteries were slowly discharged by the telemetry isolation resistance. The next recharge occurred 112 days after launch and the batteries were used to support additional subsystem tests.

Figure X-1 Viking Lander Battery Usage after Launch

Figure X-1

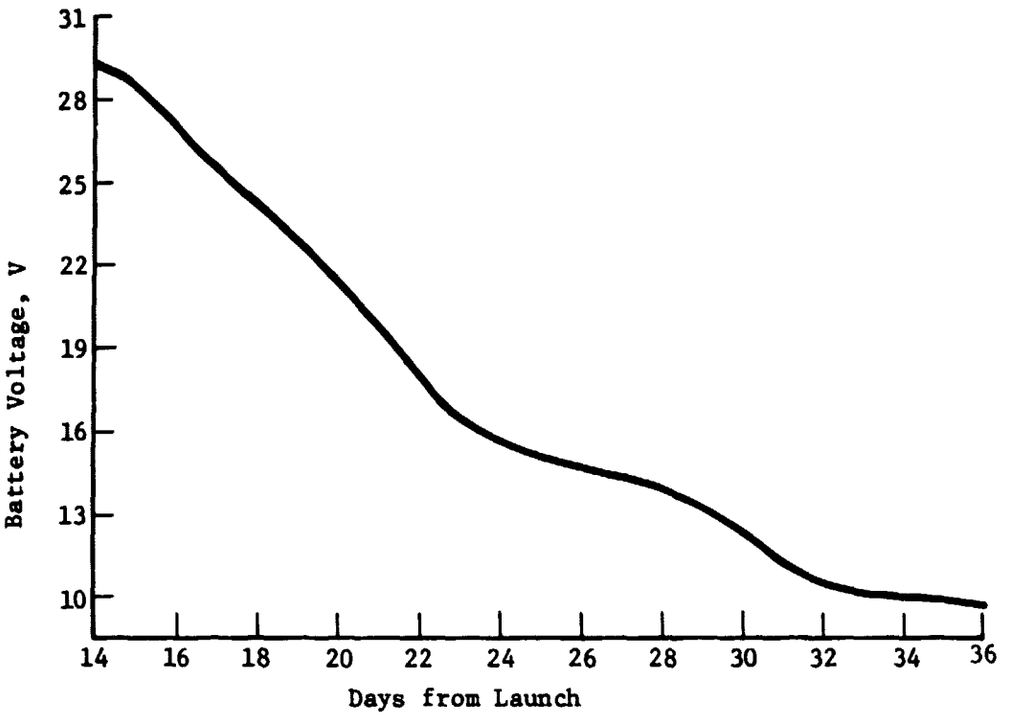

Figure X-2 Battery Discharge after Launch under 19.3 kΩ Load

A change to the operating mode was made because one of the two redundant battery chargers on VLC-2 failed. These chargers provide battery charge current from the Orbiter power system. If one additional charger had failed, the vehicle would have been lost if all four lander batteries had been totally discharged as was originally planned.

An operating mode was developed in which one battery was maintained in a charged condition throughout the remainder of the interplanetary cruise. This battery could be used to transfer the Lander subsystems from the Orbiter-supplied power to the Lander RTG power source. Once this was accomplished, the remainder of batteries could be charged using the RTGs as the primary source of energy. To maintain uniformity in the software and for performance comparison purposes (both Lander vehicles) were configured to maintain one battery in a charged state. This battery was placed on a C/40 trickle charge and maintained in this condition for the remainder of the cruise phase.

The remaining three batteries were sequentially discharged to 27.3 Vdc using a 19.3-Ω load bank beginning on the 153rd day after Launch.

Concurrent with the change in battery usage on VLC-1 and VLC-2, two test batteries were placed on a float charge test in the laboratory at a C/40 rate. Battery temperatures were adjusted to coincide with the in-flight conditions. Details of this test are given in Section IX.

The in-flight checkout tests on VLC-2 were similar to the tests performed on VLC-1. The first charge occurred 57 days after launch and the first recharge at 77 days. Approximately 1.6 to 1.8 hr of charging at a C/5 rate were required to recharge each of the batteries. The second recharge occurred 100 days after launch and each battery was charged for approximately 1.5 hr at the C/5 rate. Beginning 154 days after launch, three of the four batteries were sequentially discharged to 27.3 V using a 19.3 Ω fixed resistance load bank. The other battery was placed on a C/40 trickle charge.

During the time period following the in-flight checkout, the batteries on trickle charging reached a temperature of 30.6 and 31.7°C on VLC-1 and VLC-2. The other batteries on each vehicle were slowly being discharged by the 19.3 k telemetry isolation resistors. The two charged batteries (one on each lander) are scheduled to remain on trickle charge at the C/40 rate for 12 weeks. The trickle charge is then scheduled to be removed and the batteries and lander allowed to cooldown before the recharging in preparation for the C/160 float charge and the preseparation checkout during Mars orbital operations.

The batteries on VLC-1 were in the charged configuration for 18 weeks and VLC-2 for 14 weeks. All batteries performed as expected during the charged period.

Battery temperatures ranged from 19.4°C to 28.3°C during charging on VLC-1. The temperatures on VLC-2 were about 5°C higher. Consequently, the last battery charged reached a temperature of 32.8°C.

The batteries on both landers exhibited a slightly depressed voltage curve upon discharge down to the voltage cutoff of 27.3 Vdc (see Fig. X-3). The depressed voltage of ∿ 0.5 to 1.0 V was attributed to lack of battery operational activity. The batteries were cycled to a very shallow depth-of-discharge no more than three times in the 14 to 18 week period. Laboratory battery test data indicated that a potential one-volt depression during discharge after a 90-day charged open circuit stand was possible. In the above case, the data from the Lander were compared to lab self-discharge tests. The results of this test are presented in Section IX.

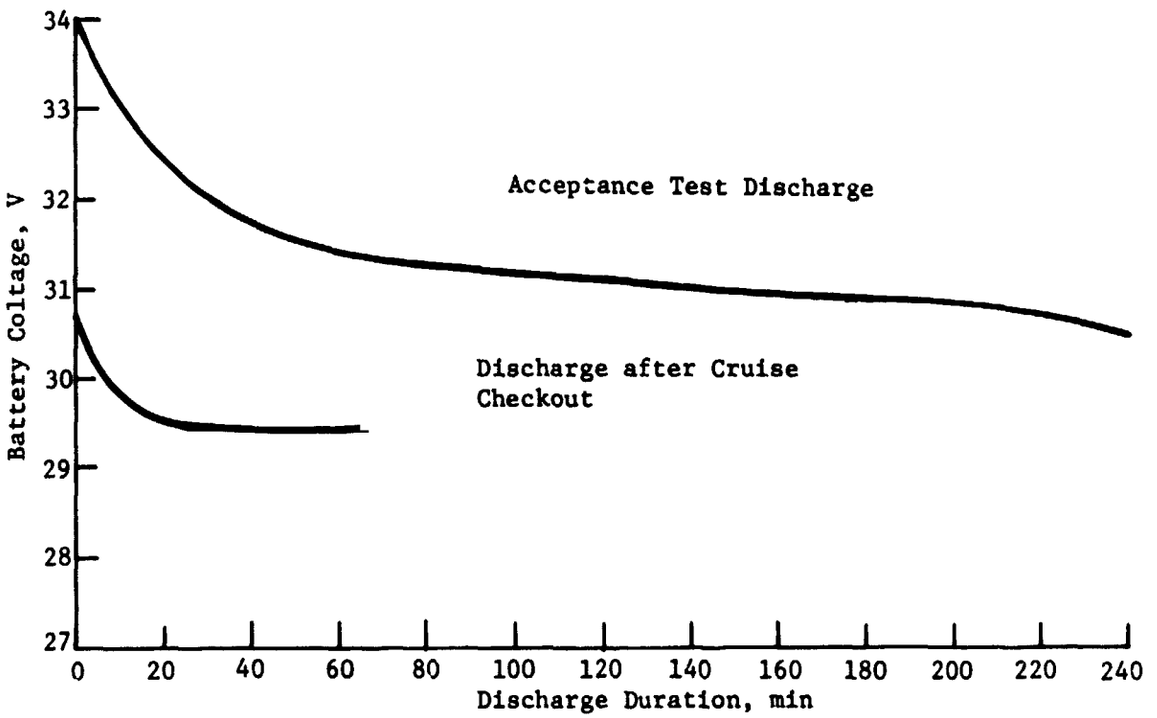

Figure X-3
Typical Battery Discharge after Cruise Checkout Compared to Acceptance Test Data

APPENDIX A

AUTOMATIC CONTROL AND DATA ACQUISITION SYSTEM (ACDAS)

Early in the Viking cell development effort, it became evident that a sizable test program was required to meet the program objectives within the allotted time span. Simultaneous evaluation of cells from three cell vendors was required and the total number of cells to be processed was estimated to be well over 1000. To provide this capability, an automated control and data acquisition system was designed and fabricated.

Two separate systems evolved, each using a PDP8/E computer as the means of control and data acquisition, to minimize the human interface. A description of the system follows.

The ACDAS is a fully automatic fail-safe system that remotely controls individual cells and or batteries through specific cycles. It also acquires test data in a readily reducible form for analysis. An overall view of the control equipment is shown in Figure A-1.

The ACDAS consists of two separate independent systems, each using a PDP8/E-8K memory computer. The first system built uses a scanner and digital voltmeter to acquire the data which are stored on a seven-track tape recorder. Real-time readout capability and access is provided by a Decwriter. This system has nine independent channels that can handle 30 cells each or one multicell battery. Figure A-2 shows a block diagram of the system.

The second system can handle up to 60 cells on each of its 12 channels for a total capability of 720 cells. The system can be expanded up to 19 channels with a total capability of 1028 cells. This system uses a sample and hold capacitor with an A/D Converter to measure and condition the test data. An additional 64 k of memory is provided by two disks which provide for additional capability such as integrating the current to provide a real-time readout of the ampere-hours supplied during charge and discharge. Again, the data is stored on seven-track magnetic tape. Real-time data and control capability is provided by a teletype and a Decwriter terminal.

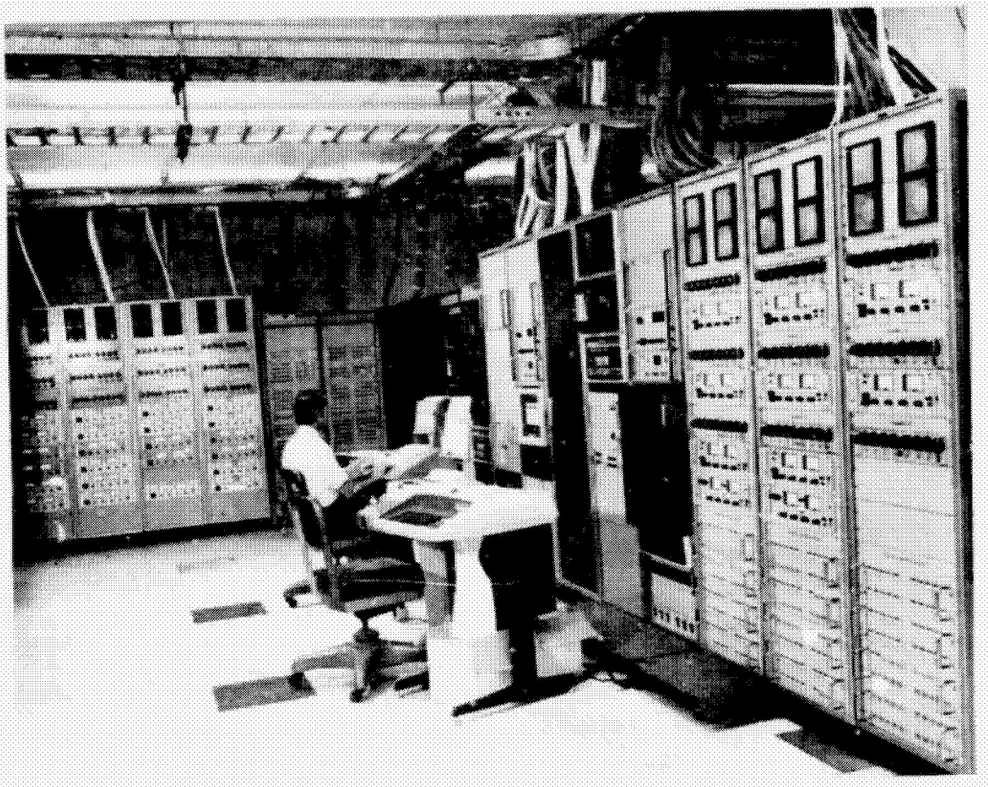

Figure A-1 Automatic Control and Data Acquisition System

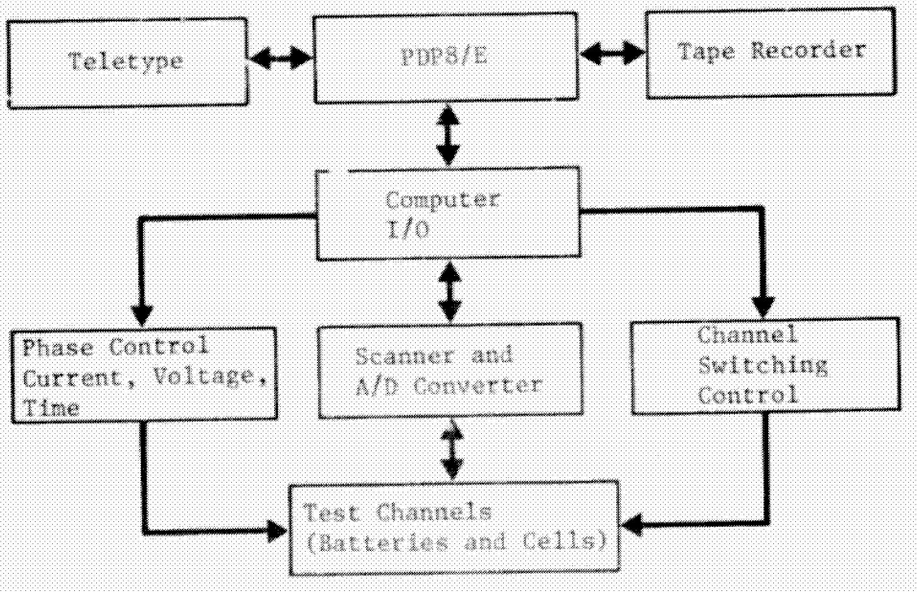

Figure A-2 ACDAS Block Diagram

Each test channel has the capability of being operated in one of four operating modes of charge, discharge, or open circuit. The four modes or phases can be operated sequentially to simulate orbital operations. The computer monitors individual cell and or battery data, compares the data with control limits, and terminates the phase when a limit has been attained. The test can then be terminated or switched to the next mode of operation. Each phase can be controlled by any of the following control parameters: (1) number of cycles, (2) cell voltage (3) cell pressure, (4) cell temperature, (5) phase duration, and (6) auxiliary electrode. In addition, battery test control may use individual cell data in the battery for phase control limits. For example, a test may require that no individual cell falls below 0.5 V on discharge. The battery test could be controlled on that basis.

Software programs using the Martin Marietta CDC 6500 computer reduce and analyze the data stored on the ACDAS magnetic tape. Present programs are capable of the following tasks:

1) Strip data into individual channels;
2) Isolate specific data or cells for individual evaluation;
3) Statistically evaluate performance parameter of groups of cells or batteries;
4) Provide predictions and trends of any parameter;
5) Provide cell matching and selection; and
6) Provide plots of test data (voltage, current, A-h, W-h, temperature, and pressure).

The data are stored on a master tape and are available on magnetic tape, microfilms, X-Y plots, and computer printout.

Support equipment housing the cells and batteries are 10, 27-ft^3 temperature chambers with a temperature range of minus 84°C to plus 182°C. Two of these chambers include a nitrogen source for heat sterilization of component parts. Figure A-3 shows some of this equipment.

Each test channel has the capability of being operated in one of four operating modes of charge, discharge, or open circuit. The four modes or phases can be operated sequentially to simulate orbital operations. The computer monitors individual cell and or battery data, compares the data with control limits, and terminates the phase when a limit has been attained. The test can then be terminated or switched to the next mode of operation. Each phase can be controlled by any of the following control parameters: (1) number of cycles, (2) cell voltage (3) cell pressure, (4) cell temperature, (5) phase duration, and (6) auxiliary electrode. In addition, battery test control may use individual cell data in the battery for phase control limits. For example, a test may require that no individual cell falls below 0.5 V on discharge. The battery test could be controlled on that basis.

Software programs using the Martin Marietta CDC 6500 computer reduce and analyze the data stored on the ACDAS magnetic tape. Present programs are capable of the following tasks:

1) Strip data into individual channels;
2) Isolate specific data or cells for individual evaluation;
3) Statistically evaluate performance parameter of groups of cells or batteries;
4) Provide predictions and trends of any parameter;
5) Provide cell matching and selection; and
6) Provide plots of test data (voltage, current, A-h, W-h, temperature, and pressure).

The data are stored on a master tape and are available on magnetic tape, microfilms, X-Y plots, and computer printout.

Support equipment housing the cells and batteries are 10, 27-ft^3 temperature chambers with a temperature range of minus 84°C to plus 182°C. Two of these chambers include a nitrogen source for heat sterilization of component parts. Figure A-3 shows some of this equipment.

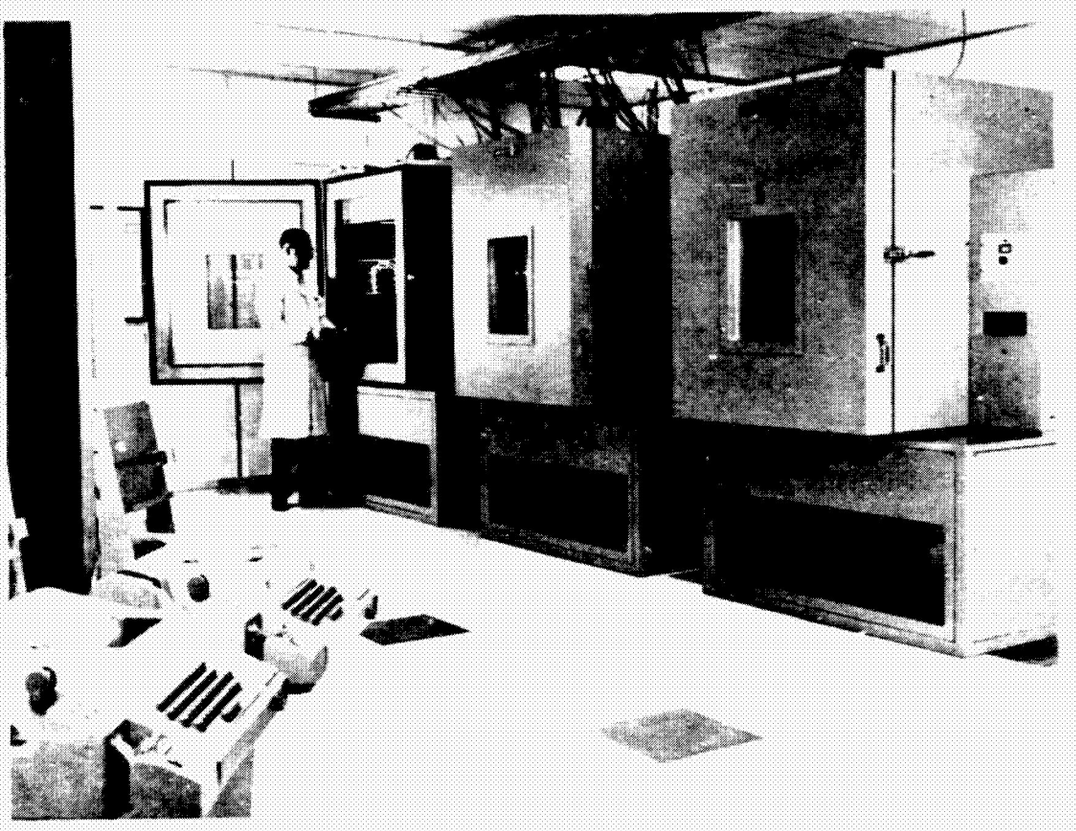

Figure A-3 Thermal Chambers for Battery Tests

APPENDIX B

PROCUREMENT SPECIFICATION REQUIREMENTS

The following are the significant requirements relative to the manufacture, inspection and test of the nickel-cadmium cell that were imposed on the cell manufacturer. These requirements were extracted from the procurement specification.

A. SEPARATOR CHARACTERISTICS

1. Electrolyte Absorption, Dimensional Change, Electrolyte Retention and Porosity

Six samples of each material shall be cut (in the machine direction) to 6.5 cm by 2.50 cm and individually measured using a standard die. The thickness of each sample shall be measured using an Ames gage Model 262 platform dial micrometer with a 1.27 cm diameter stainless steel anvil or a Cady gage, Model DW-1. The dial shall be graduated in 0.001 mm. An equivalent thickness measurement system is acceptable. Each sample shall be weighed to the nearest one milligram of an analytical balance and then immersed in approximately 100 cc of aqueous potassium hydroxide (KOH) solution in noncorrosive containers with air tight covers. Vacuum may be used for nonwetting separator material. The concentration of the KOH solution shall be the same percent as used in the cell filling and shall be of the same quality. Dimensional changes shall be measured after the samples have been subjected to the following conditions: six samples shall be conditioned while in the containers at 21.1°C. The samples shall be returned to their individual containers for an additional hour at 21.1°C. At the end of one hour, the equilibrated samples shall be wiped across a clean lucite plate until no droplets are left on the plate. Then reweigh the sample.

Electrolyte Absorpiton - Electrolyte absorption is the difference between the wet equilibrated samples and the dry sample weights. Data shall be submitted in accordance with the procurement agreement.

Electrolyte Retention - Electrolyte retention shall be measured on the same samples after draining for 15 ± 5 min on a clean lucite plate positioned at 45 ± 2 deg angle. The samples shall be reweighed. During draining, the samples shall be enclosed in an inert atmosphere. Data shall be submitted in accordance with the procurement agreement.

Porosity - Data shall be submitted in accordance with the procurement agreement.

2. Separator Wettability

Separator wettability of three samples of separator material shall be measured. Each sample shall be cut from a different roll. Separator wettability shall be measured by placing the dry separator sample in the resistivity cell, filling the cell with electrolyte, and recording the time required to attain a stable resistance. Vacuum may be used for nonwetting separator material. Measurements shall be made at five-second intervals. Data shall be submitted in accordance with the procurement agreement.

3. Tensile Strength at Break

Tensile strength at break shall be measured on at least six samples, each cut from a different roll. Separator tensile strength measurements shall be made on die cut specimens 12.7 by 2.5 cm, cut in the roll direction; each of which must be carefully examined for flaws. Samples containing obvious flaws shall be discarded. At least five samples of each material shall be run and the mean value reported. The tensile strength at break shall be measured on samples which are conditioned both at 22.2°C and 50 ± 5% relative humidity for 24 hr. A cross head speed of two inches per min shall be used and the specimens positioned in rubber-faced jaws so that the grip separation is three inches. Elongation measurements can be obtained by measuring the grip separation as the test progresses using the value at break to calculate percent elongation. For the tensile measurement, the load is in pounds shall be measured at the breaking point. Samples breaking outside the areas between the jaws are not included.

The testing shall be performed at 22.2°C, 50 ± 5% relative humidity.

Perform calculations as follows:

Calculations

$$\text{Tensile Strength} = \frac{\text{Breaking Load, lb}}{\text{C.S.A.}}$$

C.S.A. = Sample cross sectional area

$$\% \text{ Elongation} = \frac{L - L_o \times 100}{L_o}$$

L = Sample length at break

L_o = Original length

Repeat the test on six samples that have been stored for 24 hr at 21.1°C in cell electrolyte CO_2 free atmosphere. The supplier may suggest alternate methods to Martin Marietta for approval.

4. Extractable Organic Content

At least three samples, each from a different roll shall be analyzed for soluble organic material. The sample size shall be 10 cm^2. The following method of extraction of organics is recommended. If a different method is used, it shall be submitted to Martin Marietta for approval.

1) Weigh the separator sample on an analytical balance.
2) Determine volume of separator sample.
3) Put the sample in a weighed container with methanol, reagent grade. Use a volume ratio of 20 solvent to one of separator cover container.
4) Stir with a magnetic stirrer overnight.
5) Remove separator sample and weigh after drying.
6) Evaporate solvent.

7) Determine the weight of residue and weight loss of separator.

8) Perform IR analysis of residue.* Submit copy of IR trace to Martin Marietta and indicate major organic constituents. (If a larger residue sample is required to perform this task, a proportionally larger sample is permissible.)

5. Inorganic Content

At least three samples, each from a different roll, shall be analyzed for inorganic materials. The sample size from which inorganics are to be extracted shall be a 10 cm^2. Qualitative spectrographic analysis of the following will be determined: carbonate, silica, zinc, chloride, nitrate, and nickel titanium.†

6. Thickness Variation

The separator thickness shall be measured at minimum intervals of one measurement for each five cells constructed. Each measurement shall be made on samples of two feet in length, taking 10 thickness readings at approximately two-inch intervals. Using the Ames Model 262 or Cady Model DW-1 gage. Measurements may be made while separator is in rolls.

B. ELECTRODE AND ELECTRODE ASSEMBLIES

1. Electrode Quality Assurance Provisions

The electrode supplier's certification for both positive and negative electrodes shall contain the following minimum information.

1) Assigned plate batch number;

2) Spiral number or lot number;

3) Date of impregnation;

---

*Residue shall be less than 2.0% by weight of total organics.

†Residue shall be less than 0.5% by weight of total inorganics as determined by ignition residue.

4) Percent porosity;*

5) Weight of active material in grams/cm^2;

6) Positive capacity obtained; and

7) Negative capacity obtained.

2. Nitrate Content

The nitrate content of the positive (Ni) and negative (Ni) electrodes shall be measured in micrograms/gram of the active material, sinter, and substrate.

3. Carbonate Content

The carbonate content of the negative (Cd) and positive (Ni) electrodes shall be measured in milligrams/gram of active material, sinter, and substrate.

4. Electrode Assembly Quality Assurance Provisions

Manufacturing and inspection operations on completed positive and negative plates shall be controlled as follows before their formation:

1) Inspection of curing, coining, and other operations affecting the integrity of the sinter and grind.

2) Four edges shall be coined to prevent flaking of sinter material.

3) Visual inspection of plates. (100% inspection on positive and negative plates before assembly into formation pack.)

4) Plates shall be rejected if the following defects are detected:†

   a) Evidence of flaking of active materials of the plate.

   b) Rough edges, burrs and snags (inspection will be made with nylon gloves to feel for pulls on fibers of glove. Inspection will include the entire electrode surface.)

   c) Blisters and peeling of sinter material. Blisters in excess of 0.05 mm above electrode surfaces or evidence of sinter material breaking away from grid.

---

*Sample results based on a reasonable sample from each positive and negative spiral or lot are acceptable for items (4) through (7). Tolerances are to be supplied by supplier.

†Inspection criteria will be established by the supplier reflecting items listed in paragraphs (4), (a) through (h).

d) Electrodes shall be uniform thickness over the entire surface area of ±0.02 mm. A 10% random sample shall be selected for thickness determination. If all samples can meet this thickness requirement, then all platcs are acceptable. If one or more plates from this sample cannot meet this thickness requirement, then a 100% sample is required to eliminate all electrodes which cannot meet this thickness. Rejection is final.

e) Plate weight screening. Establish the average weight of the positive electrode and negative by a screening method before edge coating. Then each plate will be screened by a GO-NO-GO technique. Each plate weight shall be within ± 3.5% of the average established plate weight. The supplier shall establish detailed procedures and submit them for Martin Marietta review and approval. The average shall be established from the weighing of a minimum of 100 positive plates and 100 negative plates.

f) Tab shall be free of sinter material in the weld area. There shall be no evidence of flaking or cracking of sinter material adjacent to the tab.

g) Grid support for sinter material shall be free of any breaks or cracks.

h) Dimensional checks shall show that plates are in accordance with applicable supplier drawings. A 10% random sample shall be selected for dimensional checks.

5. Plate Samples

The supplier shall provide 25 acceptable positive electrodes and 25 acceptable negative electrodes from each plate lot used in the production of the cell lot. The electrodes shall have received inspection as required but shall not have been subjected to any electrical operation. Each electrode shall be placed in a polyethylene bag, heat sealed, and permanently marked with the plate lot number.

C. QUALITY ASSURANCE

1. Quality Assurance Provisions for Production Processing of Electrode Assemblies

Production processing and test operations on cell electrode assemblies consisting of initial inspection of plates, through formation, addition of KOH, and sealing of cell with gage assembly shall be controlled as follows:

2. Atmospheric Environment

The environment of the formation facility shall be monitored with respect to humidity and temperature.

3. Handling of Materials

All plates, separators, and materials shall be handled with gloves and shall be sealed in cleanroom grade plastic bags or sealed plastic boxes.

4. Formation Pack Identification

Sufficient numbers of previously inspected positive and negative electrodes constituting a cell pack shall have a formation pack identification number assigned. Formation pack identification numbers shall be referred to for all data recording during formation. Numbers shall be visible on each formation pack.

5. Separator Material (or materials)

Separator material or materials used to wrap plate groups for formation shall be inserted such that the outside surface of the two outer electrodes is covered with separator material.

6. Formation Pack Fabrication

All formation packs shall be fabricated from alkali resistant materials such as nylon, plexiglass, etc. The adhesive or epoxy used to assemble the containers shall also be alkali resistant.

7. Electrical Clips and Leads

Electrical clips and leads must be stainless steel, nickel, or nickel-plated steel. Means for attaching leads to clips must be alkali resistant.

8. Formation Pack Connectors

The connectors holding the plates together in the formation packs shall be constructed of stainless alloy, nickel, or nickel-plated steel.

9. Addition of Electrolyte and Water to Formation Packs

Electrolyte bubbling out of the packs during formation shall be avoided. At the end of the first formation cycle, electrolyte shall be added to a preset mark. Maintain the preset mark.

D. FORMATION AND ELECTROCHEMICAL CLEANING

1. Assembled Formation Packs

Assembled formation packs shall be soaked in KOH concentration as specified by supplier ± 0.5 deg Be for a minimum of 16 hr and a maximum of 24 hr before first electrical operation of formation. Each pack shall consist of the same number of positive and negative plates as will be used in a finished cell.

2. Operational Conditions

The following conditions shall be observed during operation:

1) KOH level in formation container shall be maintained above top of plate stack;
2) Charge and discharge times shall be maintained as specified by supplier within ± 2% of designated time periods;*†
3) Where constant currents for charge or discharge are specified, and/or current measurements are used for calculations of ampere-hour capacity, currents shall be regulated within ± 2.0% of specified value.

---

*Exact time of each charge and each discharge shall be recorded to nearest minute. Deviation from periods specified shall be subject to immediate Martin Marietta notification and joint material review board action.

†In case of power failure, a notation shall be made, clearly visible, on the data sheets.

4) Positive and negative current leads of each formation series circuit shall have an ammeter inserted in series with each lead. One ammeter shall be marked "control"; the second ammeter marked "monitor". Readings of two meters shall always be within ± 2.0%.

5) Voltage of each formation pack and current of series formation circuit measurements shall be made not more than five minutes before end-of-all-charge or end-of-all-discharge periods.

3. Cell Formation

Formation shall be performed in accordance with supplier's schedule. Exceptions to certain operations are listed below and apply to all cells manufactured herein. The following steps shall be adhered to during the final capacity determination of positive electrodes and setting of relative state-of-charge of cadmium electrodes.

1) Last formation discharge to determine capacity of positive electrodes shall be made at the C/2 constant current rate from full charge to a cell voltage of 0.75 ± 0.25 V.

2) Time for each cell to reach a voltage of +0.75 ± 0.25 V shall be recorded.

3) Each cell shall be removed from the discharge circuit at the specified voltage and individually placed under a 0.1-Ω or greater resistor load such that the cell voltage is decreased to less than 0.1 V.

4) The ampere-hour capacity of positive plates (as determined in paragraph 2) shall be adequate to provide 100% cell-rated capacity to 1.1 V after exposure to heat sterilization.

5) Formation discharge shall continue at a 0.718 A-h when all cell voltages in a series circuit are less than 0.1 V. Discharge shall continue for a time period to obtain a 1.5 negative to positive ratio. Record voltage of each cell before starting the 0.718 A discharge.

6) Positive electrodes shall be verified as limiting electrodes by sampling one cell from each series formation circuit. Series formation circuit consists of up to 26 cells.

7) Cells not capable of meeting the requirements of paragraph 7 shall be rejected. The time rate is excess negative capacity.

8) Cell voltages and series string current shall be recorded at intervals not to exceed 30 min during the 0.718 A discharge. The total time each cell is on the 0.718 A discharge shall be recorded.

4. Plate Stacks

Traceability of plates in semi-formation shall be maintained. Plates shall not be exposed to air for more than five minutes before complete neutralization. Deionized water, having a resistivity of 1.0 MΩ-cm, shall be used for rinsing plates. The sample shall be collected from plates when the runoff has slowed to approximately one drop/second. The supplier's procedure for pH measurement shall be submitted to Martin Marietta for approval.

5. Drying

Plates shall be vacuum dried or dried in an inert atmosphere. Drying temperature shall not exceed 55°C. Oven temperature not exceeding the maximum limits specified during drying operation shall be demonstrated. "Time in" and "time out" of oven on each group of plates shall be recorded.*

6. Chemical Analysis

A chemical analysis of one dry cell per plate lot shall be performed to determine the loading of the positive (Nickel) electrode, negative (Cadmium) electrode, and the negative electrode residual charge.

---

*All internal cell components shall be handled with lint-free cotton gloves in an area designated for aerospace cells. Good housekeeping procedures are required.

7. Inspection and Weighing of Electrode Assemblies

Inspection on each electrode shall be performed. Particular attention shall be given to bent corners of grid and blisters on sintered material. Positive, negative, and auxiliary electrodes for each cell shall be grouped and their weight per cell shall be recorded to the nearest 0.1 gram.

8. Plated Welds

Weld tabs to plates and terminals to combs, whichever is applicable. Welds shall be in accordance with MIL-W-8611 or supplier's Martin Marietta Corporation-approved equivalent specification.

9. Plate Stack Wrap (separator material)

Separator material shall be tested in accordance with Section A. Lot number and type of separator material shall be recorded on cell data sheets. Alignment of plate edges using an alignment gage shall be performed.

10. Resistance Test of Plate Stack Assembly

Electrode assemblies shall be compressed to 8.9 to 13.34 kN before assembly of packs into cell containers.*

11. Radiographic Examination

Radiographs shall be taken of each unit for inspection for workmanship, foreign metallic particles, and drawing compliance. No more than three cells shall be included in each radiograph taken of the flat view and no more than four cells shall be included in each radiograph taken of the edge view. As a minimum, each radiograph shall contain cell serial number, positive or negative terminal location, view number, suitable control number, date radiograph was taken, and an image quality indicator. All radiographs shall have good clarity.

---

*Controlled periodic calibration required if conducted on a test jig.

12. Rejection Criteria

Cells shall be rejected if the following is observed:

1) Tab bends greater than 90 deg;
2) Poor workmanship and nonconformance to drawings; and
3) Auxiliary electrode strips and/or tabs misaligned or exhibiting unusual bends or kinks at any point.

13. Rework

Three mechanical cycles on defects detected before welding of cover to case are permissible provided that a repeat log is maintained and submitted to Martin Marietta Corporation. A complete repeat radiographic examination shall be conducted on the repaired unit. Any cells failing to meet any of the electrical requirements stated herein shall be removed from the assembly area and held for Martin Marietta Corporation review and approval of any electrical rework. No rework shall be permitted on units where defects are detected after cover weld and pinch-off is completed.

14. KOH Fill

KOH shall be prepared and tested in accordance with 4. Electroyte (see page B-18). Data from the batch card on the cell data sheet shall be recorded. Each cell with dust cap shall be weighed to the nearest 0.1 grams before KOH is added. Contamination of KOH shall be prevented by using burettes while filling and by minimizing KOH exposure to atmospheric conditions. The amount (in ·) and the concentration of KOH shall be as specified by the supplier. Prior to KOH fill, the covers shall be welded and the insulation resistance measured. Methods used to clean burretes shall be specified by the supplier and submitted to Martin for approval. An alternate fill procedure may be submitted to Martin Marietta for review and approval.

15. Postfill Protection

Each cell with a dust cap shall be weighed immediately after fill. Cell weight shall be recorded to the nearest 0.1 gram. Weight gain must be within ± 3% of nominal value specified by the supplier. A gage or dust cap shall be placed on cells immediately after filling electrolyte. Cells left unsealed longer than 10 min shall be rejected. After installation of gage assembly, cells shall be evacuated to 25 in. minimum gage vacuum. All fittings, gages, and associated components of the gage assembly shall be noncorrosive material in a KOH environment. Jackets must be put on cells ensuring surface of plates are parallel, then torque to a specified value. Alternate procedures may be submitted for Martin Marietta review and approval if the above requirements are not compatible with the supplier's manufacturing processes.

16. Leak Test of Cells and Gage Assembly

The cell, before electrolyte filling shall be leak-tested on a Veeco or comparable leak testing device to assure that leak rate is less than 10^{-6} cc/sec. After the gage assembly is attached to the cell, the entire assembly shall be pressurized to 413.7 kPa (60 psi) as read on a standard pressure gage. Record variation and whether positive or negative (reject all gages below 393 kPA [57 psi] and above 434 kPa [43 psi]). Leave pressure in cell and set aside for two hours minimum. At the end of the two hours, repair and retest all gages that do not read the same as when pressure was applied.

E. PRECHARGE ADJUSTMENT

1. State-of-Charge Adjustment

Precharge shall be set by an oxygen venting technique established by the supplier. A minimum of one charge-discharge cycle is required after KOH [illegible] before the precharge adjustment is made. The procedure and amount used is subject to Martin Marietta approval. The distribution of negative capacity shall be determined.

F. CAPACITY TEST

1. Quality Assurance Provisions for Electrode Capacity Check

The electrode capacity check shall provide a measure of the discharge capacity of the positive (nickel) electrode and of the negative (cadmium) electrode of nickel-cadmium cells as separate data under a standard set of conditions. This test shall be run in a manner such that the excess negative capacity beyond complete discharge of the positive (or excess positive beyond the negative in case of cells that may be negative limited on discharge) may be determined in addition to the total capacities of the electrodes. These data may be used to establish one or more of the following:

1) Range and distribution of positive capacities;
2) Range and distribution of negative capacities;
3) Difference between and/or ratio of total negative and positive capacities;
4) Excess negative (or positive) on discharge; and
5) Excess negative on charge.

A total negative/positive capacity ratio of 1.50:1 minimum is required. Any ratio less than 1.50:1 obtained under the following conditions specified shall be cause for rejection of the plate lots from which the cell was manufactured. Retest can be performed with Martin Marietta Corporation approval.

Sampling Rate

1) A minimum of one pack from each plate lot group of 26 cells (or less) shall be random selected at the conclusion of electrical formation cycles. The test cells shall be selected before further processing. Test shall start as soon as possible but not to exceed three days from formation.

2) A minimum of one cell from each plate lot group of 52 cells (or less) shall be random selected immediately after the negative precharge is set. Following the standard one-ohm and dead short periods, the test sample shall be opened by removal of the gage assembly and flooded with KOH. Tests shall be performed on sample cells immediately after the negative precharge is set.

G. PRECHARGE TEST

1. Precharge Determination

Short cell into 6/C-ohm resistor for 16 to 24 hr. Remove gage and immediately flood with 34% KOH to insure no oxygen discharge of the negative occurs. Reverse at C/2 to -0.5 V. Check gas evolved while cell is on plateau with hydrogen sniffer to determine limiting electrode. Record time to -0.5 V.

Since the cell is in a stainless steel container and both electrode terminals are insulated from the container, the container itself may be used as a substitute for a reference electrode. Even though the container potential is a function of the pressure O_2 or H_2 in the cell, the changes in electrode voltage at end of capacity are relatively large and usually can be clearly identified using the container as a reference

2. Cell Preparation

Remove excess KOH under vacuum. Cut case to cover weld and remove plate pack from case. Insert cellophane separater between each plate (cellophane should be slightly larger than plate). This will provide a gas barrier to make charging the negative easier and prevent shorts. Place cell in a suitable container and add 34% KOH to approximately 1/4 in. from above top of plates.

3. Charge

Charge cells at C/8 for 16 to 48 hr (minimum cell voltage 1.510 V.)

4. Discharge

Discharge cell at C/2 to -0.5 V. After cell reaches zero volts and begins to gas, check for hydrogen with a hydrogen sniffer. Record time to +0.5 V. Record time to -0.5 V.

5. Applicable Conditions

The following conditions are applicable:

1) Cell temperature shall be between 24 and 29°C;
2) Cell terminal voltage shall be recorded; and
3) Voltage from both positive and negative terminals to the reference electrode shall be recorded continuously or at intervals not to exceed 15 min.

6. Calculations

Let

T_{N_1} = time to -0.5 V

= time to discharged precharged negative

T_{P_3} = time from start of discharge (full charge) to +0.5 V

= time to discharge positive electrode

T_{N_3} = time from full charge to -0.5 V

= time to discharge total negative electrode

I_o = discharge current = C/2 rate

Then

$I_o \left[T_{N_3} - T_{P_3} \right]$ = excess capacity of total negative over positive

$I_o \left(T_{N_1} \right)$ = precharged negative capacity

$I_o \left[\left(T_{N_3} \right) - \left(T_{P_3} \right) - \left(T_{N_1} \right) \right]$ = excess discharged negative capacity

at the charged end

$\frac{\left(T_{N_3} \right)}{\left(T_{P_3} \right)}$ = "negative-to-positive ratio"

H. CONTAMINATION CONTROL

1. Control and Testing of Water and Electrolyte

The electrolyte solutions and wash water used for cells specified herein shall be of high purity. Data shall be submitted in accordance with the procurement agreement.

2. Deionized Water

Deionized water used in all wash water, dilutant, or additive shall have a resistivity of greater than 1.0 MΩ-cm. In the event the resistivity drops below 1.0 MΩ-cm, the process shall be stopped until the resistivity is restored to the specified limits. The resistivity is to be determined before each operation in which the water is used. A suitable conductivity cell is calibrated less than two weeks before the start of water requirements tests used on cells constructed under this specification shall be used. Criteria for calibration shall be as follows:

1) The conductivity cell shall be recalibrated at two-week intervals (maximum) until completion of the water requirement tasks.

2) The calibration shall be conducted in a 0.1% potassium-chloride solution and shall record a conductivity of 1410 ± μΩ at 25°C (a temperature correction as per the handbook of "Chemistry and Physics" may be used). If conductivity is not within these tolerances, the conductivity cell must be replaced or replatinized.

3) The silica content in the water shall not exceed 1 ppm.

4) The solids content of the water must be determined by the supplier. Maximum solids content shall not exceed 50 ppm.

3. Distilled Water

Distilled water used either as wash water, dilutant, or additive shall be tested and shall meet the requirements of 3) and 4) of paragraph 2 above.

4. Electrolyte

The supplier, batch number, grade, analysis, date of purchase, and when the date container is opened must be recorded. The potassium hydroxide "mercury cell" grade electrolyte concentrate (as defined by Allied Chemical Company) or equivalent shall be mixed with the distilled water to make up a solution with a tolerance of ± 0.4% by weight. Each batch of electrolyte shall be analyzed for carbonate content and hydroxyl ion concentration using the double titration method of phenolphthalein end point followed by methyl purple or orange end point. Carbonate concentration shall not exceed 4.0 gram/liter. The hydroxyl ion concentration shall be determined by analytical methods. The electrolyte shall be analyzed for nitrate content. The supplier shall prepare procedure details and submit them to Martin Marietta for approval. The shelf life of the standard acid used in the titration method shall not be exceeded.

5. Electrolyte Sample

Electrolyte samples shall be submitted to Martin Marietta in accordance with the procurement agreement. A 100-cc sample of electrolyte shall be supplied to Martin Marietta from each batch of electrolyte used in the manufacture of cells. These samples will be supplied in sealed polyethylene containers and marked to identify the cell serial numbers for which that batch was used.

I. CELL CLOSURE

1. Cover-to-Case Junction

The cover shall be electric arc welded to the container using inert gas shielding as per specification MIL-W-8611. No welds beyond dimensional limits shall be permitted. Weld joints shall not be ground or polished. Weld beads shall be smooth and free of folds. Porosity and cracks are not acceptable.

2. Pinch-Off of Fill Tube

After cells have been drained for 16 hr with a 1.0-Ω resistor, each cell shall be back-filled with a gas mixture of 95% oxygen and 5% helium to 34.4 ± 20.7 kPa (5 ± 3 psi). Within five minutes from the time of the back-fill, each cell-filled tube shall be pinched close and welded as per MIL-W-8611A.

3. Fill Tube Welding Quality Assurance Provision

No welds beyond dimensional limits shall be permitted. Weld joints shall not be ground or polished. The weld head shall be smooth and free of folds. Porosity and cracks are not acceptable.

4. Leak Rate Test

Each cell shall be leak-checked with a helium leak detector within four hours of back-fill. Any cell with a leak rate greater than 1×10^{-8} std cc/sec of helium will be permanently rejected.

J. DATA REQUIREMENTS

1. Manufacturing Data

The manufacturer shall maintain a log on the history of each cell by recording the following data:

1) Serial number of cell;
2) Date of manufacture;
3) Date of activation;
4) Type and duration of electrical tests performed on cells;
5) Charge and discharge method and rate used in electrical tests;
6) End of charge and discharge voltages to the nearest 0.001 V;
7) Test conditions;
8) Test results, including failures; and
9) Material traceability (consisting of complete records of cell components, including batch numbers and components).

The log shall be maintained on all cells manufactured for Martin Marietta and shall be available to Martin Marietta on request.

APPENDIX C

CELL MANUFACTURING DESCRIPTION

A. MANUFACTURING TECHNIQUES

Conventional manufacturing techniques are used for fabrication of cell plates. These include the slurry process for plaque production, impregnation of the plaque with nickel or cadmium nitrates and the conversion of the nitrates in a caustic solution into nickel or cadmium hydroxides. A special proprietary process for controlling the amount of carbonate in the plates and a heat treatment for improving the wettability of the separator material were added to the conventional manufacturing processes. Figure C-1 presents a manufacturing flow diagram which traces the manufacturing steps from the selection of the steel ribbon thickness to the sealing of the fill tube and final acceptance tests. A description of the significant manufacturing steps follows; however, certain information is classified as proprietary by the cell manufacturer and will not be presented.

1. Substrate

The manufacturing process begins with the perforation and nickel plating of a steel ribbon which is used for the cell plate substrate. The perforation hole pattern and area is selected to provide the capability of blanking out two plates across the width of the standard 17.78-cm wide steel ribbon.

2. Plaque Production

Plaque production consists of loading the perforated substrate with a controlled thickness of carbonyl-nickel slurry which is then sintered at a temperature just below the melting point of the nickel powder (1025°C). The fine nickel particles are heated to just below the melting point which welds the touching surfaces producing a highly porous (80) nickel matrix. Sintering temperature, duration of exposure to heat, cool-down rate, and oven atmospheric composition all contribute to the final plaque porosity and strength of the

Figure C-1 Manufacturing Flow Diagram

Figure C-1

sintered matrix. Carbonyl nickel water mixture ratios, slurry viscosity, sintering temperature and duration are process variables usually classified as proprietary by the manufacturer.

3. Coining

The plates used for the Viking cells were coined on four sides to minimize the possibility of the sintered nickel matrix cracking and flaking. The width of the coined edges is controlled to 2.03 ± 1.02 mm and the depth of 15% of the minimum plate thickness. The sintered nickel matrix thickness is controlled to between 0.67 and 0.77 mm for positive plate and 0.85 to 0.45 mm for negative plates. Indexing holes for moving the plaque through the stamping operation and a die locator indentation for positioning the dies over the coined areas are stamped on the plaque at the same time that the plaque is coined.

4. Plaque Impregnation

The impregnation procedure consists of immersing the plaque in a solution of nickel-nitrate (positive plate plaque) or cadmium-nitrate (negative plate plaque). During this time, the nitrate solution is absorbed in the porous matrix. The plaque is then immersed in a caustic solution of NaOH and then rinsed and dried. This procedure is repeated until the desired amount of nickel or cadmium-nitrate is loaded, which is determined by measuring the weight of a sample cut from the plaque.

Once the desired loading is achieved, a polarization current is applied to the plaque to first charge the plaque and then discharge it. During this time, the residual nitrate is driven off as ammonia (NH^3), leaving the activated material in the nickel matrix as either nickel or cadium-hydroxide. The final step consists of washing the plaque in deionized water to remove any remaining traces of sodium-hydroxide. Several wash cycles are performed until the water dripping from the plaque has reached a pH of less than 0.8. The plaque is then dried in preparation for the blanking operation.

The impregnation process requires precise control of process variables to produce plates with the desired porosity, loading, and

active material utilization. Density of the nitrate solution, acid content, temperature, and impregnation time are some of the process variables controlled to achieve the desired plate performance. The caustic solution type, specific gravity, temperature and amount of impurities (i.e., NH_3, CO_2 and OH) are variables that also affect the plaque quality. The polarization current density and time duration are controlled to specific limits for each type of plate being processed.

5. Blanking

The blanking operation consists of stamping out the plates from the plaque using dies which are sized to the required plate dimensions. One die is used for both the positive and negative plates. The weld tab on the negative plates are trimmed to the required configuration in a later operation. This operation is performed to provide a means of distinguishing the negative plates from the positive during handling and x-ray inspections.

6. Plate Inspection

Following the blanking operation, the plates are inspected for defects. Inspection criteria for rejection include: (1) cracks in sinter exceeding 12.7 mm long; (2) rough edges, burrs, and snags; (3) blisters and pimples exceeding 0.0508 mm above the plate surface or peeling of sinter material; (4) electrode thickness variations exceeding ± 0.025 mm; (5) sinter material on tab; (6) coining width uniformity exceeding 0.381 mm; (7) cracks or breaks in grid support for sinter material, and (8) dimensional tolerances are exceeded.

7. Plate Weight Screening

Plate weight screening was initiated to achieve uniformity in characteristics among plates used in a cell. Previous studies had shown that the plate weight was directly relatable to the amount of active material loaded and ampere-hour capacity uniformity could be achieved by controlling the allowable dispersion in plate weight. The technique implemented required weighing and computing the average plate weight for a production lot. Each plate was then weighed and rejected if its weight deviated by more than ±3.5% from the lot average. The allowable deviation was selected based on an analysis

performed by NASA Goddard Space Flight Center. (Note: The NASA GSFC specification for the Manufacture of Aerospace Nickel-Cadmium Storage cells (74-1500) uses the same criteria for plate weight.)

8. Electro-Chemical Tests

Plate formation is accomplished using temporary plate packs of 11 positive and 12 negative plates. The plate packs are placed in a test fixture using perforated PVC sheets as separators and flooded with KOH. The temporary packs are then electrically cycled to measure the plate capacities. The amount of charge is controlled to insure that both the positive and negative plates are fully charged. This was accomplished by a large amount of overcharge (150 to 200%), to fully charge the negative plates.

The ampere-hour capacity of the positive plates is required to be between 120 and 150% of the rated (nameplate) capacity of the cell. The negative plate to positive plate ampere-hour capacity ratio must be 1.50:1.00 as a minimum.

Following the formation cycling and capacity test, the plate packs are disassembled, washed, and dried. Deionized water having a resistivity of one megohm-cm or greater and a silica content of less than one part per million is used for the plate washing and scrubbing operation. Exposure to air is minimized to control carbonate contamination. The drying operation is performed in a temperature-controlled oven in a nitrogen atmosphere. The drying temperatures and duration are controlled.

The electrical capcity test is the last electrical functional test performed before the plates are assembled into a cell. The sequence of operation in assembling the plates into finished cells is as follows.

The plates are sorted into groups of 11 positive plates and 12 negative plates. Each group of plates is weighed and the data recorded. The positive and negative groups are then combined into a cell plate pack and the thickness determined. Any plate pack exceeding 1.758 cm (thickness of 11 positive and 12 negative plates

with an average thickness of 0.071 cm and 0.0813 cm, respectively) is reworked by substituting thinner plates until the thickness criteria are met. These criteria prevent assembly plate packs with excessive thickness and consequently, excessive pressure in the cell cases. The final plate pack weight is measured and recorded.

9. Plate Pack Assembly

The plates are assembled into a pack of alternating negative and positive plates with negative plates on the outside of the pack. The plates are aligned in a jig and then welded to the comb. After the tab welding is completed, the plates are inspected and cleaned by flowing air over the plates. The plate pack assemblies are then compressed in a hydraulic press to 8.896×10^3 to 1.334×10^4 N (1 to 1.5 tons) to insure that any structurally weak sinter material is broken loose and removed before the separator bags are installed. Another air cleaning is performed after the compression test.

Before installing the separator bags on the plates, the bags are stacked in groups of 11 and each group is subjected to a compression using a 1.067×10^5 N (24,000 lb) hydraulic press to compress and flatten the folded edges of the bags. The bags are then slipped over the positive plates and the plate pack vacuum cleaned.

A plate pack short test is performed before inserting the completed pack in the cell case. The pack is compressed by a hydraulic press to 1.33×10^4 N (1.5 tons), and the impedance between the positive and negative plates measured. A plate pack that failed the 100,000 Ω isolation requirement could be reworked once to correct the leakage problem. This rework limitation was imposed to prevent failure of the plate weld tabs due to bending.

Special precautions are taken to insure that the plate positions are not disturbed during the insertion of the plate pack in the cell case. X-rays are taken of each cell to check on plate position and to verify that no sharp bends were made to the weld tabs. After the x-rays are inspected, the cell covers are heliarc welded to the cell case and a leak test performed using a helium leak detector. Leakage rate was limited to 1.0×10^{-8} Std ATM cc/sec helium.

10. Electrolyte Filling

The cells are weighed before the electrolyte fill operation and then reweighed after the operation to determine the weight gain for each cell. This weight increase is held to between 29.66 and 31.66 grams to insure that the correct amount of electrolyte is added (22.3 to 23.8 cc).

11. Cell Formation Tests

Three separate test sequences are performed by the manufacturer after electrolyte fill operations have been completed. The first test sequence consists of electrical pretests to prepare the cells for the evaluation tests to follow. These pretests consist of formation cycles, negative precharge adjustment, and pressure stabilization. Details of these tests are classified as proprietary by General Electric.

B. MANUFACTURING TESTS DESCRIPTION

Manufacturing tests include subjecting the cells to a heat compatibility test, final precharge adjustment, cold temperature charge and capacity test, ambient temperature capacity test, charge retention test, and internal impedance test.

1. High Temperature Exposure

A special high temperature compatibility test was inserted in the test sequence after the formation and pressure stabilization test of the electrical pretest procedures. Before the high temperature exposure, the cells were conditioned by discharging them to a voltage less than 0.1 V with a one-ohm resistor for a minimum of 16 hr. The cells were then evacuated to a 760 mm Hg (30 in. Hg) vacuum and then backfilled with a 95 to 5% oxygen-helium mixture.

The high temperature test consisted of a controlled temperature rise at a rate of 29.4 to 32.2°C per hour to a temperature of 125 ± 1.67°C. The cells were maintained at this temperature for 20 hr at which time the temperature was lowered at a rate of 29.4 to 32.2°C per hour.

An improvement in separator wettability and consequently an increase in oxygen recombination capability was realized by this procedure, which in most cases, resulted in an increase in the electrolyte quantity over the initial amount provided when the overcharge pressure adjustment was made.

2. Reconditioning

Following the high temperature exposure, each cell was reconditioned by charging at a C/2 rate for 150 min and then discharging at a C/2 rate to 1.0 V in a 23°C environment. This charge/discharge test was performed twice to recondition the cell following high temperature exposure. Each cell was discharged with a one-ohm resistor following the last conditioning charge and discharge.

3. Overcharge Test

During the C/10 overcharge for 48 hr, a small quantity of electrolyte is added if the pressure during overcharge is less than 172 kPa (25 psig). Conversely, if the pressure exceeds 448 kPs (65 psig), electrolyte may be removed. A negative plate precharge adjustment is also made during the overcharge test by venting a predetermined quantity of oxygen. Electrolyte adjustment techniques and oxygen venting is considered proprietary by the vendor.

4. Low Temperature Test

A charge/discharge test is performed at an ambient temperature of 0°C to verify the low temperature performance of the cells during the manufacturing tests. This test may be omitted based on an engineering evaluation and only performed during the final acceptance tests as required by the procurement specification. The test consists of a C/20 charge for 48 hr followed by a C/2 discharge to 1.0 V. During charge, a pressure limit of 689 kPa (100 psig) is allowed.

5. Cell Capacity

The cell manufacturer uses a C/10 charge for 16 hr followed by a C/2 discharge to a cell voltage of 1.0 V to measure the cell capacity. Each cell is totally discharged using a one-ohm load for 16 hr before the capacity test. During the test, the ambient temperature is maintained at 23.3 ± 3°C and the cell voltage limited to 1.48 V. The minimum capacity required by the vendor is 9.5 A-h.

6. Internal Impedance

The internal impedance is measured by the vendor using a 60-Hz sine wave source to produce a 0.01 V drop across a 0.1-Ω resistor which is in series with a totally discharged cell. The impedance is calculated by dividing the voltage drop across the cell by 0.1 A.

7. Charge Retention

Charge retention is performed by discharging the cell with a one-ohm load for 16 hr and then shorting the cells for one hour. The short is then removed and the cell voltage measured after a 24-hr open circuit stand at room temperature. The minimum acceptable voltage is 1.15 V. Cells failing this test are rejected.

8. Internal Resistance

The final test performed before releasing the cells for the formal acceptance tests consists of a C/2 charge for five minutes from a completely discharged condition and recording the cell voltages at 0.25, 0.5, and the 5-min time. The maximum allowable voltage is 1.5 V.

C. PROCUREMENT SPECIFICATION ACCEPTANCE TESTS

Formal acceptance tests, which were imposed by the procurement specification, included a low temperature overcharge test, cell capacity test, a voltage retention test, and a final leakage test. This limited amount of acceptance testing was imposed since the cell characterization and capacity matching testing was performed at the buyer's facility. The tests were required to be performed in the order given in the following paragraphs.

1. Low Temperature Overcharge

The low temperature (0°C) overcharge test was designed to verify the capability of the cell to be charged at a low rate for long periods (72 hr) without developing excessive voltages and pressures. The cell was allowed to cold soak for four hours before starting the test. During the C/20 charge, the allowable voltage was 1.52 V and the pressure was 689 kPa (100 psig). Cells exceeding these limits were rejected. The discharge was conducted using a C/2 rate to a cell voltage of 1.0 V followed by a one-ohm load for 16 hr minimum.

2. Cell Capacity

The cell capacity was measured in a chamber controlled to a temperature of 21.1°C using a C/10 charge for 16 hr followed by a C/2 discharge to 1.0 V. The beginning of life capacity for the eight ampere-hour (nameplate capacity) cell was set at 9.5 A-h.

3. Voltage Retention

A test to detect high impedance leakage paths between the cell plates was imposed on the vendor. The test selected consists of totally discharging the cell with a one-ohm load for a minimum of 16 hr. The load was then removed and the cell placed on an open circuit stand for 24 hr. At the end of the 24-hr period, the cell voltage was required to be 1.15 V or more.

4. Pinch-off and Leak Test

Following the data review and acceptance by Quality Assurance, the cells are back-filled with a gas mixture of 95% oxygen and 5% helium to 34.4 kPa (5 psig). The fill tube is pinched off and welded within five minutes of back filling. A leak test is made to insure that any leakage is less than 1×10^{-8} Std cc/sec of helium using a leak detector.

5. Cleaning

The Viking contamination control criteria required the imposition of special handling and cleanliness controls on the cells. Special precautions were taken to remove organic contaminants from the surface of the cells before delivery. Solder flux was removed from the solder terminals after tinning and fluoride-chloride test was performed on the wash water to detect the presence of solder fluxes. The cell cases were washed in demineralized water which was tested using the water break test of ASTM 21 or 22 to verify the absence of organic contaminants. The cells were dried by immersing them in acetone in preparation for packaging for shipment.

6. Packaging and Shipping

Each cell was shorted with a jumper wire connected between the terminals and placed in a plastic bag before the final packaging for shipment to the Martin Marietta facility. Each cell was individually protected with foamed packaging material while being shipped to prevent damage. Packing cases were identified with special handling stickers to minimize the possibility of damage during shipment. Air freight was chosen as the means of shipping the cells from the vendor to the Martin Marietta facility.

D. QUALITY ASSURANCE

Mandatory Quality Assurance inspections, tests, and reports were imposed by the procurement specification for several of the manufacturing steps and processes. Separator material characteristics, plate quality and weight screening, plate processing procedures, monitoring, test evaluation, case, cover, wash water purity, and electrolyte contamination controls were identified as requiring stringent quality assurance surveillance. One of the Quality Assurance requirements was to prepare a Reliability Program Plan which delineated the organization, the management, the authority, and the implementation procedures imposed throughout the program.

In addition to the specification-imposed Quality Assurance requirements, the cell manufacturer developed and used a series of quality procedure instructions for each of the manufacturing steps. Operation of equipment, inspection standards, and operator certification were controlled by these procedures.

Quality inspection requirements were identified in the manufacturing process plan.

1. Vendor Data and Material Submittal

Compliance with the intermediary design requirements was implemented by requiring the vendor to submit copies of certain data acquired during the various stages of cell production. These data submittal requirements were identified in the cell specification and further defined in the purchase agreement. Data that were required for each cell included weights of the positive and negative plate stacks, cell weight before and after electrolyte fill, negative plate stack and positive plate stack thicknesses, and total plate stack thickness. Sample cells from each lot were tested to determine negative precharge positive plate capacity, negative plate capacity, and discharged excess negative capacity.

Each roll of separator material was analyzed for wettability, porosity, absorptivity, organic and inorganic contents, tensile strength, thickness variation, and dimension stability. These data were submitted once since only one lot of separator material was used for the total Viking production.

Wash water was periodically checked for resistance and silica content and the data submitted.

In addition to the data submittal, component parts of the cell were required to be supplied to the purchaser for retention. Twenty-five samples from each of the positive and negative plate lots were delivered separately. One hundred milliliter samples of each batch of electrolyte were also delivered.

APPENDIX D

GLOSSARY

CDR	Critical Design Review - final review before production hardware build
c/a	Charge or discharge rate in amperes determined by dividing the cell nameplate capacity by the factor "a"
DOD	Depth-of-discharge as a percentage of the cell name plate capacity
Hydrophobic	Used to describe the poor wettability characteristic of a material
KOH	Potassium Hydroxide
PDR	Preliminary Design Review - review of preliminary design concepts.
PTV	A partially completed Lander vehicle used to verify test equipment and facilities before usage by the flight vehicle
SAEF	Facility at the Eastern test range for checkout of spacecraft before launch
η_{WH}	Efficiency based on the energy supplied and lost during charge and discharge. Charge, discharge, and cycle efficiency are defined.